# Title page

Understanding cell source and extracellular matrix contributions to cartilage and bone repair for regenerative medicine applications

**Inaugural dissertation**

to
be awarded the degree of Dr. sc. med.
presented at
the Faculty of Medicine
of the University of Basel

by
Benjamin PIPPENGER
from Nashville, Tennessee, USA

(Basel, 2019)

# Backside of title page

Approved by the Faculty of Medicine

On application of

Prof. Dr. Ivan Martin

Prof. Dr. Andrea Barbero

Prof. Dr. Bert Müller

Prof. Dr. Nadia Benkirane-Jessel

Prof. Dr. Daniel Kalbermatten

Basel, 27 May, 2017

……..

Prof. Dr. Primo Leo Schär

# I. Introduction

Human skeletal elements are grossly divided into three main tissue categories: bone, cartilage and muscle. While skeletal muscle is closely associated and interacts with the bony element, this thesis focuses specifically on the repair mechanisms involved in bone and cartilage and how to better mediate these mechanisms from a regenerative medicine perspective; muscle will not be treated hereafter and any reference to skeletal tissue refers either to bone or cartilage. To begin, I will first define key concepts in skeletal tissue repair that give background to the regenerative strategies chosen during this thesis. Following this, I will introduce the concept of tissue engineering and the parameters that are necessary to take into account when preparing a living tissue graft. After this brief introduction, I will present the experimental work performed during this thesis in which the specific strategies employed towards skeletal tissue engineering are presented. Finally, I conclude with a summary of accomplishments and suggest further work that could be performed to help advance the presented topics towards a translational technology.

## 1) Bone and cartilage gross anatomy

### a. Bone tissue

Bone is the densest tissue found in the human body, serving principally as support for the body's soft tissues and giving them a template upon which to attach or grow. Due to bone's remarkable mechanical properties (resistant to loads and strains), it serves as a protective organ, for example encasing the brain and spinal cord or resisting under the immense loads subjected to the human body under normal daily movements. Depending on its function and anatomical location, bone has evolved into two major tissue types: long and flat bones. While both bone types are characterized by their hard, ceramic surface composition, both harbor varying amounts of bone marrow, which is comprised of a loose connective tissue and various cell types. Indeed, these bone marrow spaces represent the second critical role of the bone organ: hematopoiesis (formation of the cellular components of blood). There are two types of bone marrow: red and yellow. While their relative quantities change throughout the lifespan of an individual, their roles remain constant. Red bone marrow, found principally in flat bones and the epiphyseal ends of long bone, is the center of

hematopoiesis. Yellow bone marrow, principally constituted of fat cells, makes up the medullary cavities of long bones. Bone marrow is a compartmentalized organ; different cell types are typically grouped together at their sites of production. Consistent with this idea of compartmentalization, the theory of bone marrow niches is generally accepted as being the sites that contain specific cell types with distinct functions, including the stem cell components of the marrow, i.e. hematopoietic stem (HSC) and mesenchymal stromal cells (MSC) (*Figure 1*). For the purposes of this thesis, only MSC will be discussed, due to their importance in bone repair.

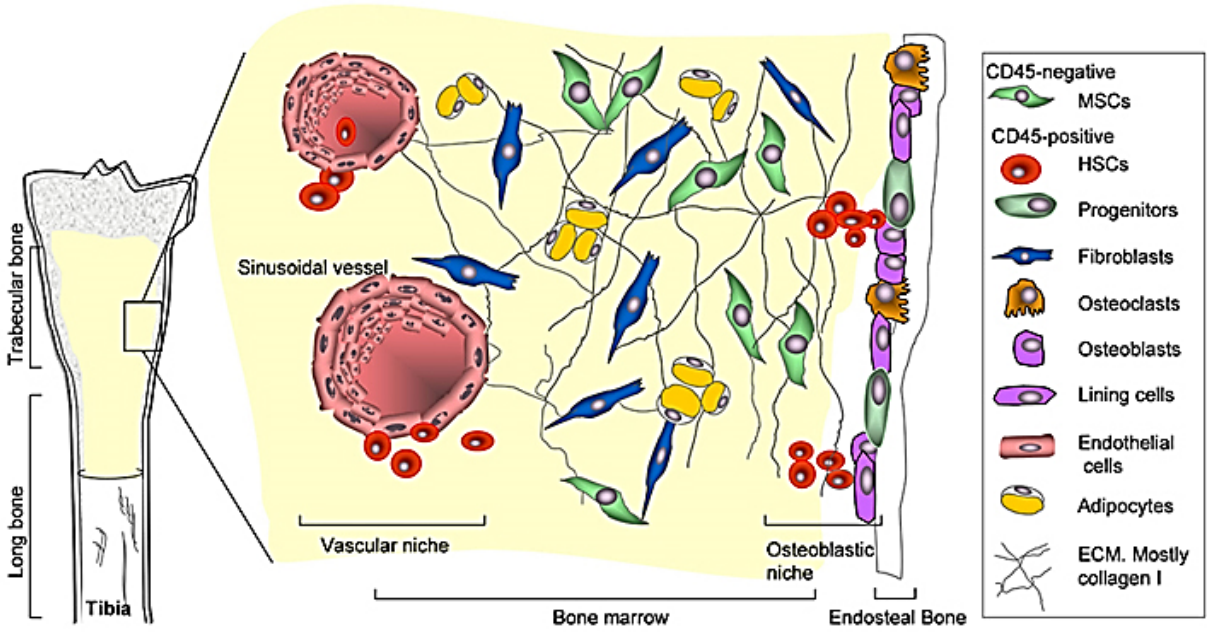


*Figure 1: The compartmentalized aspect of bone marrow within which different niches can be found. Figure source: [1]*

### 2) Skeletal tissue – Repair

To better understand skeletal tissue repair, one must first understand that bone and cartilage tissues, while both derived from the same progenitor cell source, differ drastically in their biology, biomechanics and function. It stands to reason that they also differ in their repair mechanisms and potentials. Bone repair, typically considered a relatively robust process, is in direct contrast to cartilage tissue repair, which is virtually nonexistent under physiological circumstances. While not all the reasons for this are yet understood, the most obvious factors that are thought to directly affect skeletal tissue repair (or the lack thereof) are tissue cellularity, vascularization and the presence of a progenitor cell source that can be mobilized to the repair site in the event of tissue

damage. Considering only these three factors is enough to establish the clear dichotomy between bone and cartilage tissue repair.

Bone is a heterogeneous organ composed of many different tissues and cell types, including the osseous, marrow, periostium, endostium, nerves and blood vessels (*Table 1*). In fact cartilage, being a tissue and not an organ, is also considered a part of the bone organ complex. Due to the complexity involved in the bone organ, it is common to employ semantic simplifications when referring to tissue components and this thesis will do the same. Therefore, when bone is mentioned, this specifically refers (unless otherwise stated) to the osseous tissue structure that is classically thought of as "bone tissue", being the extremely dense mineralized tissue that characterizes the hard endoskeleton of animals and, therefore, humans. The number and types of cells present in the bone organ is relatively high (when compared to cartilage). Common cell types that are critical to the homeostasis of bone are summarized in Table 1 and the relative distribution of these cells a schematized in Figure 1. Included in the bone tissues, as previously mentioned, are vessels, which constitute the second element critical to tissue repair. The bone organ is irrigated with a dense, ramified vasculature which reaches throughout the majority of the organ (excluding cartilage tissue), never leaving more than ~300 µm of space between an individual cell and a vessel wall. The density of the vascularization ensures nutrient delivery to and waste removal from the cells constituting the various tissues. Present in the bone marrow and, when mobilized into action, travel either through the blood or along the outside of the vessels themselves, are bone marrow-derived mesenchymal stromal cells (bMSC). Intimately associated with the vascular system, bMSC (the progenitor cell source for the bone organ) represent the third element associated with tissue repair. As BMSC rely on the vasculature for transport to the repair site, bone has an obvious advantage over cartilage tissue, which is avascular under physiological conditions.

Having considered these three elements critical to skeletal tissue repair (cellularity, vascularization and progenitor cell source), the mechanisms of tissue repair can now be better understood.

| *skeletal tissues* | *cell type* | *role* |
|---|---|---|
| ***osseuse tissue*** | osteoblast | Responsible for bone building through the secretion of a bone matrix (osteoid) that will subsequently be mineralized and form bone. Bone lining cells are also osteoblasts but in their resting state. |
| | osteoclast | Responsible for the breakdown (resorption) of bone. Derived from monocytes, they are specialized macrophages that excrete catalytic enzymes onto the surface of bone tissue. |
| | osteocyte | These are mature bone cells. Originating from osteoblasts, they have become surrounded by the osteoid matrix they secreted. They function in bone formation, calcium homeostasis and matrix maintenance. |
| ***bone marrow stroma*** | bone marrow-derived mesenchymal stromal cells (BMSC) | Osteo- and chondroprogenitor cells found in the bone marrow niche that are capable of differentiating into a variety of cell types including osteoblasts and chondrocytes. |
| | adipocytes & adipose-derived mesenchymal stromal cells (ASC) | the most abundant stromal cell phenotype in adult human bone marrow, adipocytes may share common functions with stromal stem cells, osteoblasts, and hematopoietic supportive cells [2,3]. |
| | fibroblasts | Regulate hematopoiesis in the bone marrow niche [4]. |
| | immune cells | leukocytes involved in host defense against infectious diseases and foreign materials. |
| | hematopoietic stem cells (and progeny) | maintain hematopoiesis. For further information, refer to the following review [5]. |
| ***vessels*** | endothelial cell | Lining the inner surface of vessels, endothelial cells constitute the direct contact barrier between the circulating blood and the surrounding tissue. Responsible for barrier properties, blood clotting and angiogenesis. |
| | pericyte | Support cells found wrapped around endothelial networks (capillaries). Responsible for the upkeep of endothelial cell maintenance and proliferation as well as the direct differentiation into mesenchymal stem cells upon tissue damage.[6] |
| ***cartilage tissue*** | chondrocyte | The only cell found in cartilage, it is responsible for the production and maintenance of a cartilage tissue. |

*3) Table 1: Tissue composition of the bone organ*

### a) Bone repair

Bone repair proceeds by the same formation patterns as bone development, but the specific mechanism of repair is determined by the biomechanical environment provided [7]. The repair of a bone organ (minus the cartilage tissue component) is a complex but relatively well understood process. As with its formation during

embryogenesis, bone repair proceeds through two archetypical routes: endochondral and intramembranous ossification. Typically, endochondral ossification occurs in long bones and intramembranous ossification occurs in flat bones, including the cranium and the scapulae. While both routes begin with mesenchymal progenitors, the differentiation process that these cells undergo will define what type of bone formation occurs.

### i. Endochondral ossification

For endochondral ossification, mesenchymal progenitors first differentiate into chondrocytes and form a stratified cartilaginous template, with resting chondrocytes towards the epiphyseal plate and hypertrophic chondrocytes towards the bone marrow space (*Figure 2*) [8,9]. This latter tissue is particularly important for bone formation and is the current focus of tissue engineering strategies aiming to recapitulate this process *in vitro*. Indeed, commonly used for histological identification purposes, the most abundant protein present in cartilage matrix is collagen type II. But, upon hypertrophic differentiation of chondrocytes, the matrix becomes calcified and begins to be remodeled through the excretion of matrix metallopeptidases, principally matrix metallopeptidase 13 (MMP13). Collagen type II is thus broken down and replaced by collagen type X (Col-X), a specific type of matrix specific to hypertrophic cartilage [10]. Col-X in histological and biochemical analyses represents the key factor whose presence marks hypertrophic tissue.

As the cartilage remodeling progresses, factors embedded in the matrix become available, the most important being vascular growth factor-1 (VEGF) [11,12]. This factor promotes the ingrowth of vessels from neighboring tissues, thereby supplying a conduit for the recruitment of cells involved in bone deposition: BMSC [13]. In fact, it is believed that vascular invasion is a prerequisite for bone formation, with osteoblasts and osteoprogenitor cells developing with endothelial cells in the newly formed blood vessels at sites where new bone is formed [14,15].

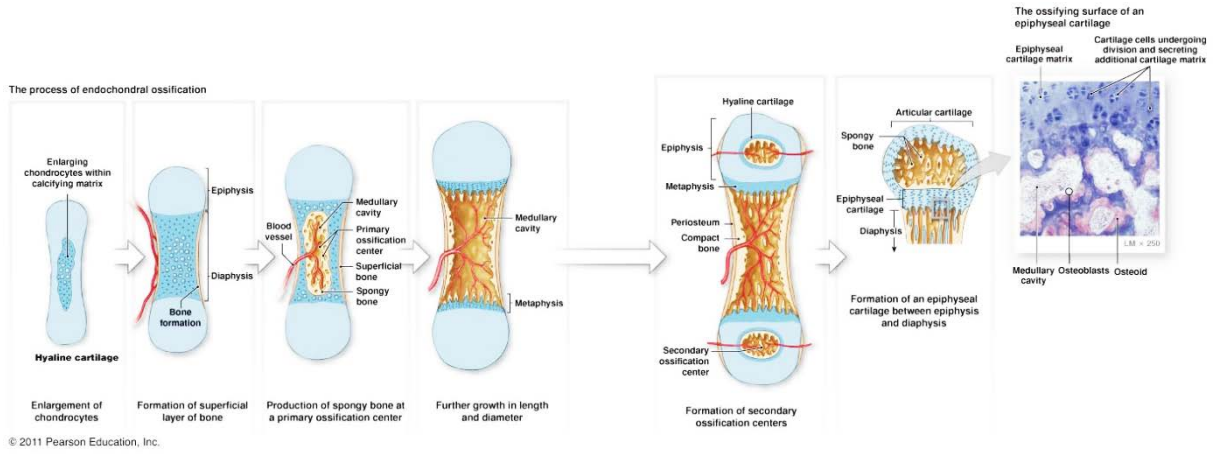


*Figure 2: Schematic of endochondral ossification. Figure source:* [16]

### ii. Intramembranous ossification

Intramembranous ossification occurs only in flat bones and is thus limited to a specific subset of bones within the body including, and importantly for this thesis, craniofacial bones such as the calvaria, maxilla and palate. Contrary to endochondral ossification, intramembranous ossification does not proceed through a cartilaginous phase but is rather characterized by BMSC differentiating directly into osteoblasts [17,18]. Intramembranous bone are classified into three categories: 1) the sesamoid, 2) periosteal and 3) dermal bones. For the interests of this thesis, we will only consider dermal bones as these include the craniofacial bones. Dermal bones are called thus because they result from mesenchymal condensations within the dermis of the skin, a process which is schematized below (*Figure 3*) [19].

Considerably more is known about endochondral ossification than dermal bone formation and several studies have demonstrated that while there are molecular similarities between the two bone formation routes, there are also events that seem to be unique to intramembranous ossification [20]. Combined with these molecular discrepancies are the differences in the bone tissue themselves as well as the ontogenetic differences. Together, they represent an evidence-based set of parameters that suggest dermal bone development and repair must be considered as unique biological events. While the specific molecular factors involved in intramembranous (and endochondral) ossification will be treated in the next section, one specific intermediate cell type that is characteristic to intramembranous

differentiation should be mentioned here: the chondrocyte-like osteoblast (CLO). This particular cell type is characterized by the co-expression of both osteogenic and chondrogenic markers [20].

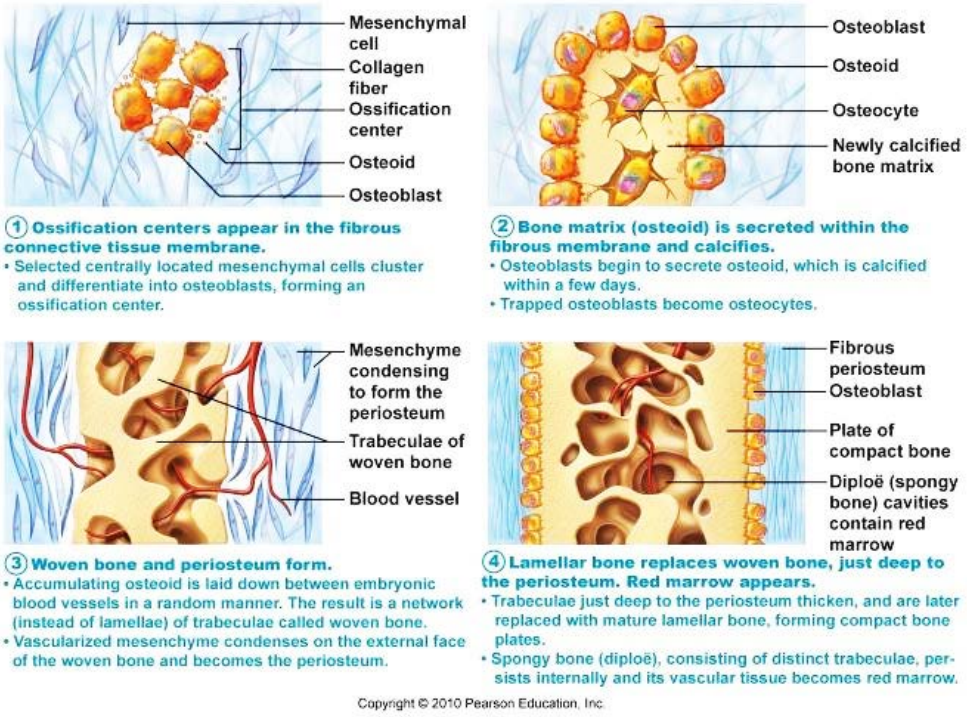


*Figure 3: Schematization of intramembraous ossification. Figure source:* [21]

### iii. Molecular regulation of osteoblastic differentiation

The molecular regulation of osteoblastic differentiation is a complex interplay of signaling pathways resulting in the gradual activation or suppression of specific transcription factors. Some of the most important pathways to date that have been shown to be critical in osteoblastic differentiation include Hedgehog, Notch, WNT, bone morphogenic protein (BMP) and fibroblast growth factor (FGF) signaling (*Figure 4*) [22]. This list does not however give a complete picture; the story complicates when considering the differences between endochondral and intramembranous ossification. Crossover does exist between pathways and markers, but certain pathways such as the Hedgehog pathway have been shown to have an opposite role in intramembranous bone formation from endochondral. For example, in long bones, indian hedgehog (IHH) and parathyroid hormone-related protein (PTHrP) form a feedback loop which serves to

regulate the onset of hypertrophic differentiation of chondrocytes [23]. However, in dermal bone formation, the IHH/PTHrP loop acts to negatively regulate the formation of osteoblasts from osteoprogenitor [20]. Also, whereas BMPs function in the later stages of endochondral bone formation, they play a fundamental role in regulating the earliest cell differentiation decisions in intramembranous differentiation [20].

Regardless the differences between the two bone formation routes, there are common factors that can be analyzed to determine if and to what extent osteoblastic and/or hypertrophic differentiation has occurred in a given cell type. Factors mentioned throughout this thesis are summarized in the table below (*Table 2*).

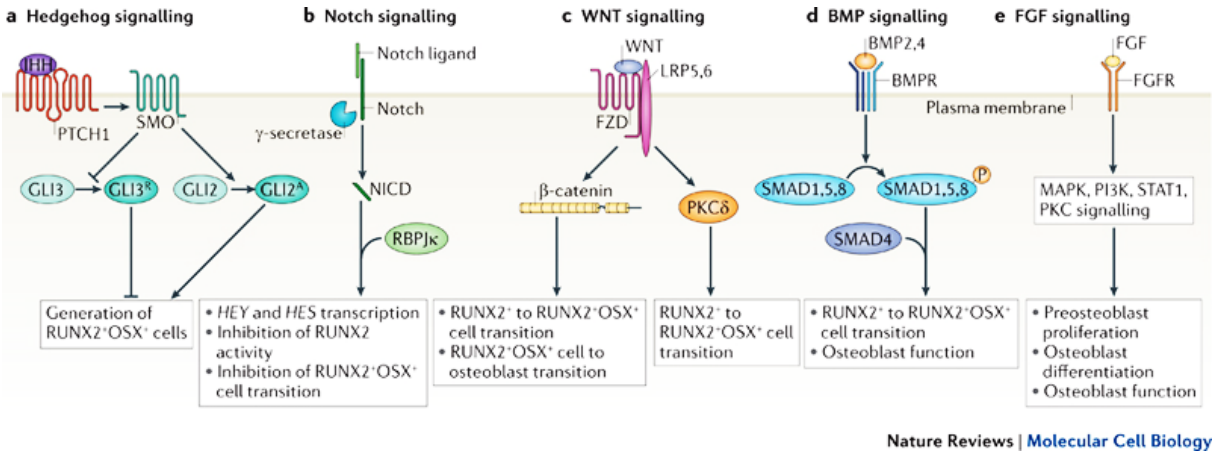


*Figure 4: Developmental signals regulating key steps of osteoblastic differentiation. Figure source:* [22]

| *factors* | *role* | *localization* |
|---|---|---|
| ***Runt-related transcription factor-2 (RUNX2)*** | considered the master organizer of gene transcription in osteoblastic differentiation [24] | nuclear |
| ***Osterix (OSX)*** | a zinc finger–containing transcription factor expressed in the osteoblasts of all endochondral and membranous bones [25] | cytoplasmic in progenitors and nuclear upon osteoblastic commitment |
| ***Collagen type X (Col-X)*** | regulates matrix mineralization and compartmentalizes matrix components. expressed exclusively by hypertrophic chondrocytes and is thus used as a marker for hypertrophic cartilage [26]. | matrix protein |
| ***Collagen type II (Col-II)*** | most abundant type of collagen in cartilage extracellular matrix. allows cartilage to entrap | matrix protein |

| | | |
|---|---|---|
| | the proteoglycan aggregate as well as provide tensile strength to the tissue [27]. | |
| ***Collagen type I (Col-I)*** | most abundant type of collagen in bone extracellular matrix. strengthens and supports many tissues in the body, including bone. | matrix protein |
| ***bone sialoprotein (BSP)*** | large component of bone extracellular matrix [28]. Thought to serve as a nucleation site for hydroxyapatite, thus initializing mineralization [29]. | matrix protein |
| ***Vascular growth factor receptor-2 (VEGF)*** | involved in both vasculogenesis and angiogenesis, the latter being critical for bone formation and repair. | membrane-bound and soluble ligand |
| ***Indian hedgehog (IHH)*** | involved in chondrocyte differentiation, proliferation and maturation especially during endochondral ossification [23]. regulates endochondral bone development through a negative feedback loop with PTHrP. | soluble ligand |
| ***Parathyroid-related protein-1 (PTHrP)*** | involved in chondrocyte differentiation, proliferation and maturation especially during endochondral ossification [23]. regulates endochondral bone development through a negative feedback loop with IHH | secreted hormone |
| ***matrix metallopeptidase 13 (MMP13)*** | restructuring the collagen matrix for bone mineralization during endochondral ossification [30]. | matrix protein |
| ***Bone morphogenic protein-4 (BMP-4)*** | Essential for early stages of BMSC condensation and commitment to osteogenic fate during dermal bone ossification [20]. | matrix protein |
| ***Bone morphogenic protein-2 (BMP-2)*** | stimulates the production of bone through autoinduction [31]. Upregulated during endochondral, but not intramembranous ossification [20]. | matrix protein |
| ***osteocalcin (OC)*** | osteoblast-specific protein thought to be involved in bone mineral homeostasis. Used as a biomarker for differentiated osteoblasts [32]. | matrix protein |
| ***osteopontin (OP)*** | a linking protein responsible for the binding calcium-based biominerals and is a a transcriptional activator of osteoblast differentiation [33]. | matrix protein |
| ***alkaline phosphatase (ALP)*** | hydrolase enzyme responsible for removing phosphate groups. Responsible for the elaboration of a bone matrix that is chemically calcifiable [34]. | excreted enzyme |

*Table 2: Selected factors involved in endochondral and intramembranous ossification*

### b. Cartilage repair

Contrary to bone tissue, articular cartilage tissue does not undergo restoration after injury. Cartilage damage results in cellular infiltration of the defect site. Included in these cells are macrophages and fibroblasts, the latter of which secretes a new extracellular matrix to "close the gap". Unfortunately, because this patch is not secreted by chondrocytes, it is lacking in key properties that define a healthy cartilage tissue: a matrix composed principally of Collagen type II and the presence of glycosaminoglycans (GAG). Without GAG, water molecules are not bound to the matrix and resistance to future loads is therefore diminished, leaving place for further articular tissue damage. One of the most important limiting factors to cartilage repair is its lack of vascularity. As an avascular tissue, BMSC recruitment to the injured joint surface is impossible. This is an important concept and forms the logic behind one of the current gold standards in surgical treatment for articular cartilage defects: microfacturing (a surgical technique that involves perforating the subchondral bone layer that underlies articular cartilage to allow BMSC infiltration into the cartilage defect site) [35]. Indeed, as cartilage restoration following injury is impossible, the development of surgical repair techniques has been the main research focus over the last decades, an overview of which can be found in (*Figure 5*). Included in these techniques are tissue engineering approaches either with or without the presence of cells. These techniques will be more thoroughly explained in section 2 of the introduction entitled "Tissue Engineering".

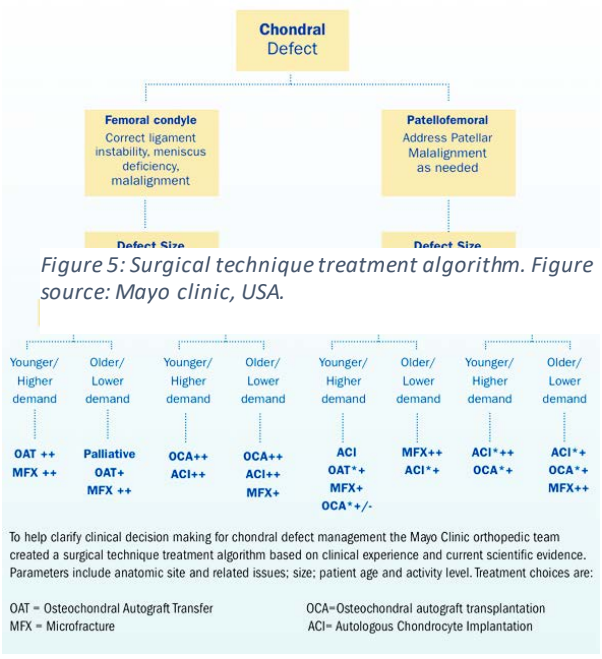


*Figure 5: Surgical technique treatment algorithm. Figure source: Mayo clinic, USA.*

### c. Embryological origin of tissues

Craniofacial skeletal tissues are derived from the neuroectoderm, whereas the remaining appendicular skeleton is derived from the mesoderm. Not only do these two skeletal tissues derive from different germ layers during embryological development,

but they also undergo disparate repair mechanisms upon injury (endochondral versus intramembranous for apical and craniofacial skeleton, respectively). These underlined differences necessitate alternative regenerative medicine strategies when considering the use of a living graft material in craniofacial bone repair applications. For example, direct experimental comparison of progenitor cells derived from craniofacial versus long bone shows in vitro differences between these two cell types in terms of cell proliferation and differentiation [36–38]. In vivo, heterotopic transplantation experiments show tibial progenitor cells (mesodermal origin) tend towards chondro- rather than osteoblastogenesis upon mandibular implantation (neurectodermal environment), a phenomenon shown to be explicable on the genetic level by mismatched Hox signatures [39]. Furthermore, mesodermal-derived progenitor cells have been shown to have little to no effect during the first month of calvarian implantation, highlighting the importance of an appropriate donor cell source for facial bone tissue engineering [40]. A final complication resides in the limited number of progenitor cells able to be harvested from the facial region, stemming principally from the fact that craniofacial bones are mainly flat bones. Therefore, common cell-based strategies to craniofacial bone repair continue to rely on bone marrow-derived stromal cells (BMSC) or apical bone-derived osteoblasts, both of which display limited repair capacities [41].

The established differences between mesodermally- and ectodermally-derived cells' *in vitro* behavior and eventual regenerative capacity can perhaps also extend to chondrocytes. Given the lack of repair capacity exhibited by articular cartilage (mesoderm), cellular-based treatments could also be a possibility if the appropriate cell source was found. Recently, cells deriving from the adult nasal septum (nasal chondrocytes, hNC) have begun to gain attention due not only to the relative ease of obtaining a septal tissue biopsy [42], but also the fact that they derive from the same astonishingly multipotent embryological segment that gives rise to the majority of the bone and cartilage of the head and face (neural crest/neuroectoderm) [43]. Human septal cartilage has long been considered the pacemaker for the growth of the face and skull, with growth potential equivalent to that of the epiphyseal growth cartilage of long bones [44]. While hNC form *in situ* a hyaline cartilage tissue biomechanically and histologically identical to that of articular cartilage [45], they also retain the capacity to

differentiate towards neuronal and osteoblastic phenotypes *in vitro* [46], suggesting that these cells can dedifferentiate in *in vitro* culture and then be pushed towards a different phenotype of interest upon appropriate morphogenic priming. However, this *in vitro* phenomenon of phenotypical plasticity has never been shown to result in a correlated *in vivo* tissue formation or repair.

A final concept associated with ectoderm/mesoderm germ layer differences resides in a group of homeobox (Hox) genes that are spatiotemporally differentially expressed during development to establish the anterio-posterio axis. As mesodermal and ectoderm tissues develop in separate regions along the anterio-posterio axis, their Hox genes status is also differentially regulated and expressed during development (*Figure 6*) [47]. Transplantation experiments in developing embryos demonstrate that the ability of implanted cells to be reprogrammed by environmental conditions is progressively restricted with the activation of Hox genes [48–51]. This principle was recently extended to Hox-negative neural crest-derived skeletal stem cells in an adult murine model, where it was shown that mesectoderm- but not mesoderm-derived skeletal stem cells can adopt the Hox-expression status of heterotopic transplantation sites, thereby leading to robust tissue repair [39]. A Hox-negative status was also proposed to reflect a higher level of self-renewal capacity in totipotent embryonic stem cells [52] and functionally distinct human stem cell populations derived from cord blood [53].

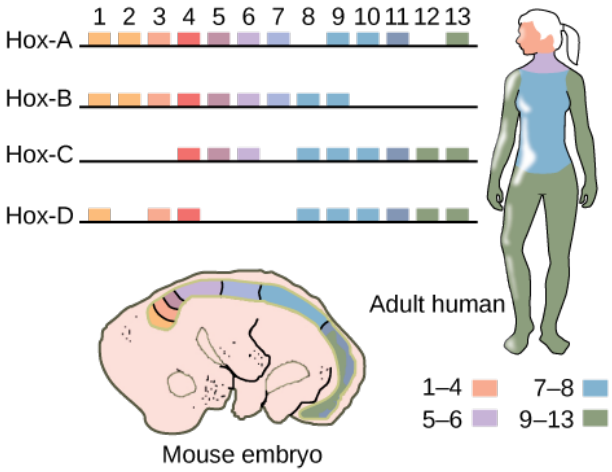


*Figure 6: Hox genes are highly conserved genes encoding transcription factors that determine the course of embryonic development in animals. In vertebrates, the genes have been duplicated into four clusters: Hox-A, Hox-B, Hox-C, and Hox-D. Genes within these clu sters are expressed in certain body segments at certain stages of development. Shown here is the*

*homology between Hox genes in mice and humans. Note how Hox gene expression, as indicated with orange, pink, blue and green shading, occurs in the same body segments in both the mouse and the human. Figure and caption source:* [54]

## 1) Tissue Engineering

"The emerging discipline of tissue engineering has the grand aim of understanding the principles of tissue growth, and applying this to produce functional replacement tissue for clinical use."[55] From lab grown organs to biomaterial tissue replacements to stem cell therapies, tissue engineering combines a vast array of scientific disciplines and much progress has been made in recent years towards real clinically-relevant treatment techniques.

### a. State-of-the-Art

Successful tissue repair is the key endpoint parameter for any tissue engineered system, whether it be cell injection, gene therapy or material-based. In order for successful tissue repair to occur, it is typically necessary to bring a bioactive signal to the defect site that would induce a repair mechanism and/or replace the damaged tissue completely. Delivery of this bioactive signal is one of the most studied subjects in regenerative medicine, with ideas ranging from bioactive materials to cell homing [56,57]. A common component of many tissue engineering strategies is that of the cell, and one of the most promising cell sources in skeletal repair is BMSC. For example, several recent early-stage clinical trials are testing the delivery of BMSCs as an intra-articular injection into the knee, but optimal dose and vehicle are yet to be established [58]. The importance of reliable and clinically relevant tissue repair approaches is evidenced in a recent European survey presenting novel cellular and engineered tissue therapies for the previous year (2011) and the results illustrate the various manners that research uses to deliver a regenerative signal to a defect site (*Table 3*) [59].

| | Cell delivery mode | | | |
|---|---|---|---|---|
| ***Indications*** | ***Intravenous*** | ***Intra-organ*** | ***Membrane/gel*** | ***3D scaffold*** |
| **Cardiovascular** | | | | |
| ***Peripheral artery disease*** | 7 | 69 | | |
| ***Cardiomyopathy*** | 1 | 52 | | |
| ***Heart failure*** | 20 | 31 | | |
| ***Myocardial ischemia*** | 11 | 84 | | |
| ***Decubitus+leg ulcers*** | | | | 58 |
| ***Other*** | 10 | 5 | | 20 |

| | | | | |
|---|---|---|---|---|
| **Musculoskeletal/rheumatological** | | | | |
| ***Bone repair (maxillofacial)*** | | | | 24 |
| ***Bone repair (orthopaedics)*** | 14 | 34 | | 12 |
| ***Osteogenesis imperfecta*** | | 2 | | 2 |
| ***Cartilage repair (orthopaedics)*** | | 47 | 120 | 80 |
| ***Muscle repair*** | | 9 | | |
| ***Tendon/ligament*** | | | 8 | |
| ***Reconstructive surgery/ tissue enhancement*** | | 268 | 118 | 6 |
| ***Scleroderma*** | 3 | | 3 | 1 |
| ***Arthritis*** | | 38 | | |
| ***Other*** | | | 13 | |
| **Neurological** | | | | |
| ***Multiple sclerosis*** | 13 | | | |
| ***Parkinson's*** | | 1 | | |
| ***Peripheral nerve regeneration (trauma)*** | | | | |
| ***Other*** | 4 | 23 | | |
| **Gastrointestinal** | | | | |
| ***Crohn's disease*** | 7 | 8 | | |
| ***Liver insufficiency*** | 3 | 1 | | |
| **Hematology/oncology** | | | | |
| ***GvHD prevention or treatment*** | 265 | | | |
| ***HSC graft enhancement*** | 55 | | | |
| **Miscellaneous** | | | | |
| ***Skin reconstruction*** | | 29 | | 67 |
| ***Cornea repair*** | | | 4 | |
| ***Diabetes*** | | 4 | | |
| ***Solid tumor*** | 14 | 24 | | |
| ***Other*** | 25 | | 21 | 12 |
| **Total** | 452 | 729 | 287 | 282 |

*3D, three-dimensional.*

*Table 3: Number of Reported Novel Cellular Therapy Treatments in Europe in 2011 Sorted by Delivery Mode. Table adapted from:* [59]

For the purposes of this thesis, I will discuss tissue engineering techniques that rely on a material as the delivery agent (scaffold) and then broadly divide these grafts into two main categories: living and extracellular matrix-based grafts. As before, the tissues of

interest remain bone and cartilage. But, overall, the common strategy applied in this thesis can be summarized in the following figure *(Figure 7)*.

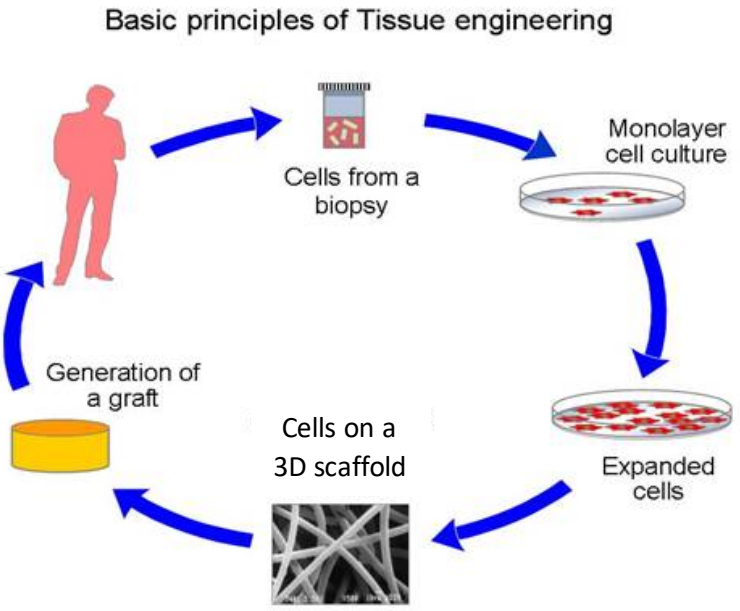


*Figure 7: Traditional tissue engineering paradigm of a closed-loop system in which cells are taken from a patient, engineerd into a graft and then reimplanted into the same patient.*

**b. "Living grafts" for tissue repair**

The concept of living grafts is based upon the combination of a scaffolding material (whether it be synthetic- or native ECM-based) with a living cell source to induce tissue repair at a defect site. Typically, this approach has relied upon internal signals (e.g. bioactive signals from the material itself [60]) or external signals (e.g. growth factors in the culture medium [61]) to push the seeded cells towards the desired differentiation status so that upon implantation, chances for engraftment and tissue repair are augmented. Indeed, the idea that a material itself could be capable of determining the differentiation status of a cell offers the possibility of "control" over an otherwise complicated biological system for regenerative medicine applications [62–64]. A logical extension to this has more often than not been the use of stem cells as seeder cells, based upon their ability to differentiate towards multiple phenotypes and therefore potentially recapitulate what occurs in vivo during development and repair of normal tissues [60,65]. There are three different types of stem cells (embryonic, induced-pluripotent

and adult stem cells), each obtained from different sources and each having different advantages and disadvantages *(Figure 8)*. Regardless the attractiveness of stem cells, the underlined disadvantages represent hurdles that must be cleared before any translation into the clinic is possible [66].

| Feature | Embryonic stem cells | Adult stem cells | Induced pluripotent stem cells |
|---|---|---|---|
| Artificial system | Yes | No | Yes |
| Pluripotent | Yes | No | Yes |
| Efficient differentiation | No | Yes | No |
| Expansion in culture | Yes | No | Yes |
| Rare cell type | No | Yes | Yes |
| Immune compatible | No | No | Yes |
| Teratoma risk | Yes | No | Yes |

*Figure 8: Current promises and limitations of stem-cell populations. Figure source:* [60]

An alternative to stem cells are somatic cells, or simply put, any other cell that is not a gamete or stem cell. For living graft production, the concept relies on the cell itself already being capable to produce an instructive ECM and/or communicate directly with the implant site for robust repair to occur. Several attractive benefits are associated with somatic cell use: 1) they are relatively easier to isolate from tissues in higher amounts, 2) they are not associated with any ethical or biological dilemmas such as embryonic tampering or teratoma formation, respectively and, 3) they are already molecularly matched to the tissue which they should repair. This last consideration helps explain what cells would be used where. For bone and cartilage applications for example, isolation of osteoblasts and chondrocytes, respectively, would allow one to create a bone or cartilage graft with cells already committed to this direction. This is precisely the topic of many studies, for both bone and cartilage, which aim to circumvent the drawbacks associated with stem cells and attempt to create autologous grafts based on somatic cells [67–70]. But, there are also certain drawbacks to the use of somatic cells that are evident in their long-term use with little to no durable treatment option having yet emerged. Damaged tissues result from either pathological processes or traumatic events. The cells that are isolated often come from these same damaged tissues and could therefore not be appropriate for a repair strategy [71]. Also, chondrocytes, upon isolation from their native tissue, must be expanded before a graft

can be prepared. During this expansion phase, the cells have been shown to dedifferentiate away from their original phenotype [72,73].

### c. "Extracellular matrix-based grafts" for tissue repair

#### i. Extracellular matrix

The extracellular matrix (ECM) is a combination of structural and functional proteins, proteoglycans, lipids and crystals that has a unique composition and physical properties for every tissue and organ in the body. Acting as a reservoir for morphogens while providing mechanical support for resident cells, ECM participates in cell communication as well as in defining the shape and stability of tissues [74]. ECM cues have been demonstrated to specifically promote cell recruitment, adhesion, migration, proliferation and differentiation in a way that reflects the functional needs and biological identity of tissues [75].

Cellular interactions with the extracellular matrix (ECM) are known to play a critical role in directing cell function and regulating development, homeostasis and repair of a variety of tissues, including bone and cartilage [76–78]. This recognition has fostered the design of biomimetic substrates for bone and cartilage regeneration aiming to provide, along with the structural support, bioactive signals mimicking some aspects of the native bone and cartilage ECM [79–82]. The hypothesis is based on the idea that such instructive elements may retain at least in part their functionality even in the absence of the living cellular component. Based on this rationale, decellularization of native and engineered tissues and organs has received increased attention in the field of regenerative medicine.

#### ii. Decelluarization

Decellularization concerns the removal of all living components from a tissue or organ with minimal disruption of the ECM component, offering the potential of an off-the-shelf and immune-compatible alternative to living grafts for tissue and organ repair (*Figure 9*). Decellularized ECM is expected to induce regenerative processes not only through specific "organomorphic" structures [83], but also by the physiological presentation of different cocktails of regulatory molecules in a mechanically suitable environment. The instructive scaffold materials derived from decellularized ECM could be activated by

living cells prior to implantation, with the assumption that ECM is capable of directing the differentiation fate of the seeded cells [61,84–86]. In an even more attractive paradigm, the decellularized ECM could be directly used to instruct resident cells towards endogenous tissue repair by leveraging principles of morphogenesis. Starting from decellularized bone as a prototype ECM graft [87], the field has received convincing proof-of-principle evidences of the latter approach for epithelial [88], musculoskeletal [89] and vascular [90] tissue regeneration, as well as for the engineering of myocardial [91], pulmonary [92], renal [93,94] and pancreatic implants [95]. More recently, thanks to the progress in guiding cell differentiation towards specific lineages, *in vitro*-engineered tissues are also being considered as a substrate for decellularization. This approach opens the perspective to the generation of large quantities of standardized, customized grafts.

Looking more specifically into osteoblastic differentiation, decellularized ECM synthesized by undifferentiated mesenchymal stromal cells (MSCs) in vitro has been shown to facilitate cell proliferation, prevent spontaneous differentiation and enhance the osteogenic capacity of freshly reseeded MSCs [96,97]. In similar studies, decellularized ECM, generated by osteogenically differentiating MSCs onto 3D porous scaffolds, enhanced and accelerated in vitro osteoblastic differentiation of newly cultured MSCs [98,99]. Decellularized bone-like ECM was also shown in rat models to enhance critical features for bone repair, namely implant vascularization and engraftment, yet no evidence of bone tissue formation could be provided [100].

A principle limiting factor of the successful translation of decellularized tissues and organs into the clinic is the decellularization method used. A variety of chemical, enzymatic and physical procedures have been developed to eliminate the cellular component of both native and engineered tissues while minimally disrupting the ECM. Protocols described in literature tend to combine several of these principal methods in order to increase the efficiency of decellularization and at the same time reduce damage to the ECM by using less destructive conditions. All of these typical methods, which have been subject of several review assays [75,101,102], can reach variable degrees of decellularization efficiency, but some problems remain common to all. First, all existing techniques rely on cell lysis. The resulting cell debris can then freely adsorb to

the remaining matrix, leading to a paradoxical increase in immunogenicity [103]. Second, existing techniques have been demonstrated to alter the ECM, leading to the degradation of some of its components [75]. Therefore, typical procedures used necessarily imply an impairment of the ECM integrity.

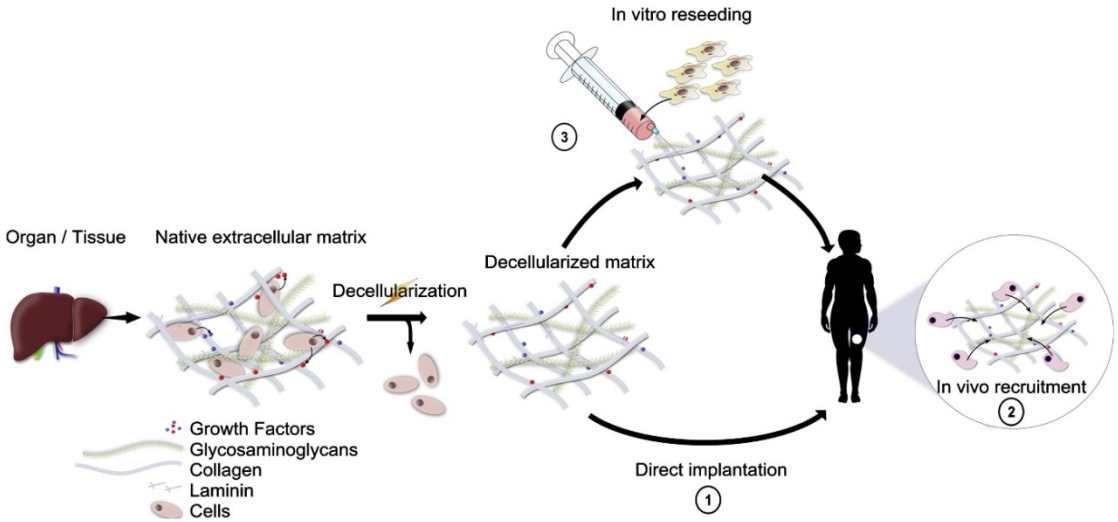


*Figure 9: Concept of tissue decellularization. Cell-free tissue can be generated by decellularization of native or engineered tissue. The resulting ECM can be directly transplanted into a patient (1), entirely relying on the capacity to instruct resident cells towards endogenous tissue repair (2). Alternatively, prior to implantation the ECM can be seeded with cells that "prime" the material (e.g., to enhance its remodeling or vascularization) and/or "get primed" toward a specific function (e.g., to proliferate or differentiate) (3). The latter implants could induce regeneration by the combined action of the seeded and recruited cells.*

### d. Standardization of graft production

One of the greatest hurdles to overcome in translating a biological into a marketable product is standardization of the production process. Unlike mechanical- or electrical-based products, the engineering of a biological system is reliant on a living source material (cells). Therein is where the problem lies: cells [104]. Regardless of the tissue source, interdonor variability is known to be so large, that using the same production process for two different donor cell sources can result in two very different grafts. It is such a problem that entire research projects concentrate on gaining a better understanding of the principles that underlie this concept as well as how to better control it. Complicating to matter, intradonor variability also contributes to production variability. Either resulting from a heterogeneous cell population or uncontrollable changes that occur within the cell source during expansion, intradonor variability often

limits graft yield. Limited source material and/or temporal changes in the living source system oblige both customized, single patient grafts and/or strongly reduced number of grafts capable of being produced. The problem of limited source material underlines another problem associated with standardization of biological graft production: current grafts are patient specific, making scaling-up of the production process impossible and dramatically increasing costs. Indeed, living grafts are typically based on the patient's own cells being first extracted, engineered into a usable graft and reimplanted into the defect site. This process intrinsically restricts the graft production process to patient-specific approach due to immune reaction considerations. This point introduces a final parameter that currently frustrates the standardization process: the support (scaffold) material associated with the biological component. Clearly not a problem for direct cellular therapy, tissue engineered grafts however must have a structure that can be manipulated by surgeons for implantation. While much work has gone and is currently going into the development of "bioactive" materials that can elicit a desired response *in vivo*, biological based materials rely on the biological component to impart bioactivity to the implant. This is an attractive alternative to material-alone options because it utilizes a "natural" biological input to evoke a regenerative response. The idea is that cells from a given tissue intrinsically know how to communicate with their own environment and can produce the signals necessary to initiate the natural regenerative process, thereby avoiding the pathological inflammation often associated with synthetic materials during biodegradation or lack of biocompatibility. Furthermore, it is poorly understood which quantities of any given bioactive factor can reliably elicit which given response.

While the material science field expands our understanding of the material/regenerative response domain, biological-based tissue engineered grafts continue to develop innovative techniques to combine biological components with support materials. Having said this (and taking into consideration the previous discussion on materials), it should be said that an ideal support material for a biological implant would therefore be one which is itself inert, biodegradable (with the biodegradation byproducts being inert as well), biocompatible and able to be handled by surgeons for implantation. For bone tissue engineering purposes, ceramics have quite often been

used in combination with cells to boost the osteogenic signals already present in the ceramic material. But, from a practical standpoint, ceramics are brittle and tend to break-up, making them inappropriate for load bearing implant sites. As the field of polymer science has evolved, several materials have made their way to the forefront because of their remarkable capacities to be shaped into almost any form needed, their biocompatibility and their capacity to support loads upon implantation. While there already exist many applications for polymers in the regenerative medicine field (artificial heart valves, breast implants and bone prostheses, for example) [105–107], no material combined with cells has yet made it to the market. As mentioned before, the main reason for this is the difficulty a biological system presents in terms of standardization.

To streamline the production of biological material-based grafts, two particular approaches were developed in this thesis: bioreactor-based graft production and extracellular matrix engineering. The first relies on a closed system in which the cell medium is forced through the cell-containing graft scaffold. Cells that are seeded onto the scaffold in the bioreactor system are then cultured under defined and controllable conditions *(Figure 10)*. This results not only in a more uniform distribution of the cells (and therefore a more uniform distribution of the produced ECM), but also a controlled environment to reduce external stimulate from affecting the culture period. Bioreactor-based graft production was developed and used in chapters 3 and 4 of the experimental work section.

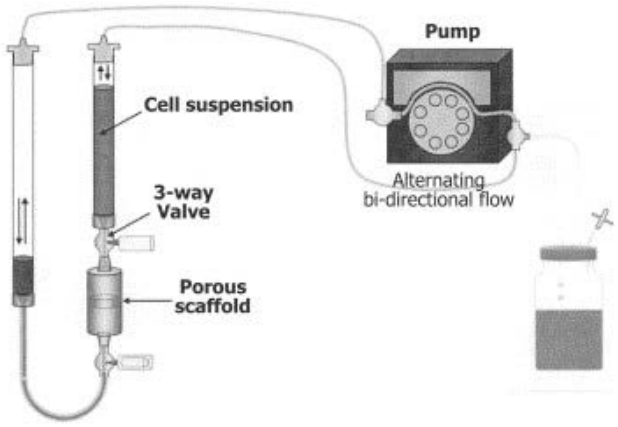

*Figure 10: 3D perfusion bioreactor system developed in the Tissue Engineering group of the ICFS. Medium and/or cell suspension is forced up and down through the porous scaffolding material, resulting in a 3D cell culture condition more reminiscent of the physiological cell environment* [108].

The second approach to aid in graft production standardization consists of the engineering of a cell-laid ECM onto the scaffolding material within the bioreactor system by using an engineered cell line. The idea consists of containing the graft production inside a bioreactor system and stimulating ECM production by the seeded cells directly onto the scaffolding material. The cells (bone marrow derived mesenchymal stromal cells in this case) are immortalized prior to graft production, allowing for a standardized cell source that is capable of producing and osteogenic ECM consistently in both quantity and quality. Both approaches are treated in more detail in the experimental work section.

**2) Aims of this thesis**

Living and/or biological material-derived grafts for regenerative medicine purposes would benefit greatly if: 1) an appropriate cell source for site-specific graft production were used and, 2) if the production process of individual, biological material-based grafts could be standardized to reduce variability. This thesis addresses possible solutions for biological-based graft materials to better incorporate into an appropriate implant environment and explores possible modes to standardize the production of these grafts. Four chapters are included in the experimental work section:

Chapter 1 focuses on a novel cell source for cartilage tissue engineering (nasal septum-derived chondrocytes). This study hypothesizes that these cells, as compared to articular chondrocytes, are more plastic in nature and maintain a self-renewal capacity. These phenomena are linked to a specific genetic expression profile associated with these cells (Hox genes), due to their unique embryological origin (neuroetodermal). The cells are further characterized for their various differentiation capacities (chondrogenic, osteogenic and adipogenic) and then used to demonstrate their regenerative capacities in both small and large animal models.

Chapter 2 extends the findings from the previous study by testing nasal chondrocytes' osteogenic capacity. We assessed the capacity of adult human nasal septum-derived

chondrocytes, appropriately primed *in vitro* through hypertrophic and osteoblastic differentiation, to form bone tissue *in vivo*. We first cultured hNC at multiclonal and clonal levels under osteoblastic differentiation conditions to both determine the extent of heterogeneity of the whole population and to test their *in vitro* osteogenic potential. Exploiting both subcutaneous and orthotopic cranial *in vivo* environments, we next assessed whether human nasal chondrocytes could be phenotypically converted to osteoblasts and actively participate in the formation of frank bone tissue. The availability of a craniofacial-derived somatic cell source capable of active participation in homotopic bone repair without pre-implantation genetic manipulation would provide a significant and clinically relevant advancement in the field of craniofacial bone repair.

Chapter 3 represents a preliminary study to test the feasibility of using a 3D perfusion bioreactor system in the development of streamlined and standardized approach to graft production. We decorated tailored synthetic substrates with decellularized ECM, in order to generate bone substitute materials with enhanced biological functionality. The developed hybrid ECM-polymer materials were shown to regulate cell osteogenic commitment while maintaining a progenitor cell pool. From this, we propose the use of bioreactors could streamline the manufacturing process and provide standardized, clinically compliant and cost-effective products. Furthermore, polymeric scaffolds decorated with decellularized matrices can also be used as models of engineered niches physiologically presenting customized signals to cells.

Chapter 4 extends the work presented in chapter 3 to include a novel, non-invasive decellularization technique to the bioreactor graft production process. Aiming at avoiding the side effects inherent to current decellularization strategies (e.g. latent immunogenicity and ECM alteration), we propose here an alternative approach to tissue decellularization based on the controlled activation of programmed cell death. The use of apoptosis as decellularization technique goes beyond the generation of grafts with enhanced performance. The concept would also offer the unprecedented possibility to investigate the properties of decellularized but theoretically intact ECM and (by correlating an observed regenerative capacity with a specific composition) to identify a set of cues critical to elicit certain functions.

## 3) References


1. Grassel, S. & Ahmed, N. Influence of cellular microenvironment and paracrine signals on chondrogenic differentiation. *Front. Biosci.* **12,** 4946–56 (2007).

2. Gimble, J. M., Robinson, C. E., Wu, X. & Kelly, K. A. The function of adipocytes in the bone marrow stroma: an update. *Bone* **19,** 421–8 (1996).

3. Martin, I. *et al.* Non-adherent mesenchymal progenitors from adipose tissue stromal vascular fraction. *Tissue Eng. Part A* (2013). doi:10.1089/ten.TEA.2013.0273

4. Rougier, F., Dupuis, F. & Denizot, Y. Human bone marrow fibroblasts--an overview of their characterization, proliferation and inflammatory mediator production. *Hematol. Cell Ther.* **38,** 241–6 (1996).

5. Dzierzak, E. & Speck, N. A. Of lineage and legacy: the development of mammalian hematopoietic stem cells. *Nat. Immunol.* **9,** 129–36 (2008).

6. Gerhardt, H. & Betsholtz, C. Endothelial-pericyte interactions in angiogenesis. *Cell Tissue Res.* **314,** 15–23 (2003).

7. Shapiro, F. Bone development and its relation to fracture repair. The role of mesenchymal osteoblasts and surface osteoblasts. *Eur. Cell. Mater.* **15,** 53–76 (2008).

8. Page-McCaw, A., Ewald, A. J. & Werb, Z. Matrix metalloproteinases and the regulation of tissue remodelling. *Nat. Rev. Mol. Cell Biol.* **8,** 221–33 (2007).

9. Kronenberg, H. M. Developmental regulation of the growth plate. *Nature* **423,** 332–6 (2003).

10. Schmid, T. M. & Linsenmayer, T. F. Immunohistochemical localization of short chain cartilage collagen (type X) in avian tissues. *J. Cell Biol.* **100,** 598–605 (1985).

11. Alini, M., Marriott, A., Chen, T., Abe, S. & Poole, A. R. A novel angiogenic molecule produced at the time of chondrocyte hypertrophy during endochondral bone formation. *Dev. Biol.* **176,** 124–32 (1996).

12. Gerber, H. P. *et al.* VEGF couples hypertrophic cartilage remodeling, ossification and angiogenesis during endochondral bone formation. *Nat. Med.* **5,** 623–8 (1999).

13. Harper, J. & Klagsbrun, M. Cartilage to bone--angiogenesis leads the way. *Nat. Med.* **5,** 617–8 (1999).

14. Deckers, M. M. *et al.* Expression of vascular endothelial growth factors and their receptors during osteoblast differentiation. *Endocrinology* **141,** 1667–74 (2000).

15. Dai, J. & Rabie, A. B. M. VEGF: an essential mediator of both angiogenesis and endochondral ossification. *J. Dent. Res.* **86,** 937–50 (2007).

16. Endochondral ossification. at <http://www.highlands.edu/academics/divisions/scipe/biology/faculty/harnden/2121/notes/skeletal.htm>

17. Yang, Y. Skeletal morphogenesis during embryonic development. *Crit. Rev. Eukaryot. Gene Expr.* **19,** 197–218 (2009).

18. Helms, J. A. & Schneider, R. A. Cranial skeletal biology. *Nature* **423,** 326–31 (2003).

19. Noden, D. M. Origins and patterning of craniofacial mesenchymal tissues. *J. Craniofac. Genet. Dev. Biol. Suppl.* **2,** 15–31 (1986).

20. Abzhanov, A., Rodda, S. J., McMahon, A. P. & Tabin, C. J. Regulation of skeletogenic differentiation in cranial dermal bone. *Development* **134,** 3133–44 (2007).

21. Intramembranous ossification. at <www.studyblue.com>

22. Long, F. Building strong bones: molecular regulation of the osteoblast lineage. *Nat. Rev. Mol. Cell Biol.* **13,** 27–38 (2012).

23. Vortkamp, A. *et al.* Regulation of rate of cartilage differentiation by Indian hedgehog and PTH-related protein. *Science* **273,** 613–22 (1996).

24. Schroeder, T. M., Jensen, E. D. & Westendorf, J. J. Runx2: a master organizer of gene transcription in developing and maturing osteoblasts. *Birth Defects Res. C. Embryo Today* **75,** 213–25 (2005).

25. Cao, Y. *et al.* Osterix, a transcription factor for osteoblast differentiation, mediates antitumor activity in murine osteosarcoma. *Cancer Res.* **65,** 1124–8 (2005).

26. Shen, G. The role of type X collagen in facilitating and regulating endochondral ossification of articular cartilage. *Orthod. Craniofac. Res.* **8,** 11–7 (2005).

27. Wikipedia. Collagen type II. at <http://en.wikipedia.org/wiki/Type-II_collagen>

28. Fisher, L. W., Whitson, S. W., Avioli, L. V & Termine, J. D. Matrix sialoprotein of developing bone. *J. Biol. Chem.* **258,** 12723–7 (1983).

29. Hunter, G. K. & Goldberg, H. A. Nucleation of hydroxyapatite by bone sialoprotein. *Proc. Natl. Acad. Sci. U. S. A.* **90,** 8562–5 (1993).

30. Leeman, M. F., Curran, S. & Murray, G. I. The structure, regulation, and function of human matrix metalloproteinase-13. *Crit. Rev. Biochem. Mol. Biol.* **37,** 149–66 (2002).

31. Urist, M. R. Bone: formation by autoinduction. *Science* **150,** 893–9 (1965).

32. Harada, S. & Rodan, G. A. Control of osteoblast function and regulation of bone mass. *Nature* **423,** 349–55 (2003).

33. Ducy, P., Zhang, R., Geoffroy, V., Ridall, A. L. & Karsenty, G. Osf2/Cbfa1: a transcriptional activator of osteoblast differentiation. *Cell* **89,** 747–754 (1997).

34. SIFFERT, R. S. The role of alkaline phosphatase in osteogenesis. *J. Exp. Med.* **93,** 415–26 (1951).

35. Mastbergen, S. C., Saris, D. B. F. & Lafeber, F. P. J. G. Functional articular cartilage repair: here, near, or is the best approach not yet clear? *Nat. Rev. Rheumatol.* **9,** 277–90 (2013).

36. Matsubara, T. *et al.* Alveolar bone marrow as a cell source for regenerative medicine: differences between alveolar and iliac bone marrow stromal cells. *J. Bone Miner. Res.* **20,** 399–409 (2005).

37. Akintoye, S. O. *et al.* Skeletal site-specific characterization of orofacial and iliac crest human bone marrow stromal cells in same individuals. *Bone* **38,** 758–68 (2006).

38. Reichert, J. C., Gohlke, J., Friis, T. E., Quent, V. M. C. & Hutmacher, D. W. Mesodermal and neural crest derived ovine tibial and mandibular osteoblasts display distinct molecular differences. *Gene* **525,** 99–106 (2013).

39. Leucht, P. *et al.* Embryonic origin and Hox status determine progenitor cell fate during adult bone regeneration. *Development* **135,** 2845–54 (2008).

40. Stockmann, P. *et al.* Guided bone regeneration in pig calvarial bone defects using autologous mesenchymal stem/progenitor cells - a comparison of different tissue sources. *J. Craniomaxillofac. Surg.* **40,** 310–20 (2012).

41. Pagni, G. *et al.* Bone repair cells for craniofacial regeneration. *Adv. Drug Deliv. Rev.* **64,** 1310–9 (2012).

42. SIEGEL, N. S., GLIKLICH, R. E., TAGHIZADEH, F. & CHANG, Y. Outcomes of septoplasty☆☆☆. *Otolaryngol.-Head Neck Surg.* **122,** 228–232 (2000).

43. Achilleos, A. & Trainor, P. A. Neural crest stem cells: discovery, properties and potential for therapy. *Cell Res.* **22,** 288–304 (2012).

44. Hall, B. K. & Precious, D. S. Cleft lip, nose, and palate: the nasal septum as the pacemaker for midfacial growth. *Oral Surg. Oral Med. Oral Pathol. Oral Radiol.* **115,** 442–7 (2013).

45. Candrian, C. *et al.* Engineered cartilage generated by nasal chondrocytes is responsive to physical forces resembling joint loading. *Arthritis Rheum.* **58,** 197–208 (2008).

46. Delorme, B. *et al.* The human nose harbors a niche of olfactory ectomesenchymal stem cells displaying neurogenic and osteogenic properties. *Stem Cells Dev.* **19,** 853–66 (2010).

47. Pearson, J. C., Lemons, D. & McGinnis, W. Modulating Hox gene functions during animal body patterning. *Nat. Rev. Genet.* **6,** 893–904 (2005).

48. Couly, G., Grapin-Botton, A., Coltey, P., Ruhin, B. & Le Douarin, N. M. Determination of the identity of the derivatives of the cephalic neural crest: incompatibility between Hox gene expression and lower jaw development. *Development* **125,** 3445–59 (1998).

49. Grapin-Botton, A., Bonnin, M. A., McNaughton, L. A., Krumlauf, R. & Le Douarin, N. M. Plasticity of transposed rhombomeres: Hox gene induction is correlated with phenotypic modifications. *Development* **121,** 2707–21 (1995).

50. Itasaki, N., Sharpe, J., Morrison, A. & Krumlauf, R. Reprogramming Hox expression in the vertebrate hindbrain: influence of paraxial mesoderm and rhombomere transposition. *Neuron* **16,** 487–500 (1996).

51. Le Douarin, N. M., Creuzet, S., Couly, G. & Dupin, E. Neural crest cell plasticity and its limits. *Development* **131,** 4637–50 (2004).

52. Lee, T. I. *et al.* Control of developmental regulators by Polycomb in human embryonic stem cells. *Cell* **125,** 301–13 (2006).

53. Liedtke, S. *et al.* The HOX Code as a "biological fingerprint" to distinguish functionally distinct stem cell populations derived from cord blood. *Stem Cell Res.* **5,** 40–50 (2010).

54. Features of the Animal Kingdom. at <http://cnx.org/content/m44655/1.8/>

55. MacArthur, B. D. & Oreffo, R. O. C. Bridging the gap. *Nature* **433,** 19 (2005).

56. Sarkar, D. *et al.* Engineered cell homing. *Blood* **118,** e184–91 (2011).

57. Renth, A. N. & Detamore, M. S. Leveraging "raw materials" as building blocks and bioactive signals in regenerative medicine. *Tissue Eng. Part B. Rev.* **18,** 341–62 (2012).

58. Barry, F. & Murphy, M. Mesenchymal stem cells in joint disease and repair. *Nat. Rev. Rheumatol.* **9,** 584–94 (2013).

59. Martin, I. *et al.* The Survey on Cellular and Engineered Tissue Therapies in Europe in 2011. *Tissue Eng. Part A* (2013). doi:10.1089/ten.TEA.2013.0372

60. Lutolf, M. P., Gilbert, P. M. & Blau, H. M. Designing materials to direct stem-cell fate. *Nature* **462,** 433–41 (2009).

61. Sadr, N. *et al.* Enhancing the biological performance of synthetic polymeric materials by decoration with engineered, decellularized extracellular matrix. *Biomaterials* **33,** 5085–93 (2012).

62. Engler, A. J., Sen, S., Sweeney, H. L. & Discher, D. E. Matrix Elasticity Directs Stem Cell Lineage Specification. *Cell* **126,** 677–689 (2006).

63. Chai, C. & Leong, K. W. Biomaterials Approach to Expand and Direct Differentiation of Stem Cells. *Mol. Ther.* **15,** 467–480 (2007).

64. Pashuck, E. T. & Stevens, M. M. Designing Regenerative Biomaterial Therapies for the Clinic. *Sci. Transl. Med.* **4,** 1–12 (2012).

65. Scotti, C. *et al.* Recapitulation of endochondral bone formation using human adult mesenchymal stem cells as a paradigm for developmental engineering. *Proc. Natl. Acad. Sci. U. S. A.* **107,** 7251–7256 (2010).

66. Daley, G. Q. & Scadden, D. T. Essay Prospects for Stem Cell-Based Therapy. *Cell* **132,** 544–548 (2008).

67. Khan, I. M., Gilbert, S. J., Singhrao, S. K., Duance, V. C. & Archer, C. W. CARTILAGE INTEGRATION: EVALUATION OF THE REASONS FOR FAILURE OF INTEGRATION DURING CARTILAGE REPAIR. A REVIEW. *Eur. Cell. Mater.* **16,** 26–39 (2008).

68. Mu, M. E. Articular cartilage repair: are the intrinsic biological constraints undermining this process insuperable? *Osteoarthritis Cartilage* **1,** 15–28 (1999).

69. Behery, O. A., Harris, M. P. H. J. D., Flanigan, D. C., Karnes, J. M. & Siston, R. A. Factors Influencing the Outcome of Autologous Chondrocyte Implantation: A Systematic Review. *J. Knee Surg.* **1,** (2013).

70. Kwan, M. D., Slater, B. J., Wan, D. C. & Longaker, M. T. Cell-based therapies for skeletal regenerative medicine. *Hum. Mol. Genet.* **17,** 93–98 (2008).

71. Candrian, C. *et al.* Are ankle chondrocytes from damaged fragments a suitable cell source for cartilage repair? *Osteoarthritis Cartilage* **18,** 1067–76 (2010).

72. Barbero, A., Ploegert, S., Heberer, M. & Martin, I. Plasticity of clonal populations of dedifferentiated adult human articular chondrocytes. *Arthritis Rheum.* **48,** 1315–1325 (2003).

73. Jakob, M. *et al.* Specific growth factors during the expansion and redifferentiation of adult human articular chondrocytes enhance chondrogenesis and cartilaginous tissue formation in vitro. *J. Cell. Biochem.* **81,** 368–377 (2001).

74. Song, J. J. & Ott, H. C. Organ engineering based on decellularized matrix scaffolds. *Trends Mol. Med.* **17,** 424–32 (2011).

75. Crapo, P. M., Gilbert, T. W. & Badylak, S. F. An overview of tissue and whole organ decellularization processes. *Biomaterials* **32,** 3233–43 (2011).

76. Rosso, F., Giordano, A., Barbarisi, M. & Barbarisi, A. From cell-ECM interactions to tissue engineering. *J. Cell. Physiol.* **199,** 174–80 (2004).

77. Allori, A. C., Sailon, A. M. & Warren, S. M. Biological basis of bone formation, remodeling, and repair-part II: extracellular matrix. *Tissue Eng. Part B. Rev.* **14,** 275–83 (2008).

78. Demoor, M. *et al.* Deciphering chondrocyte behaviour in matrix-induced autologous chondrocyte implantation to undergo accurate cartilage repair with hyaline matrix. *Pathol. Biol. (Paris).* **60,** 199–207 (2012).

79. Owen, S. C. & Shoichet, M. S. Design of three-dimensional biomimetic scaffolds. *J. Biomed. Mater. Res. A* **94,** 1321–31 (2010).

80. Bueno, E. M. & Glowacki, J. Cell-free and cell-based approaches for bone regeneration. *Nat. Rev. Rheumatol.* **5,** 685–97 (2009).

81. Nguyen, L. H., Kudva, A. K., Guckert, N. L., Linse, K. D. & Roy, K. Unique biomaterial compositions direct bone marrow stem cells into specific chondrocytic phenotypes corresponding to the various zones of articular cartilage. *Biomaterials* **32,** 1327–38 (2011).

82. Klein, T. J. *et al.* Strategies for zonal cartilage repair using hydrogels. *Macromol. Biosci.* **9,** 1049–58 (2009).

83. Toni, R. *et al.* Ex situ bioengineering of bioartificial endocrine glands: A new frontier in regenerative medicine of soft tissue organs. *Ann. Anat. - Anat. Anzeiger* **193,** 381–394 (2011).

84. Decaris, M. L., Binder, B. Y., Soicher, M. A., Bhat, A. & Leach, J. K. Cell-Derived Matrix Coatings for Polymeric Scaffolds. *Tissue Eng. Part A* **18,** 2148–2157 (2012).

85. Evan, G. Getting One's Fak Straight. *Dev. Cell* **19,** 185–186 (2010).

86. Kang, Y., Kim, S., Bishop, J., Khademhosseini, A. & Yang, Y. The osteogenic differentiation of human bone marrow MSCs on HUVEC-derived ECM and β-TCP scaffold. *Biomaterials* **33,** 6998–7007 (2012).

87. FREIBERG, R. A. & RAY, R. D. STUDIES OF DEVITALIZED BONE IMPLANTS. *Arch. Surg.* **89,** 417–27 (1964).

88. Doillon, C. J. Porous collagen sponge wound dressings: in vivo and in vitro studies. *J. Biomater. Appl.* **2,** 562–78 (1988).

89. Turner, N. J. & Badylak, S. F. Biologic scaffolds for musculotendinous tissue repair. *Eur. Cell. Mater.* **25,** 130–43 (2013).

90. Quint, C. *et al.* Decellularized tissue-engineered blood vessel as an arterial conduit. *Proc. Natl. Acad. Sci.* **108,** 9214–9219 (2011).

91. Ott, H. C. *et al.* Perfusion-decellularized matrix: using nature's platform to engineer a bioartificial heart. *Nat. Med.* **14,** 213–21 (2008).

92. Petersen, T. H. *et al.* Tissue-engineered lungs for in vivo implantation. *Science* **329,** 538–41 (2010).

93. Song, J. J. *et al.* Regeneration and experimental orthotopic transplantation of a bioengineered kidney. *Nat. Med.* **19,** 646–51 (2013).

94. Humes, H. D., Buffington, D. A., MacKay, S. M., Funke, A. J. & Weitzel, W. F. Replacement of renal function in uremic animals with a tissue-engineered kidney. *Nat. Biotechnol.* **17,** 451–5 (1999).

95. Daoud, J., Rosenberg, L. & Tabrizian, M. Pancreatic islet culture and preservation strategies: advances, challenges, and future outlook. *Cell Transplant.* **19,** 1523–35 (2010).

96. Chen, X.-D., Dusevich, V., Feng, J. Q., Manolagas, S. C. & Jilka, R. L. Extracellular matrix made by bone marrow cells facilitates expansion of marrow-derived mesenchymal progenitor cells and prevents their differentiation into osteoblasts. *J. Bone Miner. Res.* **22,** 1943–56 (2007).

97. Pei, M., He, F. & Kish, V. L. Expansion on extracellular matrix deposited by human bone marrow stromal cells facilitates stem cell proliferation and tissue-specific lineage potential. *Tissue Eng. Part A* **17,** 3067–76 (2011).

98. Datta, N., Holtorf, H. L., Sikavitsas, V. I., Jansen, J. A. & Mikos, A. G. Effect of bone extracellular matrix synthesized in vitro on the osteoblastic differentiation of marrow stromal cells. *Biomaterials* **26,** 971–7 (2005).

99. Datta, N. *et al.* In vitro generated extracellular matrix and fluid shear stress synergistically enhance 3D osteoblastic differentiation. *Proc. Natl. Acad. Sci. U. S. A.* **103,** 2488–93 (2006).

100. Pham, Q. P. *et al.* Analysis of the osteoinductive capacity and angiogenicity of an in vitro generated extracellular matrix. *J. Biomed. Mater. Res. A* **88,** 295–303 (2009).

101. Lu, H., Hoshiba, T., Kawazoe, N. & Chen, G. Comparison of decellularization techniques for preparation of extracellular matrix scaffolds derived from three-dimensional cell culture. *J. Biomed. Mater. Res. A* **100,** 2507–16 (2012).

102. He, M. & Callanan, A. Comparison of Methods for Whole-Organ Decellularization in Tissue Engineering of Bioartificial Organs. *Tissue Eng. Part B Rev.* **19,** 194–208 (2013).

103. Böer, U. *et al.* The effect of detergent-based decellularization procedures on cellular proteins and immunogenicity in equine carotid artery grafts. *Biomaterials* **32,** 9730–7 (2011).

104. Langer, R. Tissue engineering: perspectives, challenges, and future directions. *Tissue Eng.* **13,** 1–2 (2007).

105. Pibarot, P. & Dumesnil, J. G. Prosthetic heart valves: selection of the optimal prosthesis and long-term management. *Circulation* **119,** 1034–48 (2009).

106. Behairy, Y. & Jasty, M. Bone grafts and bone substitutes in hip and knee surgery. *Orthop. Clin. North Am.* **30,** 661–71 (1999).

107. Helyar, V., Burke, C. & McWilliams, S. The ruptured PIP breast implant. *Clin. Radiol.* **68,** 845–50 (2013).

108. Wendt, D., Jakob, M. & Martin, I. Bioreactor-based engineering of osteochondral grafts: from model systems to tissue manufacturing. *J. Biosci. Bioeng.* **100,** 489–94 (2005).

109. Development of New Therapeutic Drugs and Biologics for Rare Diseases. (2010).

110. Langer, R. Perspectives and challenges in tissue engineering and regenerative medicine. *Adv. Mater.* **21,** 3235–6 (2009).

111. Gonfiotti, A. *et al.* The first tissue-engineered airway transplantation: 5-year follow-up results. *Lancet* **383,** 238–44 (2014).

112. Raya-Rivera, A. *et al.* Tissue-engineered autologous urethras for patients who need reconstruction: an observational study. *Lancet* **377,** 1175–82 (2011).

113. Raya-Rivera, A. M. *et al.* Tissue-engineered autologous vaginal organs in patients: a pilot cohort study. *Lancet* (2014). doi:10.1016/S0140-6736(14)60542-0

114. Maher, B. Tissue engineering: How to build a heart. *Nature* **499,** 20–2 (2013).

115. Bourgine, P. *et al.* Combination of immortalization and inducible death strategies to generate a human mesenchymal stromal cell line with controlled survival. *Stem Cell Res.* **12,** 584–98 (2014).

116. Bourgine, P. E., Pippenger, B. E., Todorov, A., Tchang, L. & Martin, I. Tissue decellularization by activation of programmed cell death. *Biomaterials* **34,** 6099–108 (2013).

# II. EXPERIMENTAL WORK

*Science Translational Medicine 2014 Aug 27;6(251):251ra119.*
*doi: 10.1126/scitranslmed.3009688*

# Adult human neural crest–derived cells for articular cartilage repair

Karoliina Pelttari[a], Benjamin E. Pippenger[a], Sandra Feliciano[a], Celeste Scotti[b], Pierre Mainil-Varlet[c], Alfredo Procino[d], Marcel Jakob[a], Clemente Cillo[d], Andrea Barbero[a], Ivan Martin[a]*

[a]Departments of Surgery and of Biomedicine, University Hospital Basel, Hebelstrasse 20, 4031 Basel, Switzerland.

[b]I.R.C.C.S. Istituto Ortopedico Galeazzi, Via R. Galeazzi 4, 20161 Milano, Italy.

[c]AGINKO Research AG, Route de l'ancienne Papeterie PO Box 30, 1723 Marly, Switzerland.

[d]Facolta' di Medicina e Chirurgia, Via S. Pansini 5, 80131 Napoli, Italy.

*Correspondence to: Prof. Ivan Martin
ICFS, University Hospital Basel
Hebelstrasse 20, ZLF, Room 405
4031 Basel, Switzerland
Phone: + 41 61 265 2384; fax: + 41 61 265 3990
E-mail: Ivan.Martin@usb.ch

## ABSTRACT

In embryonic models and stem-cell systems, mesenchymal cells derived from the neural crest ('mesectoderm') can be distinguished from mesoderm-derived cells by their 'Hox-negative' profile, a phenotype associated with enhanced capacity of tissue regeneration (1,2,3,4). We investigated whether developmental origin and Hox-negativity are related with self-renewal and environmental plasticity also in differentiated cells from adult individuals. Using hyaline cartilage as a model we show that adult human mesectoderm-derived nasal chondrocytes (NC) can be constitutively distinguished from mesoderm-derived articular chondrocytes (AC) by lack of expression of specific HOX genes (e.g., HOXC4, HOXD8). In contrast to AC, serially cloned NC can continuously revert from differentiated to de-differentiated states, conserving the ability to form cartilage tissue in vitro and in vivo. NC can also be reprogrammed to stably express HOX genes typical of AC upon implantation into articular cartilage defects, directly contributing to their repair. Our findings identify previously unrecognized regenerative properties of HOX negative differentiated mesectoderm cells in adults and imply a role for NC in the yet unsolved clinical challenge of articular cartilage repair.

REGENERATIVE MEDICINE

# Adult human neural crest–derived cells for articular cartilage repair

Karoliina Pelttari,[1] Benjamin Pippenger,[1] Marcus Mumme,[1] Sandra Feliciano,[1] Celeste Scotti,[2] Pierre Mainil-Varlet,[3] Alfredo Procino,[4] Brigitte von Rechenberg,[5] Thomas Schwamborn,[6] Marcel Jakob,[1] Clemente Cillo,[4] Andrea Barbero,[1] Ivan Martin[1]*

**In embryonic models and stem cell systems, mesenchymal cells derived from the neuroectoderm can be distinguished from mesoderm-derived cells by their Hox-negative profile—a phenotype associated with enhanced capacity of tissue regeneration. We investigated whether developmental origin and Hox negativity correlated with self-renewal and environmental plasticity also in differentiated cells from adults. Using hyaline cartilage as a model, we showed that adult human neuroectoderm-derived nasal chondrocytes (NCs) can be constitutively distinguished from mesoderm-derived articular chondrocytes (ACs) by lack of expression of specific *HOX* genes, including *HOXC4* and *HOXD8*. In contrast to ACs, serially cloned NCs could be continuously reverted from differentiated to dedifferentiated states, conserving the ability to form cartilage tissue in vitro and in vivo. NCs could also be reprogrammed to stably express *Hox* genes typical of ACs upon implantation into goat articular cartilage defects, directly contributing to cartilage repair. Our findings identify previously unrecognized regenerative properties of *HOX*-negative differentiated neuroectoderm cells in adults, implying a role for NCs in the unmet clinical challenge of articular cartilage repair. An ongoing phase 1 clinical trial preliminarily indicated the safety and feasibility of autologous NC–based engineered tissues for the treatment of traumatic articular cartilage lesions.**

## INTRODUCTION

Although the first clinical report of cell-based cartilage repair by autologous chondrocyte transplantation now dates back more than 20 years (*1*), the predictable and durable regeneration of articular cartilage remains an unmet clinical need. Currently available cell-based techniques to treat hyaline articular cartilage mainly consist in the recruitment of mesenchymal stem/stromal cells (MSCs) from the subchondral bone (microfracturing) or in the grafting of ex vivo–expanded autologous articular chondrocytes (ACs). These techniques typically result in an unpredictable long-term outcome (*2*), likely related to the phenotypic instability of the cartilage tissue formed by MSCs (*3*) or the large inter-donor variability in the cartilage-forming capacity of ACs (*4*). To bypass the aforementioned critical issues, a more reproducibly chondrogenic cell source should be identified.

As compared to ACs, nasal chondrocytes (NCs) were shown to have a higher capacity to generate functional cartilaginous tissues, with lower donor-related dependency (*5*–*7*). NCs could respond similarly to ACs to physical forces resembling joint loading (*8*) and could efficiently recover after exposure to inflammatory factors typical of an injured joint (*9*). Moreover, NCs are easily accessible from a small biopsy of the nasal septum, with minimal donor site morbidity. NCs and ACs derive from tissues sharing a common hyaline nature and produce a similar pattern of extracellular matrix molecules. However, NCs and ACs originate from different germ layers, and the developmental or genetic compatibility of NCs with an articular cartilage environment has never been addressed.

*Hox* genes play a key role during development by encoding for transcription factors that control the three-dimensional (3D) body plan organization according to the rules of spatiotemporal colinearity (*10*, *11*). Transplantation experiments in developing quail-chick embryos have demonstrated that the ability of implanted cells to be reprogrammed by environmental conditions is progressively restricted with the activation of *Hox* genes (*12*–*15*). In particular, it was demonstrated that *Hox*-positive neural crest–derived cells from posterior rhombomeres could not substitute for *Hox*-negative cells after transplantation into anterior domains, but by contrast, *Hox*-negative neural crest–derived cells could replace *Hox*-positive cells, leading to normal tissue formation (*12*). The terms "*Hox*-positive" and "*Hox*-negative" are here used for cells respectively expressing or not expressing defined sets of *Hox* genes. This principle was recently extended to an adult murine model, where it was shown that *Hox*-negative neuroectoderm-derived skeletal stem cells, but not *Hox*-positive mesoderm-derived skeletal stem cells, can adopt the *Hox* expression status of heterotopic transplantation sites, thereby leading to robust tissue repair (*16*). A *HOX*-negative status was also proposed to reflect a higher level of self-renewal capacity in totipotent human embryonic stem cells (*17*) and functionally distinct human stem cell populations derived from cord blood (*18*).

Here, using hyaline cartilage as a model, we first investigated whether *HOX* genes are differentially expressed in human NCs (neuroectodermal, and more specifically neural crest, origin) and ACs (mesoderm origin). We then assessed whether developmental origin and *HOX* negativity remain associated with self-renewal capacity and environmental plasticity in differentiated cells from adult tissues. Finally, we tested the compatibility of NC-based engineered tissues for articular cartilage repair by implantation in experimental defects in goats and by acquiring early observations in a pilot clinical trial. We report a previously unexpected capacity of *HOX*-negative, human adult NCs to self-renew in

[1]Departments of Surgery and of Biomedicine, University Hospital Basel, University of Basel, Hebelstrasse 20, 4031 Basel, Switzerland. [2]Istituto Di Ricovero e Cura a Carattere Scientifico (IRCCS) Istituto Ortopedico Galeazzi, Via R. Galeazzi 4, 20161 Milano, Italy. [3]AGINKO Research AG, Route de l'ancienne Papeterie, P. O. Box 30, 1723 Marly, Switzerland. [4]Department of Medicine and Surgery, Federico II Medical School, Via S. Pansini 5, 80131 Napoli, Italy. [5]Musculoskeletal Research Unit, Equine Hospital, University of Zurich, Winterthurerstrasse 260, 8057 Zurich, Switzerland. [6]Cross-klinik, Bundesstrasse 1, 4009 Basel, Switzerland.
*Corresponding author. E-mail: ivan.martin@usb.ch

serial cloning assays and to be reprogrammed upon implantation in mesoderm environments by activating otherwise constitutively silent *HOX* genes. The finding that NCs can directly participate in the repair of experimental cartilage defects in goats, combined with the early observations of safety and feasibility in human, opens the clinical perspective of using nonhomotopic chondrocytes for enhanced cell-based articular cartilage repair.

## RESULTS

### *HOX* expression profile of human NCs

Comparative qualitative analysis of the whole *HOX* gene network in NCs and ACs by duplex polymerase chain reaction (PCR) showed several differentially expressed genes (Fig. 1A). Specific genes in the loci *HOXC* and *HOXD* were consistently expressed only by ACs. Quantitative reverse transcription PCR (qRT-PCR) confirmed expression of *HOXC4*, *HOXC5*, *HOXC8*, *HOXD3*, and *HOXD8* in ACs, and only at baseline or undetectable levels in NCs (Fig. 1B). The differential gene expression was observed in chondrocytes from native human cartilage and following dedifferentiation or subsequent chondrogenic redifferentiation in vitro, thus establishing a set of markers constitutively distinguishing NCs from ACs (Fig. 1B), independent of the differentiation stage. The expression pattern of the identified *HOX* genes was assessed in other cartilage types from neuroectodermal (ear cartilage) and mesodermal (ankle cartilage) germ layers (Fig. 1C), confirming a consistent association with the tissue developmental origin. The findings thus outline a general possibility to distinguish neuroectoderm-from mesoderm-derived chondrocytes.

Comparison of NCs and ACs with mesenchymal stromal/stem cells from human bone marrow (BMSCs, mesoderm-derived) or from human dental pulp (DPCs, neuroectoderm-derived) indicated that the *HOX* expression pattern is more similar in cells of a common embryologic origin (NCs and DPCs versus ACs and BMSCs) than in cells with a common phenotype (for example, cells from hyaline cartilage such as NCs and ACs versus mesenchymal progenitor cells such as DPCs and BMSCs) (fig. S1). Furthermore, chondrogenic differentiation of BMSCs did not alter the activation of *HOX* genes (fig. S1). Our data confirm that *HOX* profiles capture developmental-related molecular identity and positional memory also in adult cells (*19*). Thus, they are well suited for studying environment-driven NC plasticity following heterotopic transplantation.

### Self-renewal capacity of human NCs

We next assessed whether *HOX* expression profiles are associated with features of self-renewal, here defined [according to assays developed



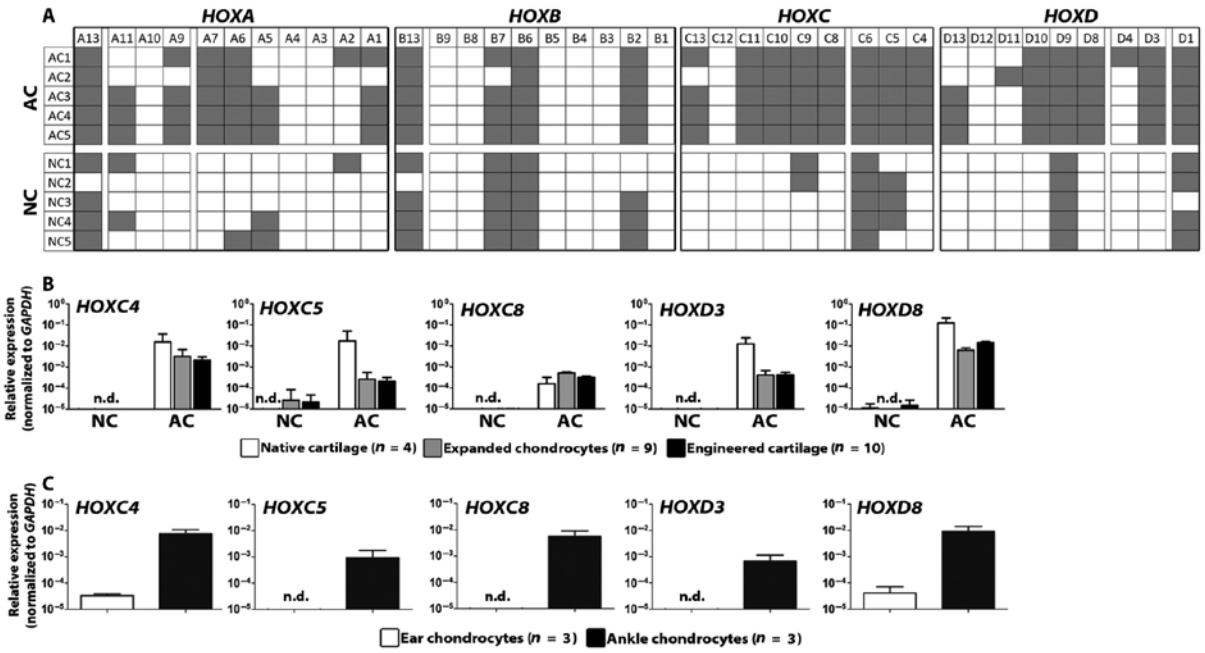


**Fig. 1. *HOX* expression profile of human NCs.** (**A**) Duplex PCR of the whole *HOX* gene network in human ACs and NCs from five donors after monolayer expansion. Actively expressed genes are depicted in gray, whereas genes whose expressions were under the limits of detection are shown in white. *HOXA*, *HOXB*, *HOXC*, and *HOXD* describe the four *HOX* clusters; each of the clusters is located on one chromosome and, together with the following number, builds up the gene name. For donors 1, 2, and 3, NCs and ACs were harvested from the same individual. (**B**) Real-time qRT-PCR analysis of *HOX* genes in ACs and NCs at different stages of differentiation. (**C**) Real-time qRT-PCR analysis of *HOX* genes in neural crest–derived ear and mesodermal ankle chondrocytes. Data in (B) and (C) were normalized to *GAPDH*. Data in (B) and (C) are means ± SD; *n* is the number of cartilage donors. All differences between cell sources in corresponding conditions were significant. For each donor, two experimental replicates were generated and analyzed; n.d., below limit of detection.

for other mesenchymal cell systems (*20*)] as the capacity to generate differentiated, functional progenies following serial cycles of cloning. Freshly isolated human NCs and ACs were clonally expanded, with associated phenotypic dedifferentiation, and subsequently redifferentiated by 3D culture in chondrogenic medium. The resulting engineered cartilaginous tissues were digested to generate new clonal strains of dedifferentiated cells (subcloning) (Fig. 2A) for ultimate assessment of their in vitro and in vivo chondrogenic ability. Compared to ACs, primary NCs contained a higher number of clonogenic cells (37% versus 21%; $P < 0.05$, Bayesian statistical modeling) (fig. S2A), and these NC-derived clones had a significantly faster proliferation rate than AC-derived clones (fig. S2B).

After the first cloning, similar percentages of NC and AC clones were capable of chondrogenic or osteogenic differentiation (Fig. 2B), as assessed by the generation of cartilaginous tissues or the deposition of mineralized matrix in vitro (fig. S2C). The percentage of AC-derived chondrogenic and osteogenic clones (40 and 30%, respectively) was in the range of the expected donor-related variability and consistent with a previous publication reporting 60% chondrogenic and 25% osteogenic clones within human AC populations (*21*). The onset of mineralization/osteogenic differentiation (fig. S2C) was associated with a 17.9 ± 3.6–fold increase (mean ± SD) of the master osteogenic transcription factor *CBFA-1* (*22*) as compared to nonmineralizing/nonosteogenic clones [$n$ = 4 clonal populations per group; $P < 0.05$ by one-way analysis of variance (ANOVA)]. The frequencies of osteochondrogenic clones (that is, populations with the ability of both osteogenic and chondrogenic differentiation) and of clones that formed cartilage in vivo were respectively 1.8- and 3.3-fold higher for NCs than for ACs (Fig. 2, B and C).

After subcloning, none of the AC strains maintained a chondrogenic capacity, whereas some NC strains formed cartilage tissues in vitro (23%) and in vivo (60%) (Fig. 2, B and C). The osteogenic differentiation capacity decreased in both NC and AC subclones compared to clones, such that the percentage of osteogenic subclones was up to fivefold lower and no osteochondrogenic subclone could be identified (Fig. 2B and fig. S3). These findings challenge the recently claimed multipotency of NCs (*23*).

### Environmental plasticity of human NCs in mice

We then investigated whether NCs display features of environmental plasticity, here defined by analogy with developmental models (*15*) as the ability to adopt the *Hox* expression profile of the recipient site. We thus implanted human NCs in the form of engineered cartilaginous



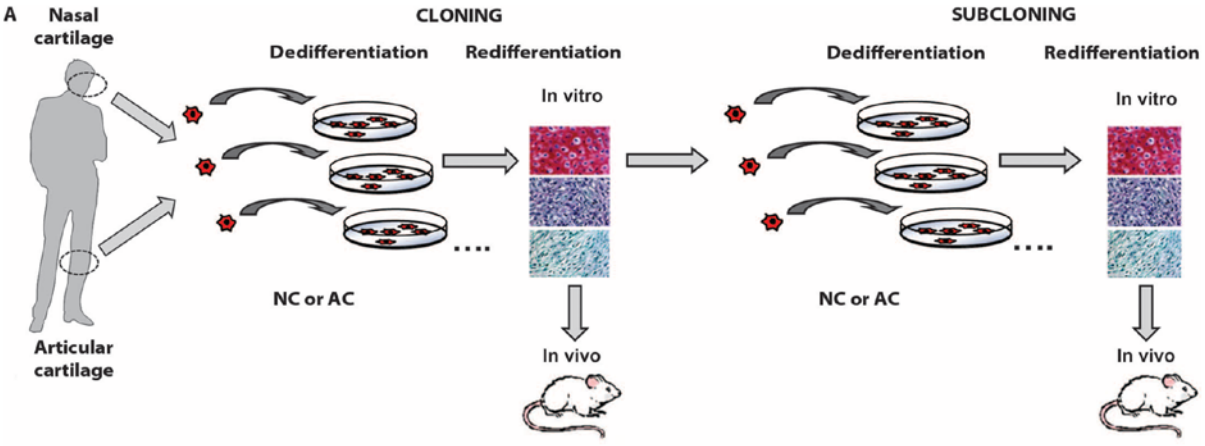


B

| | NC | | AC | |
|---|---|---|---|---|
| | Cloning | Subcloning | Cloning | Subcloning |
| Osteogenic | 29.6% (8/27) | 5.7% (2/35) | 30.0% (3/10) | 14.3% (4/28) |
| Chondrogenic | 37.0% (10/27) | 22.9% (8/35) | 40.0% (4/10) | 0.0% (0/28) |
| OC | 18.5% (5/27) | 0.0% (0/35) | 10.0% (1/10) | 0.0% (0/28) |
| Null | 14.8% (4/27) | 71.4% (25/35) | 20.0% (2/10) | 85.7% (24/28) |
| Total O (O + OC) | 48.1% (13/27) | 5.7% (2/35) | 40.0% (4/10) | 14.3% (4/28) |
| Total C (C + OC) | 55.6% (15/27) | 22.9% (8/35) | 60.0% (6/10) | 0.0% (0/28) |

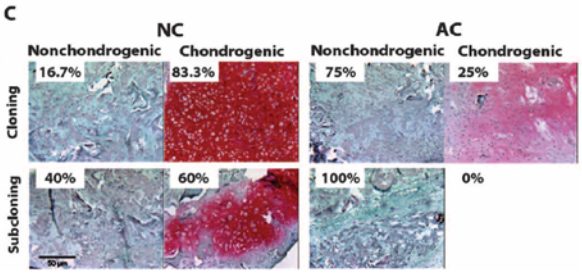


**Fig. 2. Self-renewal capacity of NCs.** (**A**) Serial clonal analysis. Cartilaginous tissue was engineered from single-cell clones derived from human nasal septum or articular cartilage (cloning) and digested for the generation of new clones (subcloning). Tests were conducted in vitro and in vivo in mice. (**B**) Summary of osteogenic (O), chondrogenic (C), and osteochondrogenic (OC) differentiation capacity of clones and subclones in vitro. (**C**) Quality of cartilage formation by NC and AC clones and subclones after 6 weeks ectopically in vivo, quantified using the Bern score (*53*). Score of 0 to 3: nonchondrogenic; score of 3.1 to 9: chondrogenic, with at least some areas positively stained for Safranin O; representative nonchondrogenic and chondrogenic clone and subclone are shown. Percentages refer to the total number of clones or subclones out of $n = 10$ and 28 for AC clones and subclones, respectively, and $n = 27$ and 35 for NC clones and subclones, respectively.

constructs into subcutaneous pockets of nude mice—a site of mesodermal origin and here verified to include *Hox*-positive cells (fig. S4). After 5 weeks, the explanted cells were identified to be of human origin by Alu in situ hybridization (Fig. 3A). Using human-specific primers, we demonstrated that *HOX* genes, which were silent or only minorly expressed in in vitro–cultured NCs (that is, *HOXC4*, *HOXC5*, and *HOXD8*), were up-regulated to levels similar to native articular cartilage (Fig. 1B) upon in vivo implantation (Fig. 3B). Induction of HOXC4 and HOXD8 expression at the protein level (Fig. 3C) confirmed the HOX reprogramming capacity of NCs. The in vivo–activated *HOX* genes remained expressed even after subsequent long-term (42 days) culture of the explanted construct in complete medium, indicating the stability of the acquired changes (Fig. 3B). *HOXC8* and *HOXD3* were not activated upon in vivo implantation, which could be attributed to site-specific conditions regulating the pattern of induced *HOX* genes.

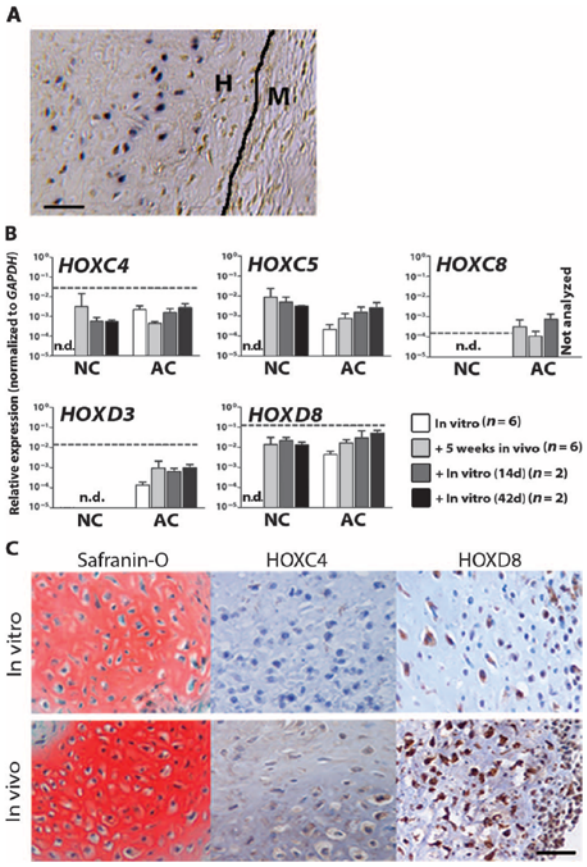


**Fig. 3. Environmental plasticity of NCs.** (**A**) Alu in situ hybridization (black nuclei) for the identification of implanted NCs of human origin after 5 weeks in the subcutaneous pouch of nude mice. H, human tissue; M, mouse tissue. Scale bar, 50 μm. (**B**) Induction and stability of induced *HOX* gene expression. Real-time qRT-PCR assessed the expression of *HOX* genes in engineered cartilage generated by human NCs on Chondro-Gide after 3 weeks of chondrogenic differentiation (In vitro) and after ectopic implantation in nude mice in vivo (+5 weeks in vivo). The explanted tissues were further cultured for another 14 days [+ In vitro (14d)] or 42 days [+ In vitro (42d)] in vitro to demonstrate the stability of the in vivo–induced expression profile. Dashed lines correspond to average expression levels in native articular cartilage in Fig. 1B. Data are means ± SD (*n* indicates the number of cartilage donors used; for each donor, two experimental replicates were analyzed). n.d., below the limit of detection. (**C**) Cartilaginous matrix deposition (Safranin O staining, left) and immunohistochemical detection of HOXC4 and HOXD8 in engineered cartilage generated with human NCs after in vitro culture and subcutaneous implantation for 5 weeks in vivo. Scale bar, 50 μm.

### Environmental plasticity of autologous goat NCs in articular defects

The environmental plasticity of NCs and their potential compatibility at an articular cartilage site were further assessed in a large-animal (goat) study. Experimental defects in a typical model (trochlear compartment) were filled with grafts based on green fluorescent protein (GFP)–transduced autologous NCs (Fig. 4A). We first verified that the *Hox* gene expression pattern in goat cartilage is similar to human, with *Hoxc4*, *Hoxc5*, *Hoxc8*, and *Hoxd3* being expressed in goat ACs (gACs) but not in goat NCs (gNCs) (Fig. 4B). Four weeks after transplantation into an articular knee defect, GFP-positive gNCs were identified in regions of the repair tissue that stained positive for proteoglycans as well as in surrounding fibrous tissue (Fig. 4C), indicating their survival and suggesting contribution to the repair process. In situ colocalization of *Hoxc4* and *GFP* expression (Fig. 4D) demonstrated the ability of gNCs to modify the memory of their biological origin and to adopt the *Hox*-positive profile of the implantation site.

### Human *HOX* gene expression regulation in vitro

Toward identifying a potential mechanism involved in the *HOX* gene profile switch, human NCs were cultured under conditions mimicking different features of the natural joint environment. *HOX* gene expression in NCs was not induced by different applied factors (fig. S5), including a synovial fluid component (hyaluronic acid); inflammatory cytokines typically produced by ACs (interleukin-1β and tumor necrosis factor–α); molecules that have been described to activate *HOX* expression in human embryonic cells [retinoic acid (*24*) and cyclic adenosine 3′,5′-monophosphate (*25*)]; a key molecule involved in articular cartilage development (growth and differentiation factor 5) (*26*, *27*); and soluble factors secreted by ACs, as tested by coculture in physically separated transwell systems or by application of AC-conditioned medium. The investigated *HOX* genes were also not activated by NC cultivation on a scaffold prepared with the extracellular matrix of articular cartilage (*28*) or under a regimen of mechanical conditioning resembling compressive deformation during joint loading (*8*) (fig. S5).

Instead, GFP-transduced NCs cocultured in direct contact with ACs or other *HOX*-positive mesodermal cells, such as synovial membrane fibroblasts, changed the expression profile for *HOXC4*, *HOXD3*, and *HOXD8* (Fig. 5A and fig. S6A). This was confirmed representatively for *HOXC4* by in situ hybridization in GFP-positive NCs (Fig. 5, B and C). The fact that *HOXD3* was activated in NCs by coculture with ACs, in contrast to coculture with synovial membrane fibroblasts or in vivo subcutaneous implantation, and that *HOXC5* was only activated in vivo suggests a different role for specific environmental parameters in selectively regulating the *HOX* gene network. When NCs were cultured together with formalin-fixed ACs, induction of *HOX* genes

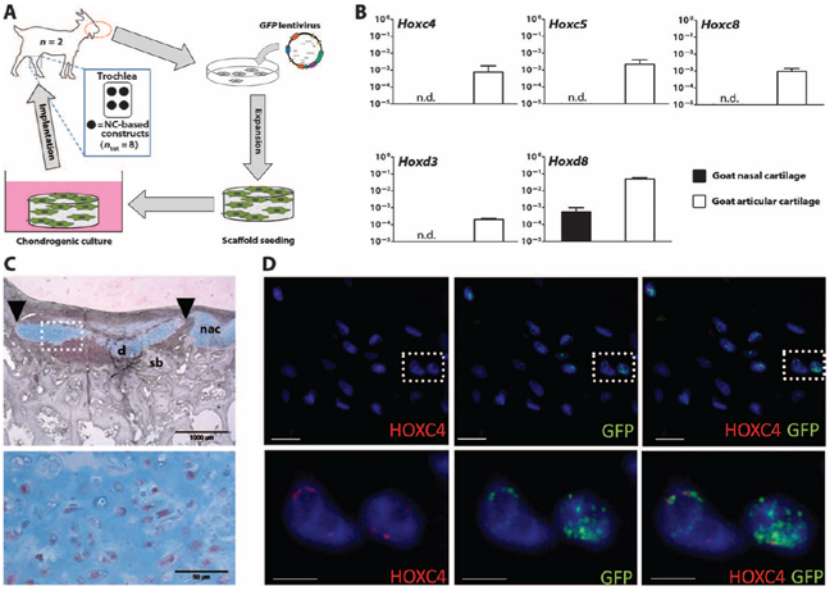


**Fig. 4. Transplantation of autologous gNCs into articular knee joints.** (**A**) GFP-transduced autologous gNCs were expanded for about 2 weeks and used for the production of cartilaginous constructs. After 2 weeks of chondrogenic differentiation, four cartilaginous constructs per goat ($n$ = 2 goats) were implanted into trochlear defects and harvested after 4 weeks with the aim to investigate the environmental plasticity of gNCs in an articular environment ($n_{tot}$ = 8 assessed explants). (**B**) *Hox* mRNA expression in gNCs and gACs from native tissues. gNCs were isolated from the biopsy harvested from nasal septum, and gACs were taken from the tissue removed when creating the articular defect. Data are means ± SD ($n$ = 2 goats). n.d., below the limit of detection. (**C**) Histological appearance of articular goat defects filled with autologous, GFP-labeled gNCs cultured on Chondro-Gide. Four weeks after implantation, sections were costained with Alcian blue for proteoglycans and with a GFP antibody to identify implanted cells (purple). Arrowheads delimit the defect area (d). The lower image is a zoomed-in view of the dotted area. nac, adjacent native articular cartilage; sb, subchondral bone. Scale bars, 1 mm (top); 50 μm (bottom). (**D**) Colocalization of *GFP* and *Hoxc4* mRNA expression detected with labeled probes in gNC-derived engineered tissue implanted into articular defect. Double-positive cells, indicated in the white dotted box, are enlarged in the lower panel. Scale bars, 40 μm (top); 20 μm (bottom).

was blocked (fig. S6B). This suggests that *HOX*-positive ACs trigger the expression of *HOX* genes either by paracrine signals acting only over a short distance or by membrane protein clustering/movement (*29*).

### NCs for repair of articular cartilage defects in goats

A longer-term study in goats was performed to obtain preclinical evidence of gNCs for the repair of articular cartilage defects. Tissue-engineered constructs were generated using autologous gNCs and gACs (serving as controls) and implanted into experimental defects created at a clinically relevant location, namely load-bearing sites of the articular condyle (Fig. 6A). Per the semiquantitative O'Driscoll scoring system (*30*) (table S1), the quality of the repair tissue significantly improved from 3 to 6 months after implantation only when using gNCs [from 10.1 ± 1.5 at 3 months ($n$ = 4) to 15.7 ± 1.7 after 6 months ($n$ = 5); means ± SEM], such that at 6 months the repair quality achieved by gNCs was statistically superior to gAC controls (11.3 ± 1.8, mean ± SEM) (Fig. 6B and table S2). The improved quality of the repair tissue using gNCs compared with gACs was histologically confirmed by a stronger and more uniform staining for glycosaminoglycans at 6 months (Fig. 6C).

### Pilot NC implantation in human articular cartilage lesions

To address the safety and feasibility of autologous NCs for the clinical treatment of posttraumatic full-thickness cartilage defects in the knee joint, in October 2012, we started recruiting patients in a pilot trial (http://clinicaltrials.gov identifier: NCT01605201; status: 7th patient treated). In the so far treated patients, followed up to 18 months after implantation, no systemic or local adverse events were observed (table S3), thus providing preliminary evidence of the safety and feasibility of the procedure. Magnetic resonance imaging (MRI) of the first patient before and 4 months after surgery indicated filling of the defect and no graft delamination, with strong reduction of subchondral bone edema (Fig. 7). The complete results of the still ongoing clinical trial will be the subject of a separate report.

## DISCUSSION

Our findings demonstrate that neural crest–derived, *HOX*-negative, differentiated cells from human adult nasal cartilage, similar to what is currently known for embryonic developmental models (*12*) or stem cell systems (*25*, *31*), exhibit features of self-renewal and environmental plasticity. These properties were respectively defined as the tissue regenerative capacity following serial cloning and the acquisition of a *HOX* pattern similar to the one of the recipient site upon transplantation. The principle was exploited for the preclinical and pilot clinical translation of autologous NCs for the unmet need of articular cartilage repair.

We initially identified a set of *HOX* genes capturing the different ontogeny of NCs and ACs, which form biochemically similar tissues but derive respectively from the neuroectoderm and the mesoderm. The same markers could distinguish ear from ankle chondrocytes, as well as DPCs from BMSCs. The data indicate that chondrocytes retain a positional signature inherited by the embryological origin (*32*–*34*), as proposed for epithelial (*19*), hematopoietic (*18*), and stromal (*35*) cells. The finding represents the basis for fundamental studies on the stability of NC molecular identity, on the assessment of reprogramming by environmental cues, as previously reported for embryonic mammalian limb bud (*36*) or thymic rat epithelial cells (*37*), and on the compatibility of their regenerative programs in heterotopic transplantation models, similar to what has been proposed for skeletal progenitors (*16*, *35*).

As compared to *HOX*-positive ACs, the identified *HOX*-negative expression profile of human NCs was associated with a higher self-renewal and regenerative capacity, here assessed by the potential of forming cartilage tissues following extensive expansion (>45 population doublings) across cycles of clonal dedifferentiation and redifferentiation [more than three orders of magnitude changes in type II collagen mRNA (*21*)]. These observations are consistent with previous reports on the close link between Hox-dependent pathways and the self-renewal program of hematopoietic stem cells in physiology and pathology (*38*). Future studies will be required to identify the factors activating *HOX* gene expression, as well as to investigate whether the lack of specific *HOX* genes, such as *HOXC4*, is merely associated with or has a direct functional role in the self-renewal/plasticity of NCs. Assessment of the functional importance of expressed or silent *HOX* genes, however, will be challenging because complex interactions between the HOX proteins, their cofactors, and multiple other genes are expected to regulate the translation of *HOX* signaling into cellular function [see review (*10*)].

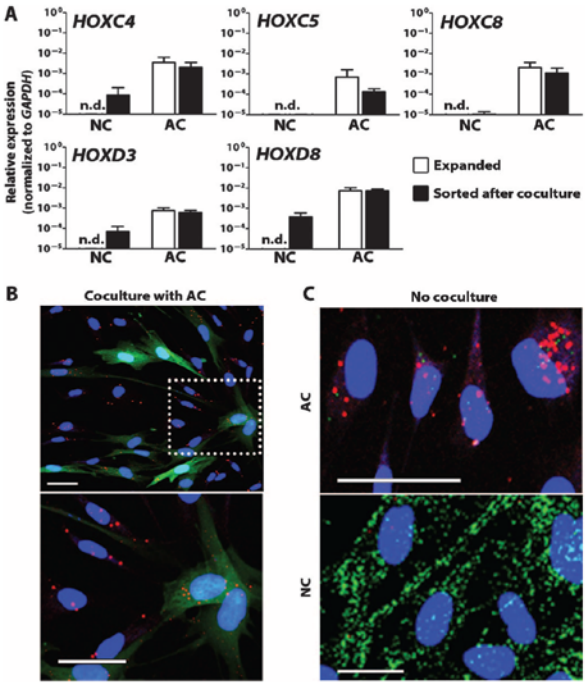


**Fig. 5. Regulation of human *HOX* genes after coculture of NCs with ACs.** (**A**) Real-time qRT-PCR analysis of *HOX* genes in human NCs after coculture with ACs for 7 days. Mixed cocultures were separated into the initial GFP-positive NC population and GFP-negative AC population by fluorescence-activated cell sorting (FACS). Separately expanded cells that were never cocultured served as controls. Data are means ± SD ($n$ = 7 experimental runs with cells from different donors). (**B**) In situ colocalization of *HOXC4* mRNA (red) and GFP protein (green) in GFP-labeled NCs when cocultured with ACs. The lower image shows a magnified view of the dotted region. Scale bars, 40 μm. (**C**) Separately cultured AC controls express *HOXC4* mRNA (red), whereas NC controls express *GFP*, but not *HOXC4*. Cell nuclei were stained with 4',6-diamidino-2-phenylindole. Scale bars, 40 μm.

Implantation of autologous, GFP-labeled NCs in experimental articular cartilage defects in goats allowed to demonstrate (i) their direct contribution to the formation of the repair tissue, similar to what was

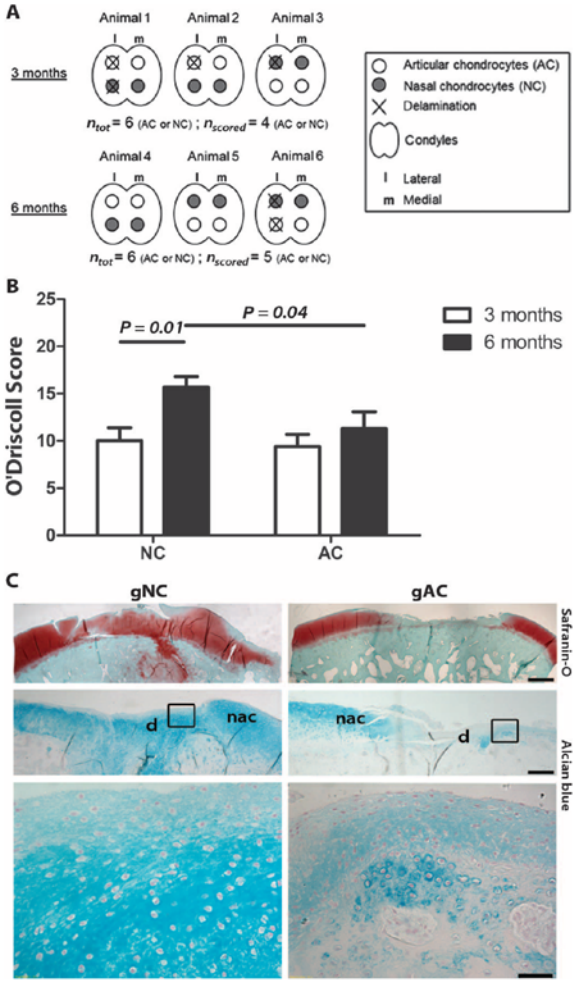


**Fig. 6. Goat NCs in articular cartilage repair.** (**A**) Two AC and two NC constructs per goat were implanted into condylar defects of a total of six goats and harvested after 3 ($n$ = 3 goats) and 6 months ($n$ = 3 goats). The diagram indicates the cases of initial construct delamination, with consequent elimination from the analysis and thus a reduction of the total number of scored explants as indicated. These delamination cases, merely related to the surgical challenges of the model, had an identical incidence for gAC- and gNC-based grafts. (**B**) O'Driscoll scores (*30*) of the repair quality of the gNC- or gAC-treated goat articular defects at 3 and 6 months ($n$ = 3 animals per time point) after implantation. Data are means ± SEM ($n$ = 4 and $n$ = 5 scored replicates per group at 3 and 6 months, respectively). The indicated $P$ values were calculated by Student's $t$ tests. (**C**) Safranin O and Alcian blue staining of representative repair tissues at the defect site (d) and of adjacent native articular cartilage (nac) 6 months after implantation of gNCs or gACs. The lower Alcian blue images show higher magnification (scale bar, 50 μm) of the regions framed in the respective upper panels (scale bar, 1 mm). Images are representative of $n$ = 5 replicates.

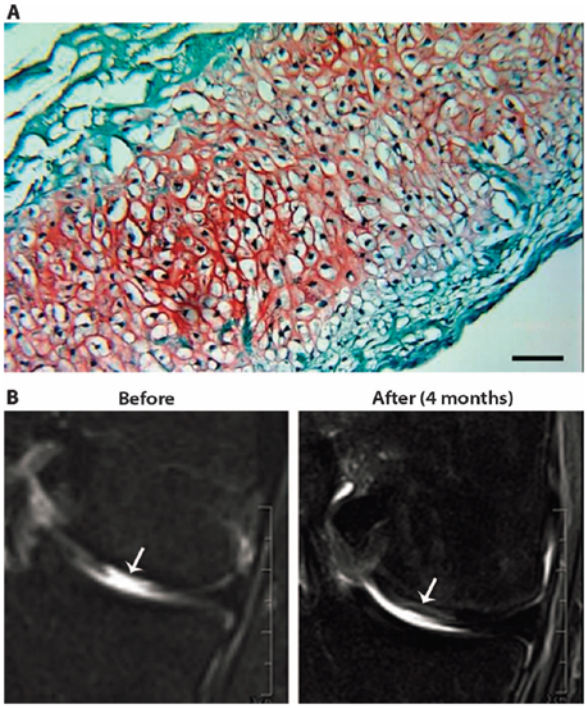


**Fig. 7. Autologous NCs in human articular cartilage repair.** (**A**) Safranin O staining demonstrated the quality of the engineered autograft at the time of implantation. Scale bar, 20 μm. (**B**) MRI before and 4 months after transplantation, displaying the maintenance of the graft or repair tissue at the defect site (white arrows).

previously reported for autologous ACs (*39*), and (ii) their activation of *Hoxc4*, which is otherwise not expressed in NCs and constitutively expressed in ACs. The finding reinforces the environmental plasticity of NCs and their compatibility with the transplantation at an articular site, which has been to date only preliminarily assessed in a rabbit model in the absence of a cell tracking system (*40*). As compared to ACs, the implantation of NCs in joint cartilage defects resulted in superior amount and quality of cartilaginous extracellular matrix at the repair sites. Here, the repair achieved by cell-based grafts was not directly compared to that of defects left empty, on the basis of previous reports that untreated cartilage defects of critical size in a large-size animal model, as those of our experimental setup, remain void or filled with fibrotic tissue (*41*, *42*). Although the goat model is among the ones that most closely resemble human cartilage (*43*, *44*), the findings should be taken with caution because indications of efficacy in animal models of cartilage repair have not been demonstrated to be predictive of clinical outcome. This is likely due to a variety of factors, including the species-related cell variability and the lack of control over the postoperative loading conditions, which critically regulate cartilage tissue regeneration (*45*).

The ongoing clinical trial was designed to test the safety and feasibility of implantation of autologous NCs in traumatic articular cartilage lesions. As compared to the traditional autologous chondrocyte implantation introduced more than 20 years ago in a clinical setting (*1*), our study differs not only in the used cell source, namely, NCs instead of ACs, but also in the grafting of a fully developed cartilage tissue as opposed to delivering cells by a gel or scaffold material. A tissue therapy rather than cell therapy for cartilage repair is expected to facilitate surgical handling and postoperative loading of the graft, as well as to protect implanted cells by the inflammatory factors at the implantation site, thanks to the deposited extracellular matrix (*46*). The tissue therapy concept is directly linked to the use of NCs because these cells, unlike ACs, allow more reproducible engineering of higher-quality cartilaginous grafts (*5*–*7*). The nasal biopsy necessitates a third operation in addition to the diagnostic arthroscopy that has to be performed in most cases to confirm the indication for a cellular therapy and during which ACs can be directly harvested. However, such operation can be performed under local anesthesia, is associated with minimal donor site morbidity (*47*), and avoids creating an additional damage to the already affected joint, shown to be potentially detrimental to the surrounding healthy articular cartilage (*48*).

Early assessments of adverse events and of maintenance in place of the repair tissue warrant proceeding with a larger cohort of patients, a longer-term follow-up, and the introduction of efficacy-related outcome parameters. Noteworthy, engineered cartilage based on autologous NCs has been recently reported to support safe and functional reconstruction of the nasal alar lobule in five patients, further underlying the regenerative capacity of the cell source (*47*). In parallel with carrying out further clinical studies, future adoption of NC-based engineered tissues for articular cartilage repair will require developing innovative manufacturing paradigms to address the standardization, scalability, and ultimately cost-effectiveness of the treatment (*49*).

## MATERIALS AND METHODS

### Study design

**Preclinical study design.** The objective of our study was to determine the self-renewal capacity and environmental plasticity of human neural crest–derived NCs and to demonstrate their compatibility and preclinical effectiveness for articular cartilage repair. Self-renewal capacity was demonstrated after serial cloning by the ability of cartilage formation in vitro and ectopically in vivo. The environmental plasticity of NCs was monitored by the cells' ability to adapt the molecular HOX expression profile to that of the subcutaneous (human NCs in mice) or articular cartilage (autologous goat cells) environment. Cartilage biopsies from a total of $n = 14$ human donors were used to compensate for a known interindividual variability. The specific number of biological replicates (=donors) used for each experiment is indicated in the figure legends. The preclinical effectiveness of NCs for articular cartilage repair was tested in a goat model, where tissue-engineered grafts generated by gNCs or gACs were implanted into articular defects of 6 mm in diameter, and tissue repair was assessed histologically 3 and 6 months after implantation. The numbers of animals and assessed replicates are indicated in the figure legends.

**Clinical study design.** A phase 1 clinical trial was initiated to test the safety and feasibility of using tissue-engineered autologous nasal cartilage for the regeneration of articular cartilage in the knee after traumatic injury (http://clinicaltrials.gov Identifier: NCT01605201). Inclusion criteria for a total of 10 patients were full-thickness cartilage lesions [from 2 to 8 $cm^2$, ICRS (International Cartilage Repair Society)

grade III to IV] on the femoral condyle and/or trochlea of the knee and age up to 55 years. Exclusion criteria were other chronic knee pathologies, previous major surgeries of the knee, or other conditions known to compromise cartilage repair. The primary outcomes for the trial were the incidence of systemic or local adverse events or reactions (including allergic reactions, wound infections, joint infections, and complications at the nasal biopsy harvest site) and the maintenance in place of the graft or of the repair tissue, as assessed by MRI up to 24 months after surgery.

### Regulatory compliance for human and animal studies

All human samples were collected with informed consent of the involved individuals. All animal experiments were performed in accordance with Swiss law, after approval by the responsible veterinary offices of Bern (Kantonales Veterinäramt Bern) and Zürich (Kantonales Veterinäramt Zürich). Human studies were approved by the cantonal ethical authority of Basel [EKNZ (Ethikkommission Nordwest- und Zentralschweiz)] and by the Swiss regulatory agency for therapeutic products (Swissmedic).

### Chondrocyte isolation, cultivation, and differentiation

ACs and NCs were isolated postmortem from articular knee joints of healthy human condyles and tibia plateau and from nasal septum, respectively. Auricular and ankle cartilages were isolated respectively from the ear and ankle joint. Chondrocyte expansion and differentiation under various conditions is described in Supplementary Methods.

### Ectopic implantation of human chondrocytes in vivo

For in vivo investigations, $3 \times 10^6$ expanded human chondrocytes were seeded onto a collagen type I/III scaffold (6 mm in diameter) (Chondro-Gide, Geistlich Pharma AG) and cultured for 1 week in differentiation medium before implantation into subcutaneous pouches of nude mice. For each donor ($n = 6$ donors), four to eight constructs were generated and implanted in mice (two replicates implanted per mouse). Constructs were harvested after 5 weeks in vivo and assessed histologically and for gene expression. For two donors, constructs were kept for another 2 or 6 weeks in complete medium. In vitro control constructs were kept in differentiating medium for 1 week followed by 5 weeks in complete medium.

### Autologous gNC constructs in articular cartilage defects

To investigate the environmental plasticity of NCs and their compatibility with articular joints, a 6-mm circular biopsy of nasal cartilage was harvested from two adult female goats after unilateral incision of the mucosa of the nasal septum. The isolated gNCs were expanded in the presence of fibroblast growth factor 2 (5 ng/ml) as previously described (*50*) before transduction with a GFP lentivirus at a multiplicity of infection of 10 and seeding ($4 \times 10^4$ gNCs/mm$^2$) on a Chondro-Gide membrane (Geistlich Pharma AG). FACS data acquisition and analysis were performed with CellQuest Pro software (Becton Dickinson). After 2 weeks of chondrogenic culture in vitro, four autologous NC–based constructs per animal ($n = 2$ animals) were implanted in four articular defects (6 mm in diameter and 1 mm in depth) generated in the same trochlea (Fig. 4A). Constructs were fixed to the surrounding articular cartilage with four stitches. Goats were sacrificed 4 weeks later, and samples were harvested for immunohistochemical and histological analyses.

To investigate the preclinical effectiveness of gNCs for articular cartilage repair, surgical procedures were performed for six adult female goats as described above with the following modifications: (i) four circular biopsies of 6 mm were additionally harvested from the articular caprine condyle; (ii) cartilaginous tissues were generated with autologous gNCs and gACs; (iii) two gNC- and two gAC-based constructs per animal were unilaterally implanted into the same condyle and followed up for 3 ($n = 3$ animals) and 6 months ($n = 3$ animals) (Fig. 6A). Repair tissues were analyzed by Safranin O and Alcian blue staining as described in the histology section and quantified according to the O'Driscoll score (*30*). In particular, mean scores from three independent observers were considered for each parameter and location (that is, medial and lateral regions adjacent to the native cartilage and central part of the defect).

### Gene expression analysis

RNA isolation and qualitative duplex PCR were performed as described previously (*51*). Complementary DNA quantification was performed in duplicates by qRT-PCR using 7300 Real Time PCR Systems (Applied Biosystems) and normalized against *GAPDH* expression as described earlier (*52*). All analyzed genes are listed in table S4. The primers used to identify gene expression of the key markers (*HOXC4*, *HOXC8*, *HOXD3*, and *HOXD8*) were confirmed to be human-specific using subcutaneous (mesodermal) mouse tissue as a control, where the primers failed to amplify the same mouse *Hox* genes. Mouse-specific primers for *Hoxc4*, *Hoxc5*, *Hoxd3*, and *Hoxd8* were used to investigate the expression of *Hox* genes in murine subcutaneous tissue (table S4).

Colocalization of *HOXC4* mRNA with *GFP* mRNA or the GFP protein was detected in situ with QuantiGene ViewRNA ISH Cell Assay or QuantiGene ViewRNA ISH Tissue Assay following the manufacturer's (Affymetrix) instructions. *GFP* mRNA was labeled with Cy3 (excitation 554 nm/emission 576 nm) and false-colored in green to coincide with the GFP color. *HOXC4* mRNA was labeled with Cy5 (excitation 644 nm/emission 669 nm) and false-colored to red.

### Clinical trial surgery

To harvest the nasal cartilage, the mucous tissue on the nasal septum was incised and lifted to punch a biopsy (6 mm in diameter) out of the anterior part of the underlying nasal septal cartilage. NCs were isolated and expanded as described above, using autologous serum instead of fetal bovine serum. Cells were then seeded ($4 \times 10^4$ NCs/mm$^2$) and cultured in a collagen sponge (Chondro-Gide; 30 × 40 mm, 1.5 mm thick) in the context of a quality management system and Good Manufacturing Practice facility established within the University Hospital Basel. Four weeks after the harvesting of the autologous nasal cartilage biopsy, the damaged cartilage tissue was removed by mini-arthrotomy, and the defect was debrided down to the subchondral bone to create a stable rim of healthy cartilage. The tissue-engineered nasal cartilage autograft was trimmed to the defect size and placed into the defect. The graft was then secured to the surrounding tissue with resorbable polyfilament suture material (Vicryl, Ethicon) and fibrin adhesive (Tisseel, Baxter), and the arthrotomy was closed layer by layer. MRI of the defect site was performed using a 3T magnetic resonance imager (Verio, Siemens Medical Solutions) with sagittal T2-weighted fast spin echo sequence (4630/91).

### Statistical analysis

With GraphPad Prism 5 statistical analysis software, the proliferation rates of NC and AC clones ($n = 27$ and $n = 10$, respectively) and subclones ($n = 35$ and $n = 28$, respectively) were analyzed by one-way ANOVA applying the Kruskal-Wallis test (significant if $P < 0.05$). A nested two-way ANOVA was performed to investigate significant

differences between native nasal ($n = 4$) and articular cartilages ($n = 6$), expanded NCs ($n = 9$) and ACs ($n = 10$), tissue-engineered cartilages generated by NCs ($n = 10$) or ACs ($n = 11$), and ear ($n = 3$) and ankle ($n = 3$) chondrocytes. Unpaired Student's $t$ tests were applied to determine statistical significance of differences measured in O'Driscoll scores in the goat cartilage repair study. Bayesian analysis using the Markov chain Monte Carlo method was applied using the WinBug program to define statistical relevance in the cloning efficiency, which was considered significant when the modeling showed 95% credible interval above 0.

## SUPPLEMENTARY MATERIALS

www.sciencetranslationalmedicine.org/cgi/content/full/6/251/251ra119/DC1
Methods
Fig. S1. *HOX* gene expression in human stromal cells from bone marrow and dental pulp.
Fig. S2. Clonogenicity and differentiation capacity of human NC and AC clones and subclones in vitro.
Fig. S3. Chondrogenic and osteogenic differentiation capacity of NC and AC clones in vitro.
Fig. S4. Expression of *Hox* genes in subcutaneous murine tissue.
Fig. S5. Effect of different factors on *HOX* gene induction in human NCs.
Fig. S6. Coculture of human nasal chondrocytes with synovial membrane fibroblasts or ACs.
Table S1. Parameters of cartilage repair quality according to O'Driscoll.
Table S2. Scoring of the repair tissue in goats.
Table S3. Summary of treated patients.
Table S4. List of TaqMan gene expression assays from Applied Biosystems.
References (*54*–*62*)

## REFERENCES AND NOTES


1. M. Brittberg, A. Lindahl, A. Nilsson, C. Ohlsson, O. Isaksson, L. Peterson, Treatment of deep cartilage defects in the knee with autologous chondrocyte transplantation. *N. Engl. J. Med.* **331**, 889–895 (1994).
2. D. J. Huey, J. C. Hu, K. A. Athanasiou, Unlike bone, cartilage regeneration remains elusive. *Science* **338**, 917–921 (2012).
3. K. Pelttari, A. Winter, E. Steck, K. Goetzke, T. Hennig, B. G. Ochs, T. Aigner, W. Richter, Premature induction of hypertrophy during in vitro chondrogenesis of human mesenchymal stem cells correlates with calcification and vascular invasion after ectopic transplantation in SCID mice. *Arthritis Rheum.* **54**, 3254–3266 (2006).
4. A. Barbero, S. Grogan, D. Schäfer, M. Heberer, P. Mainil-Varlet, I. Martin, Age related changes in human articular chondrocyte yield, proliferation and post-expansion chondrogenic capacity. *Osteoarthritis Cartilage* **12**, 476–484 (2004).
5. N. Rotter, L. J. Bonassar, G. Tobias, M. Lebl, A. K. Roy, C. A. Vacanti, Age dependence of biochemical and biomechanical properties of tissue-engineered human septal cartilage. *Biomaterials* **23**, 3087–3094 (2002).
6. W. Kafienah, M. Jakob, O. Démarteau, A. Frazer, M. D. Barker, I. Martin, A. P. Hollander, Three-dimensional tissue engineering of hyaline cartilage: Comparison of adult nasal and articular chondrocytes. *Tissue Eng.* **8**, 817–826 (2002).
7. A. G. Tay, J. Farhadi, R. Suetterlin, G. Pierer, M. Heberer, I. Martin, Cell yield, proliferation, and postexpansion differentiation capacity of human ear, nasal, and rib chondrocytes. *Tissue Eng.* **10**, 762–770 (2004).
8. C. Candrian, D. Vonwil, A. Barbero, E. Bonacina, S. Miot, J. Farhadi, D. Wirz, S. Dickinson, A. Hollander, M. Jakob, Z. Li, M. Alini, M. Heberer, I. Martin, Engineered cartilage generated by nasal chondrocytes is responsive to physical forces resembling joint loading. *Arthritis Rheum.* **58**, 197–208 (2008).
9. C. Scotti, A. Osmokrovic, F. Wolf, S. Miot, G. M. Peretti, A. Barbero, I. Martin, Response of human engineered cartilage based on articular or nasal chondrocytes to interleukin-1β and low oxygen. *Tissue Eng. Part A* **18**, 362–372 (2012).
10. M. Kmita, D. Duboule, Organizing axes in time and space; 25 years of colinear tinkering. *Science* **301**, 331–333 (2003).
11. R. Krumlauf, *Hox* genes in vertebrate development. *Cell* **78**, 191–201 (1994).
12. G. Couly, A. Grapin-Botton, P. Coltey, B. Ruhin, N. M. Le Douarin, Determination of the identity of the derivatives of the cephalic neural crest: Incompatibility between *Hox* gene expression and lower jaw development. *Development* **125**, 3445–3459 (1998).
13. A. Grapin-Botton, M. A. Bonnin, L. A. McNaughton, R. Krumlauf, N. M. Le Douarin, Plasticity of transposed rhombomeres: Hox gene induction is correlated with phenotypic modifications. *Development* **121**, 2707–2721 (1995).
14. N. Itasaki, J. Sharpe, A. Morrison, R. Krumlauf, Reprogramming *Hox* expression in the vertebrate hindbrain: Influence of paraxial mesoderm and rhombomere transposition. *Neuron* **16**, 487–500 (1996).
15. N. M. Le Douarin, S. Creuzet, G. Couly, E. Dupin, Neural crest cell plasticity and its limits. *Development* **131**, 4637–4650 (2004).
16. P. Leucht, J. B. Kim, R. Amasha, A. W. James, S. Girod, J. A. Helms, Embryonic origin and Hox status determine progenitor cell fate during adult bone regeneration. *Development* **135**, 2845–2854 (2008).
17. T. I. Lee, R. G. Jenner, L. A. Boyer, M. G. Guenther, S. S. Levine, R. M. Kumar, B. Chevalier, S. E. Johnstone, M. F. Cole, K. Isono, H. Koseki, T. Fuchikami, K. Abe, H. L. Murray, J. P. Zucker, B. Yuan, G. W. Bell, E. Herbolsheimer, N. M. Hannett, K. Sun, D. T. Odom, A. P. Otte, T. L. Volkert, D. P. Bartel, D. A. Melton, D. K. Gifford, R. Jaenisch, R. A. Young, Control of developmental regulators by Polycomb in human embryonic stem cells. *Cell* **125**, 301–313 (2006).
18. S. Liedtke, A. Buchheiser, J. Bosch, F. Bosse, F. Kruse, X. Zhao, S. Santourlidis, G. Kögler, The *HOX* Code as a "biological fingerprint" to distinguish functionally distinct stem cell populations derived from cord blood. *Stem Cell Res.* **5**, 40–50 (2010).
19. J. L. Rinn, J. K. Wang, N. Allen, S. A. Brugmann, A. J. Mikels, H. Liu, T. W. Ridky, H. S. Stadler, R. Nusse, J. A. Helms, H. Y. Chang, A dermal *HOX* transcriptional program regulates site-specific epidermal fate. *Genes Dev.* **22**, 303–307 (2008).
20. B. Sacchetti, A. Funari, S. Michienzi, S. Di Cesare, S. Piersanti, I. Saggio, E. Tagliafico, S. Ferrari, P. G. Robey, M. Riminucci, P. Bianco, Self-renewing osteoprogenitors in bone marrow sinusoids can organize a hematopoietic microenvironment. *Cell* **131**, 324–336 (2007).
21. A. Barbero, S. Ploegert, M. Heberer, I. Martin, Plasticity of clonal populations of dedifferentiated adult human articular chondrocytes. *Arthritis Rheum.* **48**, 1315–1325 (2003).
22. P. Ducy, R. Zhang, V. Geoffroy, A. L. Ridall, G. Karsenty, Osf2/Cbfa1: A transcriptional activator of osteoblast differentiation. *Cell* **89**, 747–754 (1997).
23. A. Shafiee, M. Kabiri, N. Ahmadbeigi, S. O. Yazdani, M. Mojtahed, S. Amanpour, M. Soleimani, Nasal septum-derived multipotent progenitors: A potent source for stem cell-based regenerative medicine. *Stem Cells Dev.* **20**, 2077–2091 (2011).
24. A. Simeone, D. Acampora, L. Arcioni, P. W. Andrews, E. Boncinelli, F. Mavilio, Sequential activation of *HOX2* homeobox genes by retinoic acid in human embryonal carcinoma cells. *Nature* **346**, 763–766 (1990).
25. V. D'Antò, M. Cantile, M. D'Armiento, G. Schiavo, G. Spagnuolo, L. Terracciano, R. Vecchione, C. Cillo, The *HOX* genes are expressed, in vivo, in human tooth germs: In vitro cAMP exposure of dental pulp cells results in parallel HOX network activation and neuronal differentiation. *J. Cell. Biochem.* **97**, 836–848 (2006).
26. C. M. Coleman, E. E. Vaughan, D. C. Browe, E. Mooney, L. Howard, F. Barry, Growth differentiation factor-5 enhances in vitro mesenchymal stromal cell chondrogenesis and hypertrophy. *Stem Cells Dev.* **22**, 1968–1976 (2013).
27. A. M. Craft, N. Ahmed, J. S. Rockel, G. S. Baht, B. A. Alman, R. A. Kandel, A. E. Grigoriadis, G. M. Keller, Specification of chondrocytes and cartilage tissues from embryonic stem cells. *Development* **140**, 2597–2610 (2013).
28. N. C. Cheng, B. T. Estes, H. A. Awad, F. Guilak, Chondrogenic differentiation of adipose-derived adult stem cells by a porous scaffold derived from native articular cartilage extracellular matrix. *Tissue Eng. Part A* **15**, 231–241 (2009).
29. C. C. DuFort, M. J. Paszek, V. M. Weaver, Balancing forces: Architectural control of mechanotransduction. *Nat. Rev. Mol. Cell Biol.* **12**, 308–319 (2011).
30. S. W. O'Driscoll, The healing and regeneration of articular cartilage. *J. Bone Joint Surg. Am.* **80**, 1795–1812 (1998).
31. J. A. Helms, D. Cordero, M. D. Tapadia, New insights into craniofacial morphogenesis. *Development* **132**, 851–861 (2005).
32. G. Couly, A. Grapin-Botton, P. Coltey, N. M. Le Douarin, The regeneration of the cephalic neural crest, a problem revisited: The regenerating cells originate from the contralateral or from the anterior and posterior neural fold. *Development* **122**, 3393–3407 (1996).
33. P. Hunt, M. Gulisano, M. Cook, M. H. Sham, A. Faiella, D. Wilkinson, E. Boncinelli, R. Krumlauf, A distinct *Hox* code for the branchial region of the vertebrate head. *Nature* **353**, 861–864 (1991).
34. V. Prince, A. Lumsden, *Hoxa-2* expression in normal and transposed rhombomeres: Independent regulation in the neural tube and neural crest. *Development* **120**, 911–923 (1994).
35. J. Picchi, L. Trombi, L. Spugnesi, S. Barachini, G. Maroni, G. B. Brodano, S. Boriani, M. Valtieri, M. Petrini, M. C. Magli, *HOX* and *TALE* signatures specify human stromal stem cell populations from different sources. *J. Cell. Physiol.* **228**, 879–889 (2012).
36. L. A. Wyngaarden, S. Hopyan, Plasticity of proximal–distal cell fate in the mammalian limb bud. *Dev. Biol.* **313**, 225–233 (2008).
37. P. Bonfanti, S. Claudinot, A. W. Amici, A. Farley, C. C. Blackburn, Y. Barrandon, Microenvironmental reprogramming of thymic epithelial cells to skin multipotent stem cells. *Nature* **466**, 978–982 (2010).
38. B. Argiropoulos, R. K. Humphries, Hox genes in hematopoiesis and leukemogenesis. *Oncogene* **26**, 6766–6776 (2007).
39. F. Dell'Accio, J. Vanlauwe, J. Bellemans, J. Neys, B. C. De, F. P. Luyten, Expanded phenotypically stable chondrocytes persist in the repair tissue and contribute to cartilage matrix formation

and structural integration in a goat model of autologous chondrocyte implantation. *J. Orthop. Res.* **21**, 123–131 (2003).
40. C. Vinatier, O. Gauthier, M. Masson, O. Malard, A. Moreau, B. H. Fellah, M. Bilban, R. Spaethe, G. Daculsi, J. Guicheux, Nasal chondrocytes and fibrin sealant for cartilage tissue engineering. *J. Biomed. Mater. Res. A* **89**, 176–185 (2009).
41. S. Miot, R. Gianni-Barrera, K. Pelttari, C. Acharya, P. Mainil-Varlet, H. Juelke, C. Jaquiery, C. Candrian, A. Barbero, I. Martin, In vitro and in vivo validation of human and goat chondrocyte labeling by green fluorescent protein lentivirus transduction. *Tissue Eng. Part C Methods* **16**, 11–21 (2010).
42. D. B. Saris, W. J. Dhert, A. J. Verbout, Joint homeostasis. The discrepancy between old and fresh defects in cartilage repair. *J. Bone Joint Surg. Br.* **85**, 1067–1076 (2003).
43. B. J. Ahern, J. Parvizi, R. Boston, T. P. Schaer, Preclinical animal models in single site cartilage defect testing: A systematic review. *Osteoarthritis Cartilage* **17**, 705–713 (2009).
44. C. R. Chu, M. Szczodry, S. Bruno, Animal models for cartilage regeneration and repair. *Tissue Eng. Part B Rev.* **16**, 105–115 (2010).
45. J. R. Ebert, W. B. Robertson, D. G. Lloyd, M. H. Zheng, D. J. Wood, T. Ackland, Traditional vs accelerated approaches to post-operative rehabilitation following matrix-induced autologous chondrocyte implantation (MACI): Comparison of clinical, biomechanical and radiographic outcomes. *Osteoarthritis Cartilage* **16**, 1131–1140 (2008).
46. K. Pelttari, A. Wixmerten, I. Martin, Do we really need cartilage tissue engineering? *Swiss Med. Wkly.* **139**, 602–609 (2009).
47. I. Fulco, S. Miot, M. D. Haug, A. Barbero, A. Wixmerten, S. Feliciano, F. Wolf, G. Jundt, A. Marsano, J. Farhadi, M. Heberer, M. Jakob, D. J. Schaefer, I. Martin, Engineered autologous cartilage tissue for nasal reconstruction after tumour resection: An observational first-in-human trial. *Lancet* **384**, 337–346 (2014).
48. C. R. Lee, A. J. Grodzinsky, H. P. Hsu, S. D. Martin, M. Spector, Effects of harvest and selected cartilage repair procedures on the physical and biochemical properties of articular cartilage in the canine knee. *J. Orthop. Res.* **18**, 790–799 (2000).
49. I. Martin, P. J. Simmons, D. F. Williams, Manufacturing challenges in regenerative medicine. *Sci. Transl. Med.* **6**, 232fs16 (2014).
50. S. Miot, F. P. Scandiucci de, D. Wirz, A. U. Daniels, T. J. Sims, A. P. Hollander, P. Mainil-Varlet, M. Heberer, I. Martin, Cartilage tissue engineering by expanded goat articular chondrocytes. *J. Orthop. Res.* **24**, 1078–1085 (2006).
51. M. Cantile, L. Cindolo, G. Napodano, V. Altieri, C. Cillo, Hyperexpression of locus C genes in the *HOX* network is strongly associated in vivo with human bladder transitional cell carcinomas. *Oncogene* **22**, 6462–6468 (2003).
52. I. Martin, M. Jakob, D. Schäfer, W. Dick, G. Spagnoli, M. Heberer, Quantitative analysis of gene expression in human articular cartilage from normal and osteoarthritic joints. *Osteoarthritis Cartilage* **9**, 112–118 (2001).
53. S. P. Grogan, A. Barbero, V. Winkelmann, F. Rieser, J. S. Fitzsimmons, S. O'Driscoll, I. Martin, P. Mainil-Varlet, Visual histological grading system for the evaluation of in vitro–generated neocartilage. *Tissue Eng.* **12**, 2141–2149 (2006).
54. M. Jakob, O. Démarteau, D. Schäfer, B. Hintermann, W. Dick, M. Heberer, I. Martin, Specific growth factors during the expansion and redifferentiation of adult human articular chondrocytes enhance chondrogenesis and cartilaginous tissue formation in vitro. *J. Cell. Biochem.* **81**, 368–377 (2001).
55. B. Johnstone, T. M. Hering, A. I. Caplan, V. M. Goldberg, J. U. Yoo, In vitro chondrogenesis of bone marrow-derived mesenchymal progenitor cells. *Exp. Cell Res.* **238**, 265–272 (1998).
56. N. Banu, T. Tsuchiya, Markedly different effects of hyaluronic acid and chondroitin sulfate-A on the differentiation of human articular chondrocytes in micromass and 3-D honeycomb rotation cultures. *J. Biomed. Mater. Res. A* **80**, 257–267 (2007).
57. U. H. Dietz, L. J. Sandell, Cloning of a retinoic acid-sensitive mRNA expressed in cartilage and during chondrogenesis. *J. Biol. Chem.* **271**, 3311–3316 (1996).
58. S. J. Park, E. J. Cheon, M. H. Lee, H. A. Kim, MicroRNA-127-5p regulates matrix metalloproteinase 13 expression and interleukin-1β–induced catabolic effects in human chondrocytes. *Arthritis Rheum.* **65**, 3141–3152 (2013).
59. L. Sun, X. Wang, D. L. Kaplan, A 3D cartilage-inflammatory cell culture system for the modeling of human osteoarthritis. *Biomaterials* **32**, 5581–5589 (2011).
60. M. Cantile, R. Franco, A. Tschan, D. Baumhoer, I. Zlobec, G. Schiavo, I. Forte, M. Bihl, G. Liguori, G. Botti, L. Tornillo, E. Karamitopoulou-Diamantis, L. Terracciano, C. Cillo, HOX D13 expression across 79 tumor tissue types. *Int. J. Cancer* **125**, 1532–1541 (2009).
61. P. Kasten, J. Vogel, R. Luginbühl, P. Niemeyer, M. Tonak, H. Lorenz, L. Helbig, S. Weiss, J. Fellenberg, A. Leo, H. G. Simank, W. Richter, Ectopic bone formation associated with mesenchymal stem cells in a resorbable calcium deficient hydroxyapatite carrier. *Biomaterials* **26**, 5879–5889 (2005).
62. C. Scotti, B. Tonnarelli, A. Papadimitropoulos, A. Scherberich, S. Schaeren, A. Schauerte, J. Lopez-Rios, R. Zeller, A. Barbero, I. Martin, Recapitulation of endochondral bone formation using human adult mesenchymal stem cells as a paradigm for developmental engineering. *Proc. Natl. Acad. Sci. U.S.A.* **107**, 7251–7256 (2010).

**Acknowledgments:** We are grateful to J. Geurts for help in generating the GFP lentivirus, to S. Güven for the surgery in mice, to A. Todorov for the statistical analyses, to E. Traunecker for cell sorting, to S. Grad for the mechanical conditioning of the cartilaginous constructs, to L. Ettinger Ferguson (University of Zürich) for technical assistance in performing histology of goat constructs, to C. Candrian and H. Jühlke for performing the goat surgery at the University of Bern, to K. Nuss for performing the goat surgeries at the University of Zürich, to B. Erne for help with confocal microscopy, to G. Jundt and L. Terracciano for their assistance in the immunohistochemical analyses, to M. Centola for critical editing of the manuscript, to S. Miot and A. Wixmerten for establishing the quality management system for the clinical trial, and to I. Fulco, M. Haug, and D.J. Schaefer for coordinating the harvest of nasal cartilage biopsies. We also thank K. Martin (Geistlich) for providing Chondro-Gide collagen scaffolds. **Funding:** This work was financed by the Swiss National Science Foundation (SNF Project No 310030-126965.1), the Marie Curie Actions FP7 Network for Initial Training (ITN)—MultiTERM grant agreement no. 238551, the European Union's Seventh Program for research, technological development and demonstration (project "Bio-Comet") under grant agreement no. 278807, and the Deutsche Arthrose Hilfe Foundation. **Author contributions:** K.P., M.J., C.C., A.B., and I.M. designed the study; K.P., B.P., S.F., and A.B. collected the human samples; K.P., S.F., A.P., and A.B. analyzed the *HOX* expression profiles; K.P., B.P., S.F., and A.B. performed the clonal studies and analyzed the data; K.P., S.F., P.M.-V., B.v.R., M.M., and A.B. performed the goat experiments or surgeries and analyzed the data; K.P. and A.B. peformed statistical analyses; M.M., M.J., and T.S. performed the clinical surgeries; K.P., B.P., M.M., C.C., C.S., A.B., and I.M. wrote and revised the manuscript; A.B. and I.M. coordinated the study design and implementation. **Competing interests:** The authors declare that they have no competing financial interests. **Data and materials availability:** No data for this study have been deposited elsewhere.

Submitted 27 August 2013
Accepted 11 July 2014
Published 27 August 2014
10.1126/scitranslmed.3009688

**Citation:** K. Pelttari, B. Pippenger, M. Mumme, S. Feliciano, C. Scotti, P. Mainil-Varlet, A. Procino, B. von Rechenberg, T. Schwamborn, M. Jakob, C. Cillo, A. Barbero, I. Martin, Adult human neural crest–derived cells for articular cartilage repair. *Sci. Transl. Med.* **6**, 251ra119 (2014).

*Journal of Cellular and Molecular Medicine 2015 February 16. [Epub ahead of print]*
*doi: 10.1111/jcmm.12526*

# Bone-forming capacity of adult human nasal chondrocytes

Benjamin E. Pippenger, Manuela Ventura[b], Karoliina Pelttari[a], Sandra Feliciano[a], Arnaud Scherberich[a], Claude Jacquiery[a], Frank X. Walboomers[b], Andrea Barbero[a], Ivan Martin[a*]

[a] Department of Surgery, University Hospital Basel, Basel, Switzerland

[b] Department of Biomaterials, Radboud University Nijmegen Medical Centre, Nijmegen, The Netherlands

*Correspondence to: Prof. Ivan Martin
ICFS, University Hospital Basel
Hebelstrasse 20, ZLF, Room 405
4031 Basel, Switzerland
Phone: + 41 61 265 2384; fax: + 41 61 265 3990
E-mail: Ivan.Martin@usb.ch

## ABSTRACT

Nasal chondrocytes (NC) derive from the same multipotent embryological segment that gives rise to the majority of the maxillofacial bone and have been reported to differentiate into osteoblast-like cells in vitro. In this study, we assessed the capacity of adult human NC, appropriately primed towards hypertrophic or osteoblastic differentiation, to form bone tissue in vivo. Hypertrophic induction of NC-based micromass pellets formed mineralized cartilaginous tissues rich in type X collagen, but upon implantation into subcutaneous pockets of nude mice remained avascular and reverted to stable hyaline-cartilage. In the same ectopic environment, NC embedded into ceramic scaffolds and primed with osteogenic medium only sporadically formed intramembranous bone tissue. A clonal study could not demonstrate that the low bone formation efficiency was related to a possibly small proportion of cells competent to become fully functional osteoblasts. We next tested whether the cues present in an orthotopic environment could induce a more efficient direct osteoblastic transformation of NC. Using a nude rat calvarial defect model, we demonstrated that (i) NC directly participated in frank bone formation and (ii) the efficiency of survival and bone formation by NC was significantly higher than that of reference osteogenic cells, namely bone marrow-derived mesenchymal stromal cells. This study provides a proof-of-principle that NC have the plasticity to convert into bone cells and thereby represent an easily available cell source to be further investigated for craniofacial bone regeneration.

J. Cell. Mol. Med. Vol XX, No X, 2015 pp. 1-10

# Bone-forming capacity of adult human nasal chondrocytes

**Benjamin E Pippenger [a], Manuela Ventura [b], Karoliina Pelttari [a], Sandra Feliciano [a], Claude Jaquiery [a], Arnaud Scherberich [a], X Frank Walboomers [b], Andrea Barbero [a], Ivan Martin [a, *]**

[a] *Departments of Surgery and of Biomedicine, University Hospital Basel, University of Basel, Basel, Switzerland*
[b] *Department of Biomaterials, Radboud University Nijmegen Medical Centre, Nijmegen, The Netherlands*

*Received: July 28, 2014; Accepted: November 27, 2014*

## Abstract

Nasal chondrocytes (NC) derive from the same multipotent embryological segment that gives rise to the majority of the maxillofacial bone and have been reported to differentiate into osteoblast-like cells *in vitro*. In this study, we assessed the capacity of adult human NC, appropriately primed towards hypertrophic or osteoblastic differentiation, to form bone tissue *in vivo*. Hypertrophic induction of NC-based micromass pellets formed mineralized cartilaginous tissues rich in type X collagen, but upon implantation into subcutaneous pockets of nude mice remained avascular and reverted to stable hyaline-cartilage. In the same ectopic environment, NC embedded into ceramic scaffolds and primed with osteogenic medium only sporadically formed intramembranous bone tissue. A clonal study could not demonstrate that the low bone formation efficiency was related to a possibly small proportion of cells competent to become fully functional osteoblasts. We next tested whether the cues present in an orthotopic environment could induce a more efficient direct osteoblastic transformation of NC. Using a nude rat calvarial defect model, we demonstrated that (*i*) NC directly participated in frank bone formation and (*ii*) the efficiency of survival and bone formation by NC was significantly higher than that of reference osteogenic cells, namely bone marrow-derived mesenchymal stromal cells. This study provides a proof-of-principle that NC have the plasticity to convert into bone cells and thereby represent an easily available cell source to be further investigated for craniofacial bone regeneration.

**Keywords:** nasal chondrocytes • craniofacial bone • intramembranous ossification • preclinical studies • stromal cells

## Introduction

Cells from the adult nasal septum (nasal chondrocytes, NC) derive from the same multipotent embryological segment that gives rise to the majority of the bone and cartilage of the head and face (neural crest/neuroectoderm) [1]. Human septal cartilage has long been considered the pacemaker for the growth of the face and skull, with growth potential equivalent to that of the epiphyseal growth cartilage of long bones [2]. Adult nasal septal tissue is known to directly interface with facial bone tissue development, thereby regulating turbinate and maxilla bone growth [3]. *In vitro* studies have demonstrated that NC retain a certain level of plasticity and can acquire traits of neuronal- and osteoblast-like phenotypes [4, 5]. However, it is unknown if NC can induce or directly from frank bone tissue *in vivo*.

There are two archetypal routes for bone formation and repair: endochondral and intramembranous ossification [6]. The primary route in bone development and repair is endochondral ossification, in which a hypertrophic cartilage template is formed and eventually remodelled into bone tissue. The bones of the head and face form and repair predominantly through intramembranous ossification. Since NC reside within cartilage tissue and are in direct contact with an environment that forms through intramembranous ossification, in principle they could have the capacity to form bone through either ossification route.

In this study, we assessed the capacity of adult human nasal septum-derived chondrocytes, appropriately primed *in vitro* through hypertrophic or osteoblastic differentiation, to form bone tissue *in vivo*. NC were cultured also at clonal levels under osteoblastic differentiation conditions to determine the extent of heterogeneity of their *in vitro* osteogenic potential. Exploiting both subcutaneous and orthotopic cranial *in vivo* environments, we then assessed whether human NC could be phenotypically converted to osteoblasts and actively participate in the formation of frank bone tissue. The relative easy availability of a craniofacial-derived somatic cell source [7], capable of active participation in homotopic bone repair without pre-implantation genetic manipulation, would provide a significant and clinically relevant advancement in the field of craniofacial bone repair.

*Correspondence to: Ivan MARTIN, Ph.D., Institute for Surgical Research and Hospital Management, Basel University Hospital, Hebelstrasse 20, Basel 4031, Switzerland.
Tel.: +41-61-265-2384
Fax: +41-61-265-3990
E-mail: ivan.martin@usb.ch

doi: 10.1111/jcmm.12526

# Materials and methods

## Methods

### Cell source and expansion

All cell sources were obtained in accordance with the local ethical committee (University Hospital Basel) and subsequent to informed consent. Nasal septal biopsies were harvested using a punch biopsy tool (6 mm diameter) by first inserting and gently pushing it into the cartilage, taking care not to perforate the opposite side. A total of 3 biopsies from 3 different donors (aged from 52 to 76 years old; two females and one male) were obtained in this manner and used for subsequent experiments. Articular cartilage tissues were harvested post-mortem from full-thickness biopsies of the femoral condyle of 3 patients (aged from 43 to 67 years old; two males and one female). Chondrocytes (both NC and articular chondrocytes, AC) were isolated by enzymatic digestion using collagenase II (Worthington, USA) according to an established protocol [8] and expanded for two passages (corresponding to approximately 7 population doublings) in DMEM complete medium [CM; containing 10% foetal bovine serum, 100 mM HEPES buffer solution, 1 mM sodium pyruvate, 100 U/ml penicillin, 100 mg/ml streptomycin and 292 mg/ml L-glutamine (Gibco, Basel, Switzerland)] supplemented with 5 ng/ml Fibroblast Growth Factor-2 (FGF-2; R&D Systems, Minneapolis, USA). Medium was changed twice a week. Upon confluence, cells were enzymatically retrieved, counted and used as described below. Human bone marrow-derived mesenchymal stromal cells (BMSC; used as a control throughout this study) were isolated from marrow aspirates (volume ~20 ml) obtained from the iliac crest [9] of three patients (37–45 years old, 2 males and 1 female) and expanded for two passages (corresponding to approximately 14 cell population doublings) in α-Modified Eagle's Medium (αMEM) based CM in the presence of 5 ng/ml FGF-2 to enhance their post-expansion bone forming capacity [10].

### Cell-based construct fabrication and culture

Constructs recapitulating the endochondral ossification route were established using a previously described pellet culture system [11]. Briefly, cells (500,000) were centrifuged in 1.5 ml conical polypropylene tubes (Sarstedt, Numbrecht, Germany) to form spherical pellets. Pellets were then cultured in serum free medium (SFM) consisting of DMEM, 4.5 mg/ml D-Glucose, 0.1 mM nonessential amino acids, 1 mM sodium pyruvate, 100 mM HEPES buffer, 100 U/ml penicillin, 100 mg/ml streptomycin, 0.29 mg/ml L-glutamine and Insulin-Transferrin-Selenium (ITS+1) supplemented with 0.1 mM ascorbic acid 2-phosphate, 10 ng/ml transforming growth factor-β1 (TGF-β1) and $10^{-8}$ M dexamethasone [12]. After 3 weeks of chondrogenic culture, medium was changed to hypertrophic induction medium, which consisted of SFM supplemented with 0.1 mM L-ascorbic acid 2-phosphate, $10^{-8}$ M dexamethasone, 50 nM thyroxine and 10 mM β-glycerophosphate [13]. For each experiment and experimental group, at least 2–3 replicate pellets were assessed for each analysis.

Constructs recapitulating intramembranous ossification were established by loading 1 million expanded cells after one passage (average of 4.5 doublings) onto porous calcium phosphate granules (Actifuse™ Microgranules, Apatech, Foxborough, MA, USA) using fibrin gel as a cell carrier, as previously described [14]. To obtain the fibrin mesh, fibrinogen and thrombin components from Tisseel VH S/D (Baxter BioScience, Vienna, Austria) were diluted and mixed as described previously [15]. The fibrinogen component (containing 75–115 mg/ml fibrinogen, +3000 KIE/ml aprotinin) and the thrombin component (containing 400–600 IU/l thrombin + 40 mmol/l calcium chloride) were diluted three and fourfold, respectively, using the specific buffers provided by Baxter. All constructs were maintained in osteogenic medium for 2 weeks before being either ectopically or orthotopically implanted. Osteogenic medium consisted of αMEM CM supplemented with $10^{-8}$ M dexamethasone, 0.1 mM L-ascorbic acid-2-phosphate and 10 mM β-glycerolphosphate. The above experimental procedure was applied for both NC and BMSC and for both cell types under equivalent conditions.

### Clonal production

Nasal chondrocytes were isolated and clonal populations generated according to a previously established procedure [16]. Briefly, cells were extracted from the native nasal septum tissue biopsy (whole population). Single cells from this whole population were plated into one well of a 96-well plate and expanded in DMEM CM supplemented with 1 ng/ml TGF-β1 and 5 ng/ml FGF-2 [17]. Colonies deriving from a single cell were expanded for 3 passages (corresponding to approximately 22 doublings) (clonal population) before testing their osteoblastic differentiation capacity in established *in vitro* assays. Individual colonies were also tested *in vivo* for 8 weeks in subcutaneous pouches using the intramembranous ossification constructs described above.

### Animal models

All *in vivo* procedures were performed in accordance with the standards and protocols of both the University Hospital Basel, Switzerland and Radboud University Nijmegen Medical Centre, Nijmegen, the Netherlands. National guidelines for care and use of laboratory animals were followed and approval was obtained from the country's governing body in which the experimentation occurred.

For subcutaneous implantations, constructs were implanted into the subcutaneous tissue of nude mice (CD1 nu/nu, athymic, 6–8 week-old females, Charles River, Sulzfeld, Germany). Constructs from the same experimental group were implanted in different mice, with up to four constructs implanted per mouse. A total of 6 replicates per experimental group resulted in the use of 5 mice. For orthotopic implantations, bilateral calvarial defects were made in 4 week-old, male nude rats (Crl:NIH-Foxn1rnu, Charles River) as previously described [18]. Constructs were placed into the defects and molded to increase as much as possible the bone to construct contact. Finally, the periosteum and the scalp were closed with 3.0 and 4.0 Vicryl® resorbable sutures (Johnson & Johnson, St. Stevens-Woluwe, Belgium). For both subcutaneous and orthotopic implantations, constructs remained *in vivo* for a total of 12 weeks, whereupon the mice or rats were killed by inhalation of $CO_2$. The constructs were harvested, fixed in 1.5% paraformaldehyde overnight and processed as described below. Redundant. Already described in first paragraph.

## Analytical methods

### Histology

Explanted constructs were fixed overnight in 1.5% paraformaldehyde at 4°C. Ceramic-based constructs were then subjected to slow decalcification in 7% w/v EDTA and 10% w/v sucrose (both from Sigma-Aldrich, Saint Louis, USA) at 37°C on an orbital shaker for 7–10 days. Decalcification solution was refreshed daily. All constructs were then paraffin

embedded (TPC15 Medite, Burgdorf, Germany), sectioned (6-μm-thick) by means of a microtome (Leica, Wetzlar, Germany) and processed for histological, histochemical and immunohistochemical stainings as follows. Standard haematoxylin and eosin (Baker) staining was performed to identify bone tissue formation and maturation stage. According to conventional definitions and in contrast to mere condensation of collagenous structures, frank bone tissue was identified as uniform eosin-pink stained regions, often including a visible rim of lining osteoblasts. Based on haematoxylin and eosin stained sections, quantification of total *de novo* bone area was performed based on 3 different depth sections of 3 different explants ($n = 9$). Total bone area was calculated automatically by totaling the sum of all traced contours of *de novo* bone spots using CellSense Dimension software (Olympus, Tokyo, Japan). Safranin-O (Fluka, Buchs, Switzerland) staining allowed investigating the presence of sulphated proteoglycans inside the construct, characteristic of cartilaginous tissue. The matrix characterization in cartilaginous constructs was assessed by immunostaining for human collagen type II (COLL II) and collagen type X (COLL X) (MP Biomedicals LLC, Santa Ana, USA and Abcam PLC, Cambridge, UK respectively). Upon rehydratation in ethanol series, sections were treated as described previously for antigen retrieval for COLL X according to the manufacturer's instructions [13]. The presence of vessels was detected by immunostaining for CD31 (Abcam 28364). The immunobinding was detected with biotinylated secondary antibodies and using the appropriate Vectastain ABC kits (Vector Laboratories, Burlingame, USA). The red signal was developed with the Fast Red kit (Dako Cytomation Dako, Glostrup, Denmark) and sections counterstained by Haematoxylin. Negative controls were performed during each analysis by omitting the primary antibodies. Human cells in the explants were identified by chromogenic *in situ* hybridisation for the human-specific sequence ALU, using a biotin-conjugated DNA probe (ZytoVision GMBH, Bremerhaven, Germany), as per the manufacturers guidelines. Histological and immunohistochemical sections were analysed using an Olympus BX-61 microscope.

### Calcium and DNA quantification

Extracellular matrix associated calcium present on all applicable constructs was determined colorimetrically on a Spectra Max 190 microplate colorimeter (Molecular Devices, Sunnyvale, USA) as previously described [19] and as per the manufacturer's protocol (Total Calcium Assay, Randox, Crumlin, UK). Total calcium was normalized to total DNA present in a replicate construct.

To quantify total DNA per construct, collected samples were digested with proteinase K solution (1 mg/ml proteinase K, 50 mM TRIS, 1 mM EDTA, 1 mM iodoacetamide, and 10 mg/ml pepstatin-A (Sigma-Aldrich) in double distilled water or potassium phosphate buffer for 16 hrs at 56°C as previously described [20]. DNA quantification was performed by means of CyQUANT® Cell Proliferation Assay (Invitrogen, Waltham, USA). Working solutions were prepared according to the manufacturer's protocols. The analyses were carried out measuring fluorescence with a Spectra Max Gemini XS Microplate Spectrofluorometer (Molecular Devices). Excitation and emission wavelengths were, respectively, 485 and 538 nm. Samples in each plate included a calibration curve. Each sample was measured in triplicate.

### Real-time PCR

Total RNA extraction, cDNA synthesis and real-time reverse transcriptase-polymerase chain reaction (RT-PCR; 7300 AB Applied Biosystems, Foster City, USA) were performed to quantify expression levels of the following genes of interest: COLL II, COLL X, bone sialoprotein (BSP), osteocalcin (OC) [16], collagen type I (COLL I), osteopontin (OP), osteonectin (ON), RUNX2, bone morphogenetic protein 2 (BMP2), bone morphogenic protein 4 (BMP4-Applied Biosystems Ref. number: Hs00181626_m1), Matrix Metalloproteinase-13 (MMP13-Applied Biosystems, Ref. number: Hs00233992_m1), alkaline phosphatase (ALP-Applied Biosystems Ref. number: Hs01029144_m1), osterix (SP7-Applied Biosystems, Ref. number: Hs00541729_m1), indian hedgehog homolog (IHH-Applied Biosystems, Ref. number: Hs01081800_m1), glioma associated oncogene homolog-1 (GLI1-Applied Biosystems, Ref. number: Hs00171790_m1), parathyroid hormone 1 receptor (PTH1R-Applied Biosystems, Ref. number: Hs00174895_m1), bone morphogenetic protein 4 (BMP-4, Applied Biosystems, Ref. number: Hs00181626_m1), and chondromodulin (LECT1, Applied Biosystems, Ref. number: Hs00993254_m1). Glyceraldehyde 3-phosphate dehydrogenase (GAPDH) was used as housekeeping, reference gene.

### Statistics

Data are presented as mean ± SD; N is indicated in the figure legends. For statistical testing one-way ANOVA was performed for multi-condition experiments using the Graphpad Prism software (Version 5.02, Graphpad Software, San Diego, USA).

## Results

### *In vitro* hypertrophic NC form stable cartilage *in vivo*

We first tested endochondral ossification as a potential bone forming route for NC. Using a previously established protocol for the production of engineered hypertrophic cartilage tissues using BMSC [13], expanded NC were cultured as pellets in chondrogenic medium followed by hypertrophic induction. After chondrogenic induction, the resulting tissues displayed clear cartilaginous features, including positive Safranin-O staining for glycosaminoglycans (GAG) (Fig. 1A) and large cells in lacunae embedded in abundant, mineral free matrix positive for COLL II (data not shown). Subsequent hypertrophic induction produced areas of enlarged cells (Fig. 1B) with associated mineral deposition (Fig. 1C) and positively stained for COLL X (Fig. 1D). The expression of genes encoding for the above proteins matched the immunohistochemical findings and paralleled the expression profiles found in BMSC undergoing the same culture regime, including up-regulation of BSP and COLL-10 (Fig. 1E). Analysis of the pathways involved in endochondral ossification on cells from the hypertrophy-induced constructs showed up-regulation of IHH, PTH1R and GLI1 to levels approaching those reached by BMSC and clearly distinct from AC (Fig. 1E).

Implantation into subcutaneous pockets of nude mice of both chondrogenic- and hypertrophy-induced constructs ($n = 3$) yielded similar results at the analysed time-points. Hypertrophic explants underwent remodelling *in vivo*, resulting after 5 weeks in a marked decrease in Safranin-O staining intensity and of positivity for COLL



Journal of Cellular and Molecular Medicine published by John Wiley & Sons Ltd and Foundation for Cellular and Molecular Medicine.

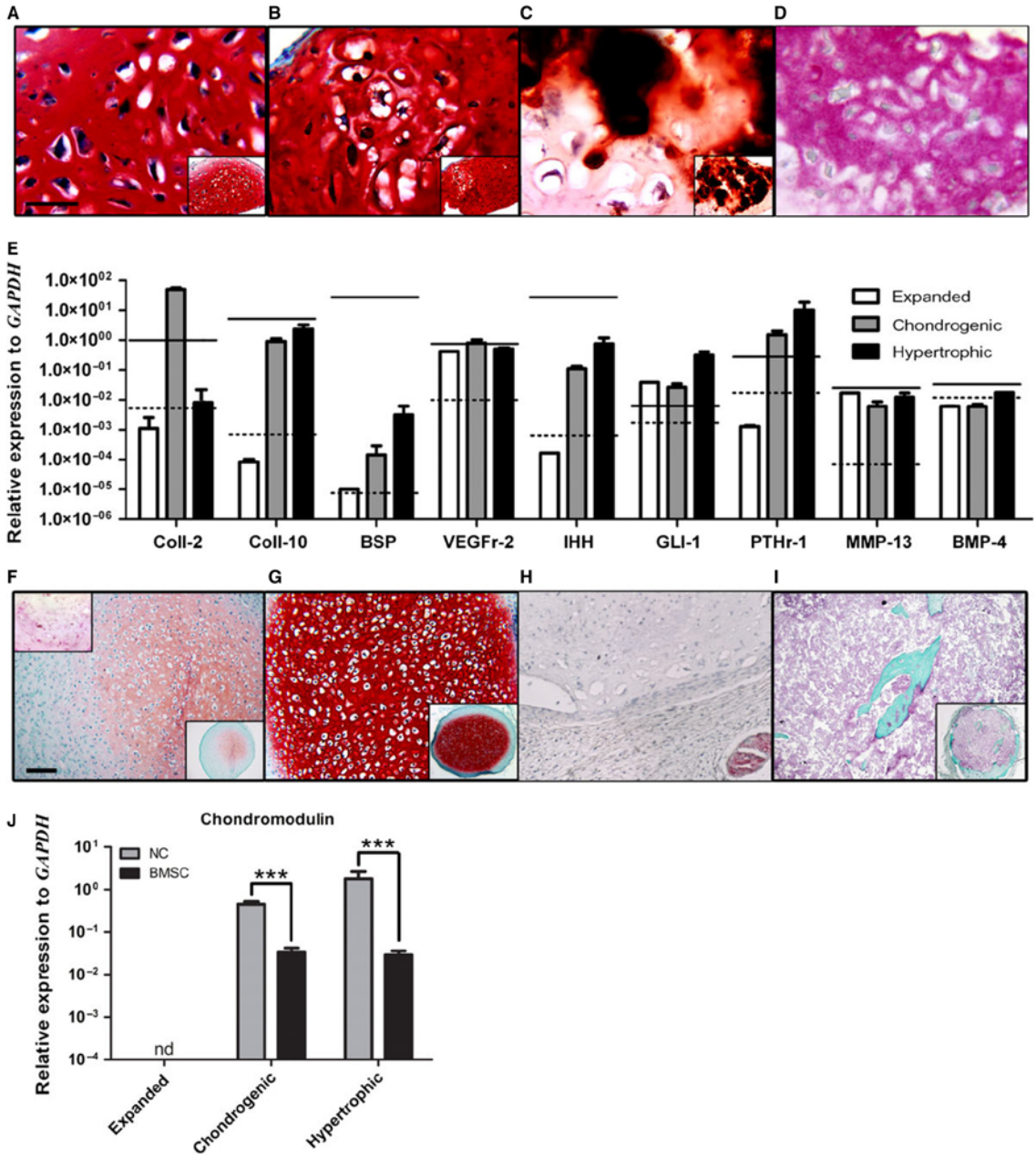


**Fig. 1** NC can form hypertrophic-like tissue *in vitro*, but revert to stable cartilage *in vivo*. *In vitro analysis*: Safranin-O staining of (**A**) chondrogenic- and (**B**) hypertrophic-induced NC constructs with (**C**) corresponding alizarin red staining of hypertrophic-induced NC constructs. (**D**) Immunohistochemistry staining of collagen type X in hypertrophic-induced NC constructs. (**E**) Gene expression analysis of NC (bars) compared to hypertrophic-induced AC (black dotted lines) and BMSC (black solid lines); $n = 3$. *In vivo analysis*: (**F**) Safranin-O and Collagen type X (upper left insert) staining of NC-based *in vitro* hypertrophic-induced constructs explanted after 5 weeks. (**G**) Safranin-O staining of NC-based *in vitro* hypertrophic-induced constructs explanted after 12 weeks subcutaneous implantation. (**H**) Immunohistochemistry staining of CD31 in 12 week explants. (**I**) Masson's trichrome staining of BMSC-based *in vitro* hypertrophic-induced constructs explanted after 12 weeks subcutaneous implantation. (**J**) Real-time RT-PCR analyses carried out using specific primers for chondromodulin expressed by expanded NC and NC cultured under chondrogenic or hyperthrophic conditions. Levels are normalized to glyceraldehyde 3-phosphate dehydrogenase (GAPDH). Values are mean ± SD of $n = 3$ donors performed in duplicates, $***P \leq 0.001$. nd = under the limit of detection. Scale bars = 100 μm; nd = under the limit of detection. scale bars are the same for **A**–**D** and **F**–**I**. For all immunohistochemical analyses negative controls omitting the primary antibodies were performed resulting in the absence of the specific signals (data not shown).

X immunostaining (Fig. 1F). After 12 weeks *in vivo*, NC-based constructs consistently established a GAG-rich cartilage tissue (Fig. 1G) negative for COLL X (data not shown), in contrast to BMSC-based constructs which proceeded throughout endochondral ossification as previously described (Fig. 1I) [13]. Successful endochondral bone remodelling is known to hinge upon the vascularization of the implanted construct [21], whereas CD31 staining of explanted NC-based constructs demonstrated a total lack of vessel invasion from the host vasculature (Fig. 1H). Additionally, the mRNA expression of chondromodulin, a potent anti-angiogenic factor specific to cartilage [22], was strongly up-regulated in NC during chondrogenic differentiation and hypertrophic induction. This was in contrast to BMSC, which maintained a statistically significant lower expression level throughout hypertrophy (Fig. 1J). In summary, we demonstrated that NC can acquire a phenotype characteristic of hypertrophic cartilage under *in vitro* stimulation, but then revert back to stable chondrocytes upon *in vivo* implantation in a subcutaneous environment.

## Intramembranous ossification of NC in a subcutaneous environment is inefficient

We next analysed the capacity of NC to differentiate directly towards an osteoblastic phenotype *in vitro* and then undergo intramembranous ossification upon implantation *in vivo*. Expanded NC were exposed to osteogenic stimuli in either monolayer cultures (2D) or after embedding within ceramic-fibrin materials (3D). In 2D cultures, accumulation of mineral deposits in the extracellular matrix reached levels similar to those of BMSC

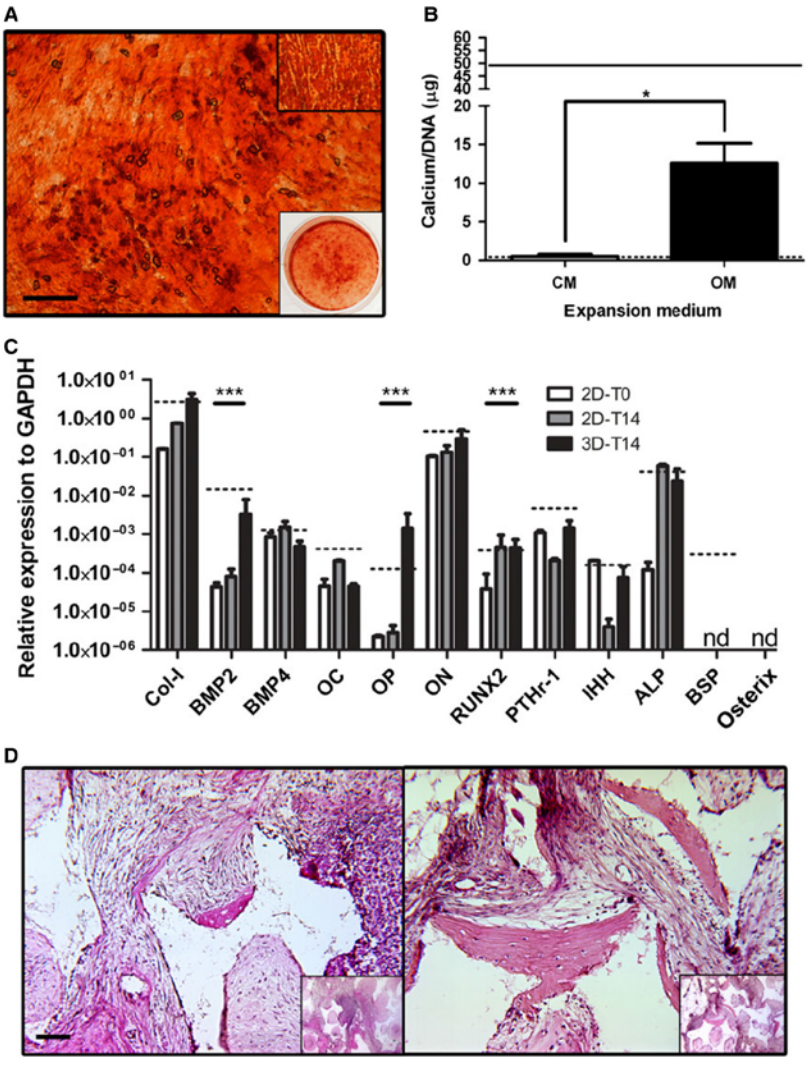


**Fig. 2** NC can osteoblastically differentiate, but do not efficiently proceed through intramembranous ossification in a subcutaneous environment. (**A**) Alizarin red staining of NC following osteogenic culture conditions (upper right box = BMSC under same conditions; lower right box = low magnification of whole well NC; scale bar = 1 mm). (**B**) Quantification of calcium matrix deposition of NC in complete medium (CM) and osteogenic medium (OM). Solid and dotted black lines represent calcium values for BMSC and AC, respectively, when cultured in OM. $*P < 0.05$; $n = 3$. (**C**) Gene expression levels of NC after expansion, after 2 weeks osteogenic induction in a monolayer (2D-T14) and after 2 weeks osteogenic induction in a 3D construct (3D-T14). Dotted line represents BMSC expression values at 3D-T14 time-point. nd = under the limit of detection. $***P < 0.001$; represented significant differences noted only for selected markers of osteoblastic differentiation comparing 2D-T0 to 3D-T14; $n = 3$. (**D**) Haematoxylin and eosin staining of NC (left; one of only two bone ossicles detected) and BMSC (right) explanted 3D constructs after 8 weeks *in vivo*. Inserts are low magnification images of the entire constructs; scale bar = 100 µm.



Journal of Cellular and Molecular Medicine published by John Wiley & Sons Ltd and Foundation for Cellular and Molecular Medicine.

(Fig. 2A). Quantification of calcium per cell deposited onto the matrix was consistent with the intensity of alizarin red staining and indicated that osteogenically cultured NC could mineralize the ECM to an intermediate level between AC and BMSC (Fig. 2B). Osteogenic stimulation in 2D culture resulted in the up-regulation of osteoblast-related genes, *e.g.* RUNX2 and ALP. Up-regulation of further osteoblastic genes, *e.g.* BMP2, OP and COLL-1, occurred in the 3D culture system, although BSP and osterix levels remained undetectable, indicating that *in vitro* osteogenically differentiated NC did not become fully functional osteoblastic cells. There was also an up-regulation of PTH1R and IHH in 3D constructs (8 and 10 times, respectively), but expression levels remained over 4 orders of magnitude lower than those seen during hypertrophic induction (Fig. 2C), suggesting minimal hedgehog pathway activity. Implantation of 3D constructs ($n = 3$) after osteogenic differentiation into subcutaneous pockets of nude mice resulted in limited bone formation (only 2 scattered small bone regions) in only 1 of the 3 donors tested, while BMSC resulted in robust bone formation (reproducible presence of several frank bone areas in each construct; Fig. 2D). We then decided to test whether this inefficient production of bone was a result of a limited fraction of cells present in the whole NC population that would be capable of osteogenic differentiation and bone matrix deposition.

## Clonal strains of NC have heterogeneous osteoblastic differentiation capacities

A clonal study was performed to investigate the percentage of cells with osteogenic capacity present within the whole extracted NC population. The colony forming efficiency of NC, here defined as the percentage of plated single cells able to form a colony, was 36.5%. During the extensive expansion phase, including two passages, NC clones maintained an average proliferation rate of 0.90 ± 0.16 doublings/day, resulting in an average of 22.6 ± 1.1 total doublings. Cells isolated from the individual colonies were cultured in 2D in osteogenic medium. Mineralization capacity of the individual NC clonal populations was highly heterogeneous, as assessed by alizarin red staining and quantification of the amount of deposited calcium (Fig. 3A). Expression analysis of the master gene for osteoblastic differentiation (RUNX2) [23–25] showed a positive correlation between its up-regulation and the mineralization capacity of the clonal strains (Fig. 3B). Upon combination with fibrin-ceramic granules and implantation into subcutaneous pouches of nude mice, variances in matrix density were observed between implanted clones. In particular, clonal populations expressing higher amounts of RUNX2 *in vitro* resulted in higher tissue densities *in vivo* (Fig. 3C). However, no individual clone was able to generate frank bone tissue.

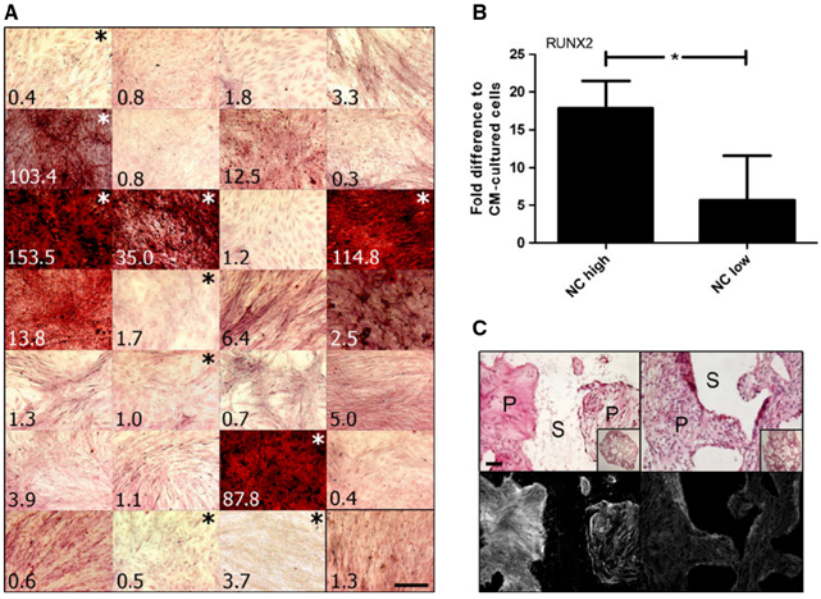


**Fig. 3** Clonal populations representing elevated intradonor heterogeneity and osteogenic capacity within a whole NC population. (**A**) Alizarin red staining of matrix obtained after 2 weeks osteogenic induction of all the individual clones from total population of NC. Numbers in bottom left of each image refer to total calcium (μg Ca/μg DNA) associated with a duplicate well. Lower right black-boxed image represents whole NC population. (**B**) qPCR of RUNX2 expression in NC clonal populations following osteogenic stimulation; $n = 4$. (**C**) Representative haematoxylin and eosin (upper row) and red filter florescence imaging of haematoxylin and eosin stained tissues to show relative collagen fibril densities (lower row) of explanted clones; Left column = NC high; right column = NC low. NC high = clones with intense alizarin red staining (indicated with white asterisk); NC low = clones with little to no alizarin red staining (indicated with black asterisk). S = decalcified scaffold (no cells present), P = pores of the scaffold (presence of cells and tissue development); scale bars = 100 μm.

## NC participate in bone formation in an orthotopic environment

We next hypothesized that an orthotopic environment could be necessary to support the NC towards more efficient bone formation. We thus implanted osteogenically induced NC and BMSC ($n = 3$) in 3D constructs into bilateral calvarial defects for 8 weeks. Upon explantation, two types of bone formation were observed: ingrowth bone from surgical margins, indicative of osteoconduction, and *detached bone*, here defined as ossicles without osseous link to the ingrowth bone, indicative of osteogenesis (Fig. 4A and B). Human cells were found throughout the repair tissue, as assessed by Alu sequence staining,

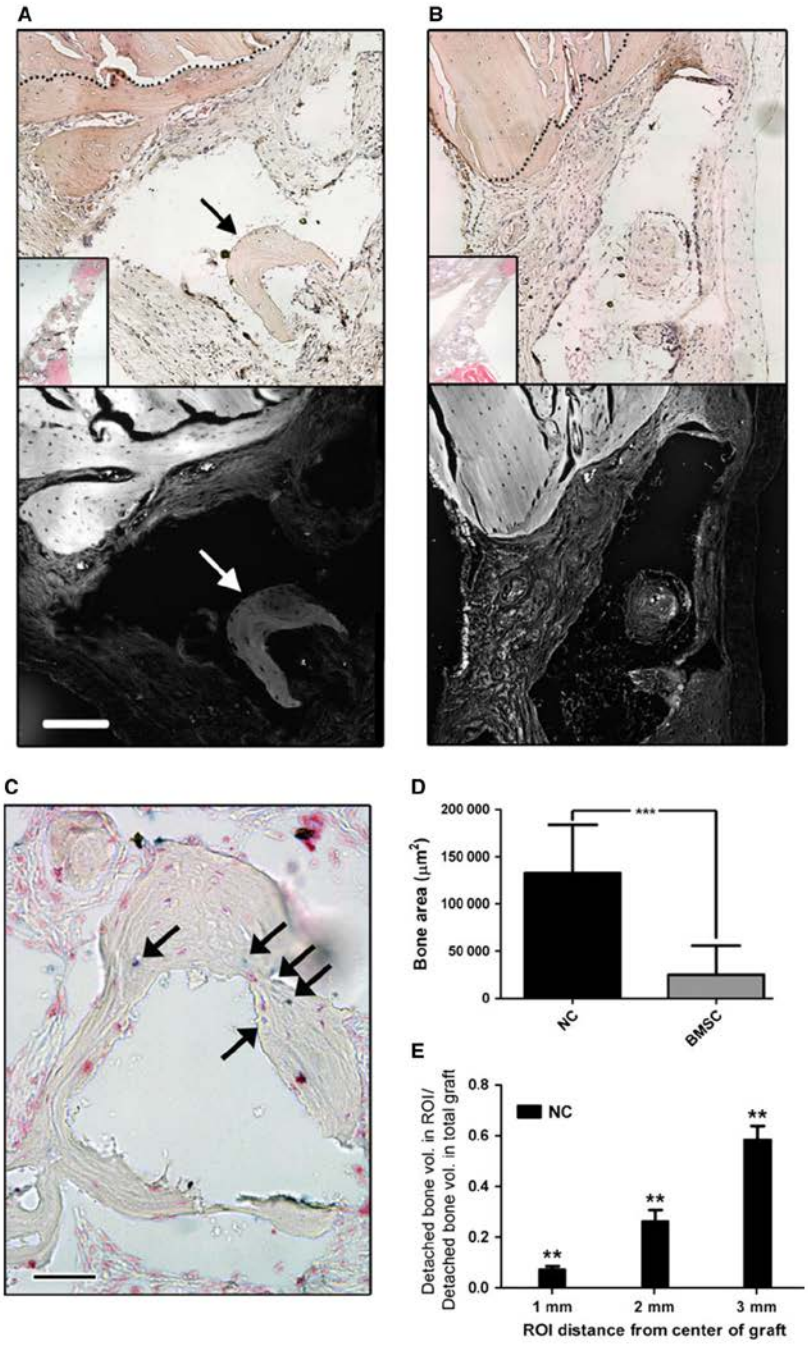


**Fig. 4** NC participate in bone formation in calvarian bone defects. Haematoxylin and eosin staining of explanted NC-based (**A**) and BMSC-based (**B**) constructs; Bottom images for both **A** and **B** are red filter florescence imaging of haematoxylin and eosin stained tissues to show relative collagen fibril densities; scale bar = 1 mm. Black and white arrows in **A** indicate detached bone ossicles. (**C**) *In situ* hybridization of human specific Alu sequences in an NC-based explanted construct; black arrows point to human nuclei; scale bar = 100 μm. (**D**) Histological section-based quantification of total detached bone volume; $n = 3$. (**E**) MicroCT-based quantification of detached bone formation (osteogenesis) 8 weeks after implantation into calvarial defects, demonstrating decreasing bone formation towards the centre of the construct. MicroCT was performed as described by Scotti *et al.* [13]. Values are means ± SD of $n = 9$ per group (for each of the 3 implants per group, 3 regions were quantified). Significant differences from one experimental group to both other groups is indicated; $^{**}P < 0.01$. ROI = region of interest.

and also within the areas of *detached bone* (Fig. 4C and Fig. S1). Quantification of *detached bone* volume areas in explanted constructs revealed an average of over 5 times more bone formation by NC than by BMSC (Fig. 4D). Micro-CT analysis indicated that, while bone was found to be present even in the centre of the constructs, total *detached bone* volume decreased with the distance from the defect edges (Fig. 4E). This finding suggests that the construct itself was not intrinsically osteoinductive, but the soluble signals from the native bone defect were responsible for the osteoblastic switch of the NC (Fig. 4E). The result could be alternatively explained by an increased mortality of NC in the inner implant regions, as a result of lack of nutrients at the time of implantation. Interestingly, no BMSC were detected in the explants, whereas NC remained viable and were present throughout the *de novo*-formed tissue within the explants (Fig. S1).

## Discussion

This study provides a proof-of-principle that NC can directly convert into bone cells and actively participate in bone tissue formation. This was not observed in ectopic implantation models, even following hypertrophic or osteoblastic *in vitro* priming or clonal selection, but critically required a craniofacial, orthotopic *in vivo* environment. In that model, the efficiency of survival and bone formation by NC was significantly higher than that of reference osteogenic cells, namely BMSC.

Considering NC normally form a cartilage tissue *in situ*, we first wanted to determine if they could proceed through endochondral ossification. The phenotype acquired by NC after *in vitro* hypertrophic induction resembled that of BMSC, not only including COLL X deposition, but also the acquisition of a genetic signature known to be reflective of endochondral ossification [13]. While BMSC could effectively form a functional bone organ *in vivo* after *in vitro* stimulation to a hypertrophic phenotype [26], under the same conditions NC did not develop into bone, but rather formed a stable cartilage tissue. The inability of NC to continue through the endochondral ossification route suggests that typical markers associated with endochondral bone formation (*e.g.*, COLL X and IHH) [27] are not sufficient to establish the process. Considering that vascularization is critically required for endochondral bone formation *in vivo* [21], our finding could be related with the elevated production by NC of chondromodulin, a strong anti-angiogenic factor implicated in blocking hypertrophic cartilage vascularization and subsequent tissue turnover to bone [28].

Direct *in vitro* osteogenic stimulation of NC demonstrated that not only could NC produce a mineralized extracellular matrix just as effectively as BMSC, but that NC acquired a genetic profile similar to BMSC under the same conditions. In 3D culture, NC up-regulation of BMP2 and OP, combined with downregulation of the chondrogenic factor BMP4, is consistent with the osteoblastic differentiation profiles previously reported in neural crest progenitors [29]. IHH was not up-regulated during osteogenic differentiation, consistent with the findings that its expression by neuroectodermally derived pre-osteoblasts inhibits further osteoblastic differentiation [30]. In a subcutaneous implant environment, NC were capable to form frank bone tissue at a very low efficiency, suggesting that either the *in vitro* pre-osteogenic commitment was not stable enough to have a relevant *in vivo* effect or that only a small proportion of cells were competent to become fully functional osteoblasts. A clonal study designed to address the latter hypothesis demonstrated that none of the clonal strains implanted ectopically resulted in bone formation. However, these findings could have been intrinsically biased by the extensive population doublings underwent by the clonal populations (average of 22) as compared to the typical ones (average of 4.5) required for expansion of a whole NC population. Extensive proliferation has in fact been associated with the loss of *in vivo* osteogenic differentiation capacity in other mesenchymal precursor cell systems [31, 32]. Although the clonal experiments designed to explain the limited efficiency were not conclusive, the results of the multiclonal implantation proved that NC have the capacity to form frank bone tissue by direct osteoblastic differentiation, in contrast to the previously targeted route of endochondral ossification. Indeed, Calloni *et al.* postulated that bone cells from the craniofacial region arise from specific progenitors distinct from the osteochondrogenic, endochondral like ones found in long bones [25], thus further supporting a preferential capacity of NC to undergo intramembranous ossification.

To induce a more efficient direct osteoblastic transformation of NC, we next tested the cues present in an orthotopic environment. The cranial defect model used in this study reflects not only a bone environment that forms and heals through intramembranous ossification [33–35], but also a mixed embryological origin site providing homotopic (neuroectodermally- and mesodermally derived) signals for both cell types implanted (NC and BMSC) [36–38]. Using this model we demonstrated, for the first time to the best of our knowledge, that a population with a previously considered stable chondrocytic phenotype could be converted into osteoblastic cells forming frank bone tissue *in vivo*. The behaviour of NC is different from that of AC, reported to form stable cartilage when implanted into calvarial defects [39], and could be reminiscent of embryonic neural crest-derived cells, which supported bone healing in a cranial defect upon differentiation into chondrocytes [40, 41]. Unexpectedly, under our experimental conditions, NC-based constructs outperformed BMSC-based ones in terms of osteogenesis and survival in the repair tissue. Indeed while large numbers of human NC could be detected in the repair tissue, no living BMSC could be observed. Obviously we cannot exclude that very few BMSC did survive, in which case their contribution to bone formation would likely be appreciated only after longer *in vivo* time. Mankani *et al.* in fact reported that bone formation by human BMSC in the calvarial defects of rats occurred at time-points superior to 8 week [42]. Collectively, these results indicate that the implanted BMSC have a positive influence on vascularization and osteogenesis primarily by the release of trophic factors [43–45] as opposed to the survival after acquisition of an osteoblastic phenotype. Instead, the direct contribution of NC to bone formation, at least in the assessed time frame, demonstrates an intrinsically different mode of action, possibly related to the homotopic neuroectoderm nature of the cell origin and implantation site [46, 47]. Further studies will be necessary to investigate which environmental cues are responsible for the osteogenic induction of NC

at the orthotopic and homotopic site, as well as to further characterize whether or not only specific subpopulations of NC can be effectively converted into osteoblasts. Indeed, it cannot be excluded that bone tissue was formed in our model by undifferentiated mesenchymal progenitors, either included within the nasal cartilage or – despite meticulous separation from the perichondral membrane – derived from a contaminant population from surrounding tissues.

A cell-based therapy has the potential to accelerate and improve the repair efficiency of critically sized craniofacial defects, but an adequate cell source has yet to be identified [48]. Common cell-based strategies rely on BMSC or apical bone-derived osteoblasts, both of which display limited repair capacities [49] and associated drawbacks (low yield, donor site morbidity and high intradonor variability). NC could represent a homotopic cell source accessible under minimally invasive conditions and possibly used in autologous settings. Autologous NC have recently been clinically used for the reconstruction of the alar lobule [50] and are currently being tested for the treatment of articular cartilage defects at the University Hospital Basel (clinicaltrials.gov identifier: NCT01605201) [51]. Their demonstrated ability to directly convert into a functional bone cell provides a proof-of-principle that the same cells may be further investigated in pre-clinical models for bone regeneration.

## Acknowledgements

The research leading to these results has received funding from the European Community's Seventh Framework Program (MultiTERM, grant agreement no. 238551) and the Swiss National Science Foundation (SNF project no 310030-126965.1). We kindly thank Waldemar Hoffmann for his technical assistance for certain experimental techniques associated with this study.

## Conflicts of interest

The authors confirm that there are no conflicts of interest.

## Author contribution

Study design: BEP, MV, KP, CJ, AS, XFW, AB and IM. Data collection: BEP, MV, KP, SF and AB. Data analysis: BEP, MV, KP, AS, XFW and AB. Data interpretation: BEP, MV, KP, CJ, AS, XFW, AB and IM. Drafting manuscript: BEP. Revising manuscript content: BEP, AB and IM. Approving final version of manuscript: BEP, MV, KP, CJ, AS, XFW, AB and IM. BEP, KP, AS, AB and IM take responsibility for the integrity of the data analyses.

## Supporting information

Additional Supporting Information may be found in the online version of this article:

**Figure S1** *In situ* hybridization for human specific Alu sequences demonstrating the large presence of remaining (A) NC after 8 weeks calvarian implementation *versus* no detected presence of (B) BMSC under the same implant regime.

## References

1. **Achilleos A, Trainor PA.** Neural crest stem cells: discovery, properties and potential for therapy. *Cell Res.* 2012; 22: 288–304.
2. **Hall BK, Precious DS.** Cleft lip, nose, and palate: the nasal septum as the pacemaker for midfacial growth. *Oral Surg Oral Med Oral Pathol Oral Radiol.* 2013; 115: 442–7.
3. **Verwoerd CDA, Verwoerd-Verhoef HL.** Rhinosurgery in children: basic concepts. *Facial Plast Surg.* 2007; 23: 219–30.
4. **Kergosien N, Sautier J, Forest N.** Gene and protein expression during differentiation and matrix mineralization in a chondrocyte cell culture system. *Calcif Tissue Int.* 1998; 62: 114–21.
5. **Shafiee A, Kabiri M, Ahmadbeigi N, *et al.*** Nasal septum-derived multipotent progenitors: a potent source for stem cell-based regenerative medicine. *Stem Cells Dev.* 2011; 20: 2077–91.
6. **Shapiro F.** Bone development and its relation to fracture repair. The role of mesenchymal osteoblasts and surface osteoblasts. *Eur Cell Mater.* 2008; 15: 53–76.
7. **Siegel NS, Gliklich RE, Taghizadeh F, *et al.*** Outcomes of septoplasty. *Otolaryngol Head Neck Surg.* 2000; 122: 228–32.
8. **Candrian C, Vonwil D, Barbero A, *et al.*** Engineered cartilage generated by nasal chondrocytes is responsive to physical forces resembling joint loading. *Arthritis Rheum.* 2008; 58: 197–208.
9. **Frank O, Heim M, Jakob M, *et al.*** Real-time quantitative RT-PCR analysis of human bone marrow stromal cells during osteogenic differentiation *in vitro*. *J Cell Biochem.* 2002; 85: 737–46.
10. **Martin I, Muraglia A, Campanile G, *et al.*** Fibroblast growth factor-2 supports *ex vivo* expansion and maintenance of osteogenic precursors from human bone marrow. *Endocrinology.* 1997; 138: 4456–62.
11. **Acharya C, Adesida A, Zajac P, *et al.*** Enhanced chondrocyte proliferation and mesenchymal stromal cells chondrogenesis in coculture pellets mediate improved cartilage formation. *J Cell Physiol.* 2012; 227: 88–97.
12. **Jakob M, Démarteau O, Schäfer D, *et al.*** Specific growth factors during the expansion and redifferentiation of adult human articular chondrocytes enhance chondrogenesis and cartilaginous tissue formation *in vitro*. *J Cell Biochem.* 2001; 81: 368–77.
13. **Scotti C, Tonnarelli B, Papadimitropoulos A, *et al.*** Recapitulation of endochondral bone formation using human adult mesenchymal stem cells as a paradigm for developmental engineering. *Proc Natl Acad Sci USA.* 2010; 107: 7251–6.
14. **Müller AM, Mehrkens A, Schäfer DJ, *et al.*** Towards an intraoperative engineering of osteogenic and vasculogenic grafts from the stromal vascular fraction of human adipose tissue. *Eur Cell Mater.* 2010; 19: 127–35.
15. **Bensaïd W, Triffitt JT, Blanchat C, *et al.*** A biodegradable fibrin scaffold for mesenchymal stem cell transplantation. *Biomaterials.* 2003; 24: 2497–502.
16. **Barbero A, Ploegert S, Heberer M, *et al.*** Plasticity of clonal populations of dedifferentiated

adult human articular chondrocytes. *Arthritis Rheum*. 2003; 48: 1315–25.

17. **Wolf F, Candrian C, Wendt D, *et al.*** Cartilage tissue engineering using pre-aggregated human articular chondrocytes. *Eur Cell Mater*. 2008; 16: 92–9.
18. **Ventura M, Franssen GM, Oosterwijk E, *et al.*** SPECT *vs.* PET monitoring of bone defect healing and biomaterial performance *in vivo*. *J Tissue Eng Regen Med*. 2014; Doi:10.1002/TERM.1862.
19. **Sadr N, Pippenger BE, Scherberich A, *et al.*** Enhancing the biological performance of synthetic polymeric materials by decoration with engineered, decellularized extracellular matrix. *Biomaterials*. 2012; 33: 5085–93.
20. **Piccinini E, Sadr N, Martin I.** Ceramic materials lead to underestimated DNA quantifications: a method for reliable measurements. *Eur Cell Mater*. 2010; 20: 38–44.
21. **Harper J, Klagsbrun M.** Cartilage to bone–angiogenesis leads the way. *Nat Med*. 1999; 5: 617–8.
22. **Hiraki Y, Shukunami C.** Chondromodulin-I as a novel cartilage-specific growth-modulating factor. *Pediatr Nephrol*. 2000; 14: 602–5.
23. **Komori T, Yagi H, Nomura S, *et al.*** Targeted disruption of Cbfa1 results in a complete lack of bone formation owing to maturational arrest of osteoblasts. *Cell*. 1997; 89: 755–64.
24. **Ducy P, Zhang R, Geoffroy V, *et al.*** Osf2/Cbfa1: a transcriptional activator of osteoblast differentiation. *Cell*. 1997; 89: 747–54.
25. **Calloni GW, Le Douarin NM, Dupin E.** High frequency of cephalic neural crest cells shows coexistence of neurogenic, melanogenic, and osteogenic differentiation capacities. *Proc Natl Acad Sci USA*. 2009; 106: 8947–52.
26. **Scotti C, Piccinini E, Takizawa H, *et al.*** Engineering of a functional bone organ through endochondral ossification. *Proc Natl Acad Sci USA*. 2013; 110: 3997–4002.
27. **Long F, Chung U, Ohba S, *et al.*** Ihh signaling is directly required for the osteoblast lineage in the endochondral skeleton. *Dev Cambridge Engl*. 2004; 131: 1309–18.
28. **Shukunami C, Hiraki Y.** Role of cartilage-derived anti-angiogenic factor, chondromodulin-I, during endochondral bone formation. *Osteoarthritis Cartilage*. 2001; 9: S91–101.
29. **Abzhanov A, Rodda SJ, McMahon AP, *et al.*** Regulation of skeletogenic differentiation in cranial dermal bone. *Development*. 2007; 134: 3133–44.
30. **Long F.** Building strong bones: molecular regulation of the osteoblast lineage. *Nat Rev Mol Cell Biol*. 2012; 13: 27–38.
31. **Banfi A, Muraglia A, Dozin B, *et al.*** Proliferation kinetics and differentiation potential of *ex vivo* expanded human bone marrow stromal cells: implications for their use in cell therapy. *Exp Hematol*. 2000; 28: 707–15.
32. **Digirolamo CM, Stokes D, Colter D, *et al.*** Propagation and senescence of human marrow stromal cells in culture: a simple colony-forming assay identifies samples with the greatest potential to propagate and differentiate. *Br J Haematol*. 1999; 107: 275–81.
33. **Rosen V, Thies RS.** The BMP proteins in bone formation and repair. *Trends Genet*. 1992; 8: 97–102.
34. **Tsuji K, Bandyopadhyay A, Harfe BD, *et al.*** BMP2 activity, although dispensable for bone formation, is required for the initiation of fracture healing. *Nat Genet*. 2006; 38: 1424–9.
35. **Couly GF, Coltey PM, Le Douarin NM.** The triple origin of skull in higher vertebrates: a study in quail-chick chimeras. *Development*. 1993; 117: 409–29.
36. **Wilkie AO, Morriss-Kay GM.** Genetics of craniofacial development and malformation. *Nat Rev Genet*. 2001; 2: 458–68.
37. **Leucht P, Kim J-B, Amasha R, *et al.*** Embryonic origin and Hox status determine progenitor cell fate during adult bone regeneration. *Development*. 2008; 135: 2845–54.
38. **Koyabu D, Maier W, Sánchez-Villagra MR.** Paleontological and developmental evidence resolve the homology and dual embryonic origin of a mammalian skull bone, the interparietal. *Proc Natl Acad Sci USA*. 2012; 109: 14075–80.
39. **Vacanti CA, Kim W, Upton J, *et al.*** The efficacy of periosteal cells compared to chondrocytes in the tissue engineered repair of bone defects. *Tissue Eng*. 1995; 1: 301–8.
40. **Montufar-Solis D, Nguyen HC, Nguyen HD, *et al.*** Using cartilage to repair bone: an alternative approach in tissue engineering. *Ann Biomed Eng*. 2004; 32: 504–9.
41. **Doan L, Kelley C, Luong H, *et al.*** Engineered cartilage heals skull defects. *Am J Orthod Dentofacial Orthop*. 2010; 137: 162–3.
42. **Mankani MH, Kuznetsov SA, Wolfe RM, *et al.*** *In vivo* bone formation by human bone marrow stromal cells: reconstruction of the mouse calvarium and mandible. *Stem Cells*. 2006; 24: 2140–9.
43. **Caplan AI, Correa D.** The MSC an injury drugstore. *Cell Stem Cell*. 2011; 9: 11–5.
44. **Osugi M, Katagiri W, Yoshimi R, *et al.*** Conditioned media from mesenchymal stem cells enhanced bone regeneration in rat calvarial bone defects. *Tissue Eng Part A*. 2012; 18: 1479–89.
45. **Zhou Y, Fan W, Prasadam I, *et al.*** Implantation of osteogenic differentiated donor mesenchymal stem cells causes recruitment of host cells. *J Tissue Eng Regen Med*. 2012; Doi:10.1002/TERM.1619.
46. **Matsubara T, Suardita K, Ishii M, *et al.*** Alveolar bone marrow as a cell source for regenerative medicine: differences between alveolar and iliac bone marrow stromal cells. *J Bone Miner Res*. 2005; 20: 399–409.
47. **Akintoye SO, Lam T, Shi S, *et al.*** Skeletal site-specific characterization of orofacial and iliac crest human bone marrow stromal cells in same individuals. *Bone*. 2006; 38: 758–68.
48. **Jheon AH, Schneider RA.** The cells that fill the bill: neural crest and the evolution of craniofacial development. *J Dent Res*. 2009; 88: 12–21.
49. **Pagni G, Kaigler D, Rasperini G, *et al.*** Bone repair cells for craniofacial regeneration. *Adv Drug Deliv Rev*. 2012; 64: 1310–9.
50. **Fulco I, Miot S, Haug MD, *et al.*** Engineered autologous cartilage tissue for nasal reconstruction after tumour resection: an observational first-in-human trial. *Lancet*. 2014; 384: 337–46.
51. **Pelttari K, Pippenger B, Mumme M, *et al.*** Adult human neural crest-derived cells for articular cartilage repair. *Sci Transl Med*. 2014; 6: 251ra119.

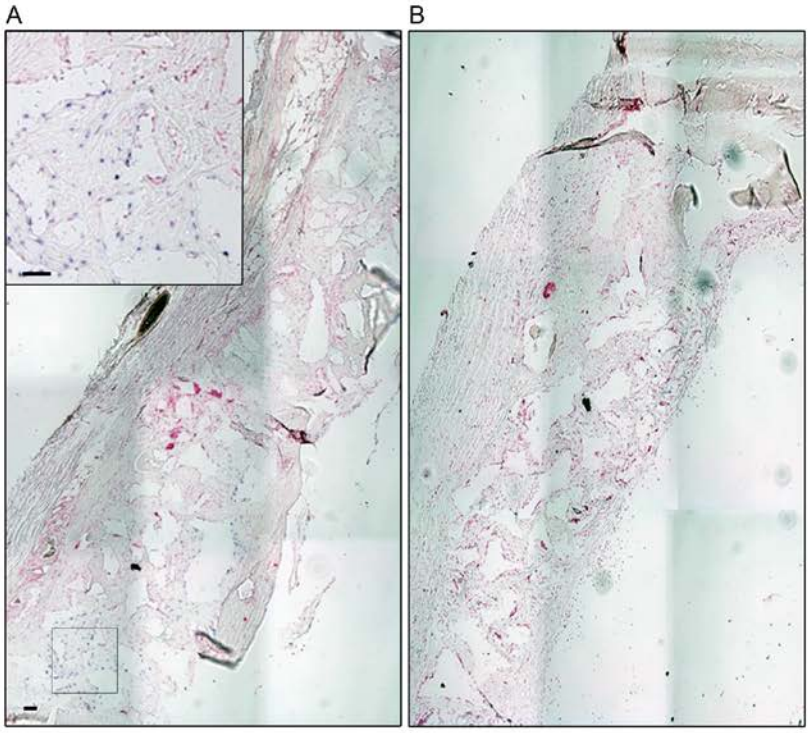


Supplemental Figure 1: In situ hybridization for human specific Alu sequences demonstrating the large presence of remaining (A) NC after 8 weeks calvarian implantation versus no detected presence of (B) BMSC under the same implant regime. Inlay for figure A represents zoomed region of black-boxed area. Blue nuclei: Alu positivity; Red nuclei: rat cells. Scale bars: 100µm.

*Biomaterials 2012 Jul;33(20):5085-93*
*doi: 10.1016/j.biomaterials.2012.03.082*

# Enhancing the biological performance of synthetic polymeric materials by decoration with engineered, decellularized extracellular matrix

Nasser Sadr[a, b, c], Benjamin E. Pippenger[a, b], Arnaud Scherberich[a, b], David Wendt[a, b], Sara Manteroc, Ivan Martin[a, b], Adam Papadimitropoulos[a, b]

[a] Department of Surgery, University Hospital Basel, Hebelstrasse 20, CH-4031 Basel, Switzerland

[b] Department of Biomedicine, University Hospital Basel, Hebelstrasse 20, CH-4031 Basel, Switzerland

[c] Bioengineering Department, Politecnico di Milano, Piazza Leonardo da Vinci 32, 20131Milan, Italy

*Correspondence to: Prof. Ivan Martin
ICFS, University Hospital Basel
Hebelstrasse 20, ZLF, Room 405
4031 Basel, Switzerland
Phone: + 41 61 265 2384; fax: + 41 61 265 3990
E-mail: Ivan.Martin@usb.ch

## ABSTRACT

Materials based on synthetic polymers can be extensively tailored in their physical properties but often suffer from limited biological functionality. Here we tested the hypothesis that the biological performance of 3D synthetic polymer-based scaffolds can be enhanced by extracellular matrix (ECM) deposited by cells in vitro and subsequently decellularized. The hypothesis was tested in the context of bone graft substitutes, using polyesterurethane (PEU) foams and mineralized ECM laid by human mesenchymal stromal cells (hMSC). A perfusion-based bioreactor system was critically employed to uniformly seed and culture hMSC in the scaffolds and to efficiently decellularize (94% DNA reduction) the resulting ECM while preserving its main organic and inorganic components. As compared to plain PEU, the decellularized ECM-polymer hybrids supported the osteoblastic differentiation of newly seeded hMSC by up-regulating the mRNA expression of typical osteoblastic genes (6-fold higher bone sialoprotein; 4-fold higher osteocalcin and osteopontin) and increasing calcium deposition (6-fold higher), approaching the performance of ceramic-based materials. After ectopic implantation in nude mice, the decellularized hybrids induced the formation of a mineralized matrix positively immunostained for bone sialoprotein and resembling an immature osteoid tissue. Our findings consolidate the perspective of bioreactor-based production of ECM-decorated polymeric scaffolds as off-the-shelf materials combining tunable physical properties with the physiological presentation of instructive biological signals.

Biomaterials 33 (2012) 5085–5093

Contents lists available at SciVerse ScienceDirect

Biomaterials

journal homepage: www.elsevier.com/locate/biomaterials

# Enhancing the biological performance of synthetic polymeric materials by decoration with engineered, decellularized extracellular matrix

Nasser Sadr [a,b,c], Benjamin E. Pippenger [a,b], Arnaud Scherberich [a,b], David Wendt [a,b], Sara Mantero [c], Ivan Martin [a,b,*], Adam Papadimitropoulos [a,b]

[a] Department of Surgery, University Hospital Basel, Hebelstrasse 20, CH-4031 Basel, Switzerland
[b] Department of Biomedicine, University Hospital Basel, Hebelstrasse 20, CH-4031 Basel, Switzerland
[c] Bioengineering Department, Politecnico di Milano, Piazza Leonardo da Vinci 32, 20131Milan, Italy

ARTICLE INFO

*Article history:*
Received 13 March 2012
Accepted 27 March 2012
Available online 15 April 2012

*Keywords:*
Polyesterurethane scaffold
Bone tissue engineering
Human mesenchcymal stem cell
Decellularized ECM (extracellular matrix)
Bioreactor

ABSTRACT

Materials based on synthetic polymers can be extensively tailored in their physical properties but often suffer from limited biological functionality. Here we tested the hypothesis that the biological performance of 3D synthetic polymer-based scaffolds can be enhanced by extracellular matrix (ECM) deposited by cells in vitro and subsequently decellularized. The hypothesis was tested in the context of bone graft substitutes, using polyesterurethane (PEU) foams and mineralized ECM laid by human mesenchymal stromal cells (hMSC). A perfusion-based bioreactor system was critically employed to uniformly seed and culture hMSC in the scaffolds and to efficiently decellularize (94% DNA reduction) the resulting ECM while preserving its main organic and inorganic components. As compared to plain PEU, the decellularized ECM-polymer hybrids supported the osteoblastic differentiation of newly seeded hMSC by up-regulating the mRNA expression of typical osteoblastic genes (6-fold higher bone sialoprotein; 4-fold higher osteocalcin and osteopontin) and increasing calcium deposition (6-fold higher), approaching the performance of ceramic-based materials. After ectopic implantation in nude mice, the decellularized hybrids induced the formation of a mineralized matrix positively immunostained for bone sialoprotein and resembling an immature osteoid tissue. Our findings consolidate the perspective of bioreactor-based production of ECM-decorated polymeric scaffolds as off-the-shelf materials combining tunable physical properties with the physiological presentation of instructive biological signals.



## 1. Introduction

Cellular interactions with the extracellular matrix (ECM) are known to play a critical role in directing cell function and regulating development, homeostasis and repair of a variety of tissues, including bone [1] and [2]. This recognition has fostered the design of biomimetic substrates for bone regeneration aiming to provide, along with the structural support, bioactive signals mimicking some aspects of the native bone ECM [3] and [4]. However, one of the main drawbacks of naturally occurring molecules is the limited ability to be processed within compliant biomaterials for bone repair applications.

Due to their tunable chemico-physical properties and compatibility with several processing techniques [5], synthetic polymer-based materials have been extensively tested for bone repair, but their use is generally limited by a sub-optimal biological interaction with cells [4]. Significant efforts have been made to improve polymers' bioactivity by combination with specific ECM components, such as calcium phosphate-based particles [6], growth factors [7] specific molecules or peptides [8]. However, this strategy is challenged by the difficulty to identify optimal amounts and combinations of defined factors, to preserve their biological functionality and to release them according to suitable kinetic profiles. Furthermore, recent studies suggest that ECM regulatory function on cell fate is unlikely to be recapitulated by a limited set of synthetic or purified components [2,9–13].

The alternative use of cell-laid ECM subsequently devitalized or decellularized has gained an increasing interest as a physiologically functional source of the complex set of naturally occurring bioactive signals. For instance, decellularized ECM synthesized by undifferentiated mesenchymal stromal cells (MSCs) in vitro has been shown to facilitate cell proliferation, prevent spontaneous differentiation and enhance the osteogenic capacity of freshly

* Corresponding author. Institute for Surgical Research and Hospital Management, University Hospital Basel, Hebelstrasse 20, ZLF, Room 405, CH-4031 Basel, Switzerland. Tel.: +41 61 265 2384; fax: +41 61 265 3990.
*E-mail address:* imartin@uhbs.ch (I. Martin).

0142-9612/$ – see front matter © 2012 Elsevier Ltd. All rights reserved.
doi:10.1016/j.biomaterials.2012.03.082

reseeded MSCs [14] and [15]. In similar studies, decellularized ECM, generated by osteogenically differentiating MSCs onto 3D porous scaffolds, enhanced and accelerated in vitro osteoblastic differentiation of newly cultured MSCs [16] and [17]. Decellularized bone-like ECM was also shown in rat models to enhance critical features for bone repair, namely implant vascularization and engraftment, yet no evidence of bone tissue formation could be provided [18] and [19]. Collectively, these studies urge for the development of streamlined approaches to decorate tailored synthetic substrates with decellularized ECM, in order to generate bone substitute materials with enhanced biological functionality and possibly osteoinductivity.

In the present work we first developed decellularized hybrid ECM-polymer materials based on the combination of 3D polyesterurethane (PEU) scaffolds and human MSC (hMSC). The process relied on the use of a perfusion-based bioreactor system in order to (i) facilitate an efficient and homogeneous cell seeding within the pores of 3D scaffolds [20], (ii) achieve uniform cell viability and tissue formation through the constructs [21], and (iii) remove the cellular debris without compromising the amounts of organic and inorganic constituents of deposited ECM. We then tested the capacity of the decellularized ECM to enhance in vitro differentiation of newly seeded hMSC or to induce osteoid tissue formation by resident precursor cells upon ectopic implantation in nude mice, using plain PEU and ceramic foams as reference materials.

## 2. Materials and methods

### 2.1. Polymeric substrate

The synthetic polyesterurethane (DegraPol®; Ab Medica, Italy) processed by thermally induced phase separation into porous cylinders was soaked in cyclohexane (Fluka, Switzerland) and frozen at −20 °C overnight. The frozen samples were cut to obtain discs (4 mm height, 8 mm diameter) and subsequently dried at room temperature (evaporation of cyclohexane). For cellular experiments the scaffolds were sterilized by repeated soaking in 70% ethanol (EtOH) followed by rinsing in phosphate buffer solution (PBS) and incubation in culture medium overnight.

Various physical parameters of the substrates were first determined. Scaffold porosity was found to be 93 ± 5% with individual interconnected pores of 153 ± 44 μm in diameter. The permeability was comprised between $2.00 \pm 0.44^{*}10^{-11}$ m$^2$ and $1.74 \pm 0.30^{*}10^{-11}$ m$^2$ (1471.5 ÷ 4414.5 Pa pressure across the samples). Eluates collected at 1, 3 and 7 days were evaluated to verify the absence of potentially cytotoxic residuals in the scaffolds. Flow cytometric assay (Apoptosis Detection kit; BD Biosciences, Germany) of hMSC incubated with the eluates for 72 h showed viability similar to the controls (Supplementary Data 1). Overall, the porous structure of the PEU substrates was found to comply with those of scaffolds used in BTE applications [22] and [23].

### 2.2. Cell source and expansion

Bone marrow aspirates (20 ml volumes) were obtained from the iliac crest of healthy donors during routine orthopedic surgical procedures, in accordance with the local ethical committee (University Hospital Basel) and subsequent to informed consent. Nucleated cells were isolated from aspirates by means of red blood cells lyses buffer (pH 7.2) containing 0.15 M $NH_4Cl$, 1 mM $KHCO_3$ (Sigma–Aldrich, USA) and 0.1 mM $Na_2EDTA$ (Fluka, Switzerland).

Freshly isolated cells were plated at a density of $1^{*}10^5$ nucleated cells/cm2. Cell expansion was carried out in complete medium (CM) which consisted of α-Modified Eagle's Medium, 10% fetal bovine serum, 100 mM HEPES buffer solution, 1 mM sodium pyruvate, 100 U/ml penicillin, 100 μg/ml streptomycin and 292 μg/ml L-glutamine (GIBCO, Switzerland) supplemented with 100 nM dexamethasone (Sigma–Aldrich, USA) and 5 ng/ml fibroblast growth factor-2 (FGF-2; R&D systems, USA). Medium was changed twice a week. At confluence, bone marrow-derived hMSC were replated for expansion (seeding density of $3^{*}10^3$ cells/cm$^2$). Upon confluence, cells were enzymatically retrieved and counted for use in the following experiments.

### 2.3. Evaluation of cell-polymer interactions

Using a previously developed perfusion bioreactor system for cell seeding and culture of 3D scaffolds [20], hMSC were perfused overnight through PEU discs at a superficial velocity of 1000 μm/s. After 24 h (cell seeding phase), the superficial velocity was reduced to 100 μm/s for perfusion culture of hMSC. CM was supplemented either with 100 nM dexamethasone, 0.1 mM ascorbic acid-2-phosphate and 5 ng/ml FGF-2 (proliferative medium; PM) or with 100 nM dexamethasone, 0.1 mM ascorbic acid-2-phosphate and 10 mM β-glycerolphosphate (differentiative medium; DM) according to the experiment. Samples seeded and cultured within the bioreactor were then analyzed to determine cell seeding efficiency, cell proliferation and differentiation as follows.

Optimal cell seeding efficiency was determined by harvesting constructs after overnight cell seeding using different cell densities (0.5, 1, and $2^{*}10^6$ cells/scaffold) and analyzed for DNA content as described below. Cell proliferation kinetics as well as osteoblastic differentiation were assessed by perfusion seeding $1^{*}10^6$ hMSC onto PEU and culturing for 3, 7 and 14 days. Constructs were harvested at the various time points and cell numbers (DNA content), gene expression (bone sialoprotein and collagen I), and cell morphology and ECM deposition (scanning electron microscopy; SEM) were assessed, as described in the analytical methods section.

### 2.4. Generation of decellularized hybrid ECM-polymer scaffold

#### 2.4.1. 3D culture to induce ECM deposition

Using the bioreactor perfusion protocol described in the cell-substrate interactions section, hMSC ($1^{*}10^6$ cells/scaffold) were seeded and cultured on PEU in PM. After a total of 4 days, culture medium was changed to DM and the scaffolds were perfused for an additional 24 days. Culture medium was changed twice a week. In order to evaluate the mineralized ECM deposition, constructs were sacrificed at various time points and characterized for total calcium, collagen, and DNA content, mineral chemistry and distribution (energy dispersive X-ray analysis, SEM, and synchrotron based microtomography) as described in the following paragraphs.

#### 2.4.2. Hybrid ECM-polymer constructs decellularization

After ECM deposition, samples were devitalized to obtain hybrid ECM-polymer constructs according to previous protocols with minor variations [24]. Briefly, samples underwent three freeze and thaw (F/T) cycles in liquid nitrogen and 37 °C water bath (10 min each), respectively. Samples were rinsed in sterile PBS after each thaw step as well as in double distilled water after the second thaw in order to hypotonically lyse remaining cells. To eliminate cellular debris, a perfusion-based washing step was added subsequent to the F/T: the constructs were placed into the bioreactor system and perfused at 100 μm/s in PBS for 30 min at room temperature. To verify if the perfusion washing step was effectively removing cellular debris but at the same time preserving ECM components, DNA, calcium and collagen were quantified as described in the analytical methods section.

### 2.5. Evaluation of hMSC-hybrid ECM-polymer scaffold interactions in vitro

In order to assess the differentiative potential of the ECM, hMSC expanded in CM supplemented with 5 ng/ml FGF-2 to maintain an immature phenotype [25] were reseeded onto decellularized hybrid constructs ($1^{*}10^6$ cells/scaffold) using the aforementioned bioreactor parameters and cultured in DM. To discriminate the effect of the mineralized ECM and compare it with known osteoconductive material, ceramic scaffolds (ENGIpore; Fin-Ceramica Faenza, Italy) was adopted as positive control, while plain PEU (without ECM) was chosen as negative control. Samples were collected after 8 and 16 days culture. The osteogenic differentiation of the hMSC was evaluated by calcium deposition quantification, gene expression and cytofluorometric analyses, as described below.

### 2.6. In vivo bone formation assays

Decellularized hybrid ECM-polymer constructs, plain polymeric substrates, and ceramic scaffolds were subcutaneously implanted ectopically into dorsal pockets of recipient nude mice (CD-1 nu/nu, 1 month old; Charles River Laboratories, Germany) in accordance with institutional guidelines. Eight weeks following implantation, explants were processed and analyzed histologically, immunohistochemically, and by synchrotron based microtomography as described in the following section.

### 2.7. Analytical methods

#### 2.7.1. DNA quantification

Samples collected as described above were digested with proteinase K solution (1 mg/ml proteinase K, 50 mM TRIS, 1 mM EDTA, 1 mM iodoacetamide, and 10 μg/ml pepstatin-A; Sigma–Aldrich, USA) in double distilled water or potassium phosphate buffer for 16 h at 56 °C as previously described [26].

DNA quantification was performed by means of a commercially available fluorescence based kit, namely CyQUANT® Cell Proliferation Assay (Invitrogen, USA). Working solutions were prepared according to the manufacturer's protocols. The analyses were carried out measuring fluorescence with a Spectra Max Gemini XS Microplate Spectrofluorometer (Molecular Devices, USA). Excitation and emission wavelengths were respectively 485 nm and 538 nm. Samples in each plate included a calibration curve. Each sample was measured in triplicate.

Seeding efficiencies were calculated dividing the values obtained for the samples by the mean DNA amount measured in 3 aliquots of cells collected at the time of bioreactor seeding.

*2.7.2. Collagen and calcium quantification*

Total calcium and collagen were determined colorimetrically on a Spectra Max 190 microplate colorimeter (Molecular Devices, USA) following the protocols provided with the respective assay kits. Briefly, calcium present in the mineralized extracellular matrix was solubilized in 0.5 N hydrochloric acid for 4 h at 4 °C before quantification (Total Calcium Assay, Randox, UK). Collagen was solubilized using 3% v/v acetic acid (Fluka, Switzerland) and 0.01% w/v pepsin (Sigma–Aldrich, USA) overnight at 4 °C and then quantified (Sircol, Biocolor, UK). Working solutions and standard curves were prepared according to the manufacturer's protocols. Samples in each plate included a calibration curve. Each sample was measured in triplicate.

*2.7.3. Scanning electron microscopy and energy dispersive X-ray analysis*

Hybrid constructs were fixed overnight in 1.5% paraformaldehyde at 4 °C and then dehydrated in graded ethanol changes (30, 50, 75, and 100% EtOH concentration) followed by critical point drying. Samples were then sputtered with gold (Baltec MED020, 25 mA by $2 \times 10^{-2}$ mBar) before examination under a Philips XL 30 ESEM microscope with energy dispersive X-ray (EDX) analyzer (Philips, Nederland). EDX analysis samples were sputtered with silver before scanning for calcium and phosphate elements with energy peaks at 3.7 and 2.1 keV, respectively.

*2.7.4. Flow cytofluorometric analysis*

Following 3D cultures, cells were extracted from the scaffold pores by sequentially perfusing a solution of 0.3% collagenase (Worthington, USA) for 40 min and 0.05% trypsin/0.53 mM EDTA (GIBCO, Switzerland) for 10 min, both at a superficial velocity of 400 μm/s. Previous studies using a similar setup indicated that the protocol allows detaching of more than 85% of the total cells in the system [27]. For each experimental group, pooling samples from multiple bioreactors chambers ($n = 3$) were rinsed and incubated in the dark at 4 °C for 30 min with an antibody against STRO-1 (R&D systems, USA) followed by incubation with a FITC conjugated secondary antibody for 30 min and analyzed using a FACSCalibur flow cytometer (BD Biosciences, Germany). Positive expression was defined as the level of fluorescence greater than 99% of corresponding control.

*2.7.5. Gene expression analysis*

Total RNA was extracted using TRIzol (Life Technologies, Basel, Switzerland) and the standard single-step acid–phenol guanidinium method. Complementary DNA (cDNA) was synthesized as previously described [28]. Quantitative real-time reverse transcriptase-polymerase chain reaction assays (qRT-PCR; 7300 Real Time PCR system; Applied Biosystem, Switzerland) were performed for the following genes of interest in accordance to the specific experiment: collagen I, core-binding factor subunit alpha-1 (Cbfa-1), bone morphogenic protein 2 (BMP-2), bone sialoprotein (BSP), osteopontin (OP), and osteocalcin (OC). Glyceraldehyde 3-phosphate dehydrogenase (GAPDH) was used as housekeeping reference gene. Primers and probes used are reported in Supplementary Data 2. Expression data were calculated, for each cDNA sample, by using the $2^{\Delta Ct}$ method [29]. Briefly, threshold cycle (Ct) value of each target sequence was subtracted from the Ct value of the reference gene to derive ΔCt. The expression level of each target gene was calculated as $2^{\Delta Ct}$. Each sample was assessed at least in duplicate for each gene of interest.

*2.7.6. Synchrotron based differential phase contrast microtomography*

Synchrotron based differential phase contrast microtomography (SR-μCT) were performed at the Tomographic Microscopy and Coherent Radiology experiments (Tomcat) beamline at the Swiss Light Source (SLS). For each construct, 1501 projections were acquired over a range of 180° at a photon energy of 25 keV with an exposure time of 250 ms using 8 phase steps per projection. The nominal pixel size amounted to 7.4 μm. Reconstructed images were obtained by applying standard filtered backprojection to the projection images.

*2.7.7. Histological staining and immunohistochemistry*

Constructs retrieved 8 weeks post-implantation were fixed overnight in 1.5% paraformaldehyde at 4 °C, paraffin embedded (TPC15 Medite, Switzerland) and sectioned (6-μm-thick) by means of a microtome (Leica, Switzerland). Paraffin sections were deparaffinized, hydrated and stained with hematoxylin and eosin (H&E), alizarin red (AlizR), followed by observation under light microscopy. Some ceramic constructs were directly embedded in methylmethacrylate (MMA) without decalcification and 6-μm-thick sections stained with Von Kossa and toluidine blue stain.

Immunohistochemical analyses were performed to characterize the extracellular matrix using anti-human bone sialoprotein (BSP; Enzo Life Sciences AG, Switzerland). The immunobinding was detected with a biotinylated secondary antibody and using the appropriate Vectastain ABC kits. The red signal was developed with the Fast Red kit (Dako, Denmark) and sections were counterstained with Haematoxylin. Chromogenic in situ hybridization (CISH; Zytovision, Germany) to detect human alu repeat

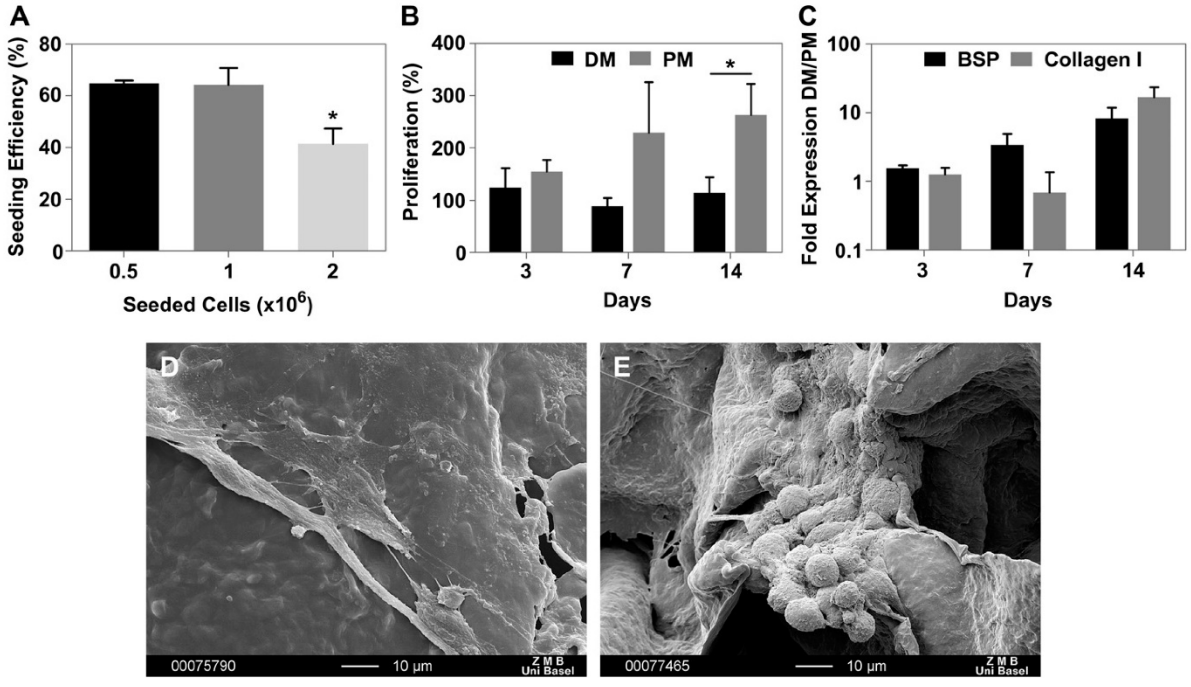


**Fig. 1.** Cell-polymer interactions. (A) Seeding efficiency on PEU was higher than 60% when up to $1*10^6$ cells/scaffold were injected in the bioreactor, and decreased below 40% for higher cell densities. (B) After seeding, cell population was stable over 14 days when cultured in differentiative medium (DM) and increased by almost 3 folds when cultured in proliferative medium (PM). (C) Conversely, osteogenic marker gene expression (collagen I and BSP) was up-regulated in DM as compared to PM up to 10 folds. Representative SEM images show that hMSC initially displayed a spindle-shape spread morphology (D) and acquired a more rounded osteoblastic-like morphology, surrounded by ECM, when cultured in DM (E). (* = Statistically significant difference).

sequences was performed as described in the kit. Histological and immunohistochemical sections were analyzed using a BX-61 microscope (Olympus, Germany).

### 2.8. Statistical analysis

Statistical analysis was performed by Student's *t*-tests for two groups of data or by analysis of variance (ANOVA) followed by Bonferroni's post-hoc tests for multiple comparisons using Prism 5 (GraphPad Software Inc., USA). Differences were considered significant for $p < 0.05$.

## 3. Results

### 3.1. Evaluation of cell-polymer interactions

To define a suitable number of initial cells seeded onto polyesterurethane (PEU) scaffolds, different numbers of hMSC were inoculated in the bioreactor system and perfused through the porous structure of the scaffold overnight. Using a DNA assay, the number of cells adhered on the scaffold was quantified and the seeding efficiency was calculated. When 0.5 and 1 million cells/scaffold were inoculated, seeding efficiency was found to be approximately 60%,corresponding to an average of 0.3 and 0.6 millions of adherent cells, respectively. However, when 2 million cells were used, cell seeding efficiency dropped to roughly 40%, corresponding to 0.8 million cells attached to the scaffold, possibly indicating a plateau in the number of cells that can be effectively seeded within our experimental setup (Fig. 1A). These results suggested that an initial seeding of 1 million cells/scaffold would maximize seeding efficiency while minimizing cell waste, and thus, this seeding density was used for the subsequent experiments.

To determine the in vitro behavior of hMSC on PEU substrates, after seeding phase the cells were cultured in either differentiative (DM) or proliferative (PM) medium for up to 2 weeks under perfusion. In PM, adherent hMSC attained 1.5 fold increase in 3 days and a further proliferation to an almost 3-fold increase over the course of 2 weeks (Fig. 1B). On the contrary, in DM, hMSC number remained stable over the 14-day culture (Fig. 1B). At the same time the cells up-regulated collagen I and BSP expression as compared to PM condition (Fig. 1C). Initially displaying spindle-like morphology (Fig. 1D), in DM cells acquired a rounded osteoblast-like morph ology surrounded by a cell-laid ECM (Fig. 1E). Taken together, these results demonstrated the feasibility to appropriately seed hMSC on the porous polymeric substrate and suggest the possibility to regulate their growth and differentiative fate with the use of exogenous factors during the perfusion culture.

### 3.2. Generation of decellularized hybrid ECM-polymer scaffold

In order to generate hybrid constructs, a two phase perfusion culture regime was adopted by firstly promoting proliferation to increase cell numbers and subsequently inducing their differentiation to stimulate ECM production and its mineralization for a total culture period of 28 days.

SEM images taken after 1 and 28 days of culture show that initially adhered hMSC progressively deposited an ECM associated with mineral spherulites within the inner pores of the scaffold (Fig. 2A ,B). EDX analysis of these deposits revealed calcium and phosphorus, main inorganic constituents in calcium phosphate apatite, typically found in bone tissues and absent in the cell-free scaffolds (Fig. 2C). DNA quantification results indicated after the first 14 days of culture, the number of cells present on the scaffold was 1.7 fold of those initially adhered on the scaffold, which was sharply decreased (84% reduction) by the end of the culture period,

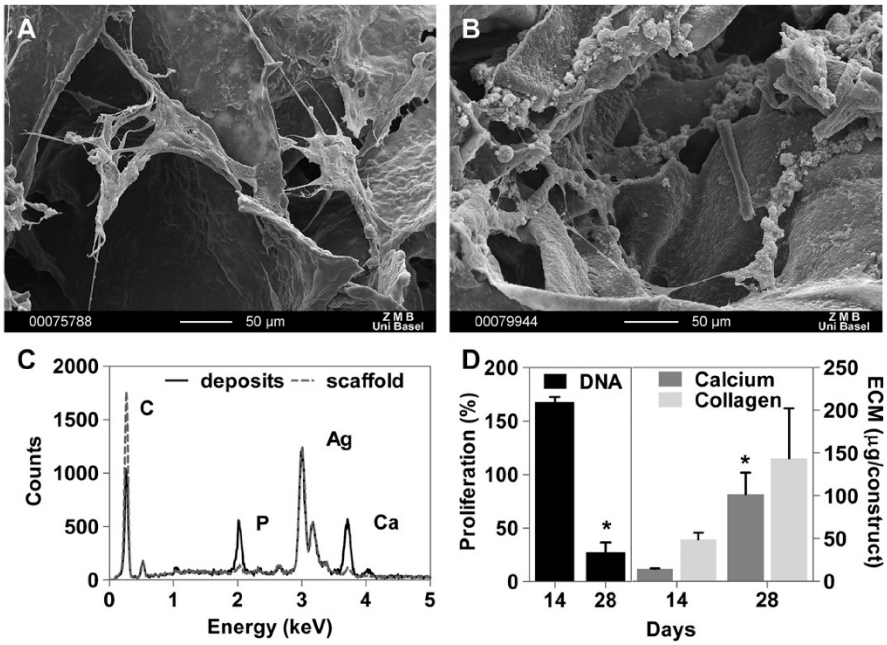


**Fig. 2.** Mineralized ECM deposition. Representative SEM images of the inner compartment of PEU scaffolds seeded with hMSC in the bioreactor show the presence of adherent cells after 1 day culture (A) and the accumulation of an ECM network composed of fibrous components and mineral spherulites by the end of 28 days culture (B). (C) EDX analyses on spherulites show the presence of calcium and phosphorus as main constituents. (D) Total DNA, calcium, and collagen quantification analyses demonstrated a drastic decrease in cell number (84%) and significant increases in total calcium (7-fold) and collagen (3-fold) content in 28 days of 3D perfusion culture. (* = Statistically significant difference as compared to 14 days).

after 28 days (Fig. 2D). Inversely, at the same time points cells were found to deposit steadily increased quantities of collagen and calcium onto the scaffold material. In particular, the relative increase for collagen and calcium between the two time points were found to be of 3- and 7-fold, respectively, mirroring the mineralized ECM deposition process carried out by the cells.

In order to decellularize the above generated hybrid constructs, a two step procedure was adopted in which 1) devitalization of the cellular component proceeded through a succession of freeze and thaw cycles with intermediate rinse in hypotonic solution and 2) the cellular debris was washed away by gentle perfusion of an isotonic solution through the construct using the aforementioned bioreactor system (Fig. 3A). The proposed decellularization process effectively removed the cellular remnants from the internal regions of the hybrid constructs (94.2 ± 6.0% DNA reduction) while preserving the previously-deposited quantities of collagen and calcium (Fig. 3B). Considering all of the previous results, a bioreactor-based protocol has been established to efficiently produce decellularized hybrid constructs composed of naturally deposited hMSC-laid ECM on polymeric substrates.

### 3.3. Evaluation of hMSC-decellularized hybrid ECM-polymer scaffold interactions in vitro

In order to investigate the effect of the ECM on cell adhesion, calcium deposition, phenotype maturation, and gene expression, hMSC (previously expanded in FGF-2 to maintain an immature phenotype) were reseeded on decellularized hybrid ECM-polymer scaffolds (PEU w/ECM) and cultured in osteogenic medium for 8 or 16 days. In addition to the plain polymeric substrate (PEU; negative control), a standard ceramic scaffold (HA) was included in this study and served as positive control for supporting hMSC osteogenic differentiation.

The seeding efficiency was evaluated after an overnight perfusion of the cell suspension. PEU w/ECM constructs showed similar DNA content to the plain PEU ones, indicating that ECM did not significantly affect initial cell seeding efficiency in our bioreactor based perfusion set up (Fig. 4A). Regarding calcium deposition, while at 8 days no differences were found between PEU w/ECM and PEU constructs, at 16 days the hMSC deposited higher amounts of newly deposited calcium (6-fold) on PEU w/ECM as compared to PEU samples (Fig. 4B).

The expression of STRO-1 surface protein, a marker of undifferentiated osteogenic precursors [30] was cytofluorometrically investigated to evaluate the differentiation stage of hMSC cultured on the various substrates. The percentage of STRO-1+ cells, initially at the level of 4.8% prior to cell loading into the scaffolds, increased after 8 days of culture on PEU w/ECM (1.7-fold) and PEU (2.5-fold) and was maintained between 7.4% and 7.9% after additional 8 days. Instead, hMSC culture on HA resulted in markedly inferior percentages of STRO-1+ cells, reaching the level of 3.6% after 16 days of culture (see Supplementary Table 1).

The differentiation of hMSC was further assessed by quantifying the mRNA expression of typical osteogenic markers. The results are displayed after normalization to the expression level of hMSC on PEU substrates at day 8 (Fig. 5). After 8 days in culture, mid-early osteoblastic genes, namely cbfa-1, BSP and BMP-2, were up-regulated in the hMSC cultured on PEU w/ECM similarly to the

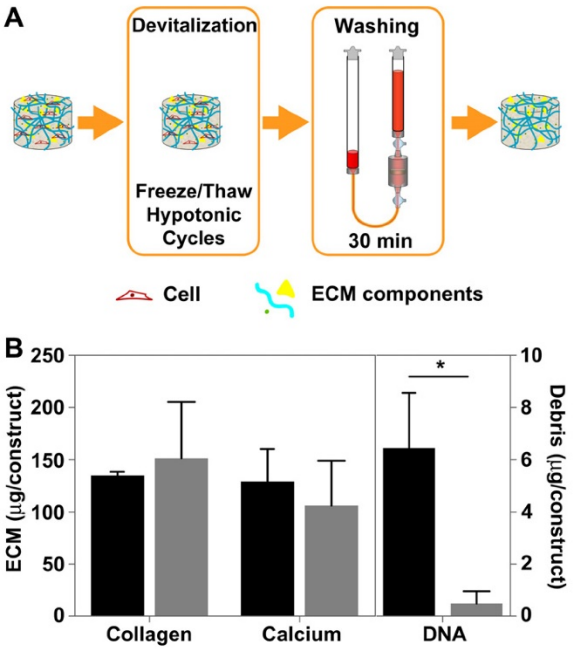


**Fig. 3.** Construct decellularization. (A) Diagram detailing the decellularization process: a chemo-physical cell lysis step, composed of F/T steps and hypotonic rinsing, provided for construct devitalization followed by cell debris wash-off step in the bioreactor. (B) Total collagen, calcium and DNA quantification analyses before (black bars) and after (grey bars) decellularization process highlighted that the adopted protocol preserved the ECM components and efficiently removed DNA remnants (94.2 ± 6.0% reduction). (* = Statistically significant difference).

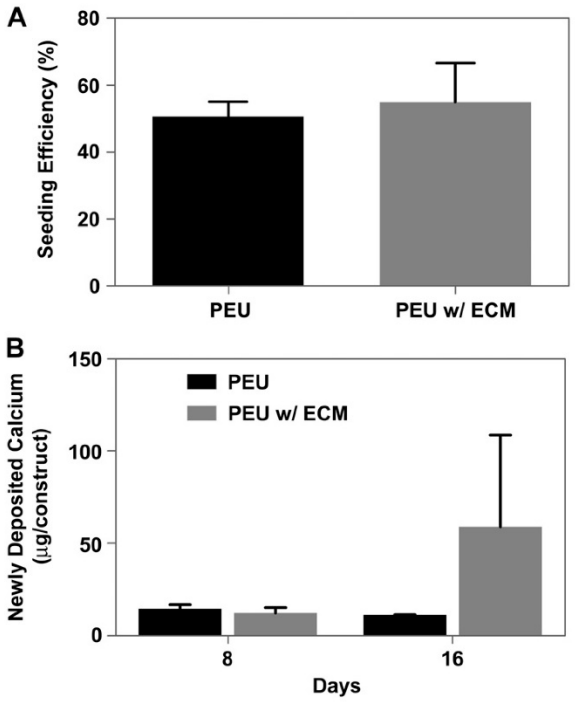


**Fig. 4.** Effect of ECM on cell seeding and calcium deposition. (A) DNA quantification after reseeding fresh hMSC pointed out similar number of adherent cells on both plain polymer scaffolds (PEU) and polymer scaffolds with in vitro deposited ECM (PEU w/ECM). (B) The presence of the cell-laid ECM favored a 6-fold higher *de novo* calcium deposition when fresh hMSC were cultured in DM on the constructs for 16 days in the bioreactor.

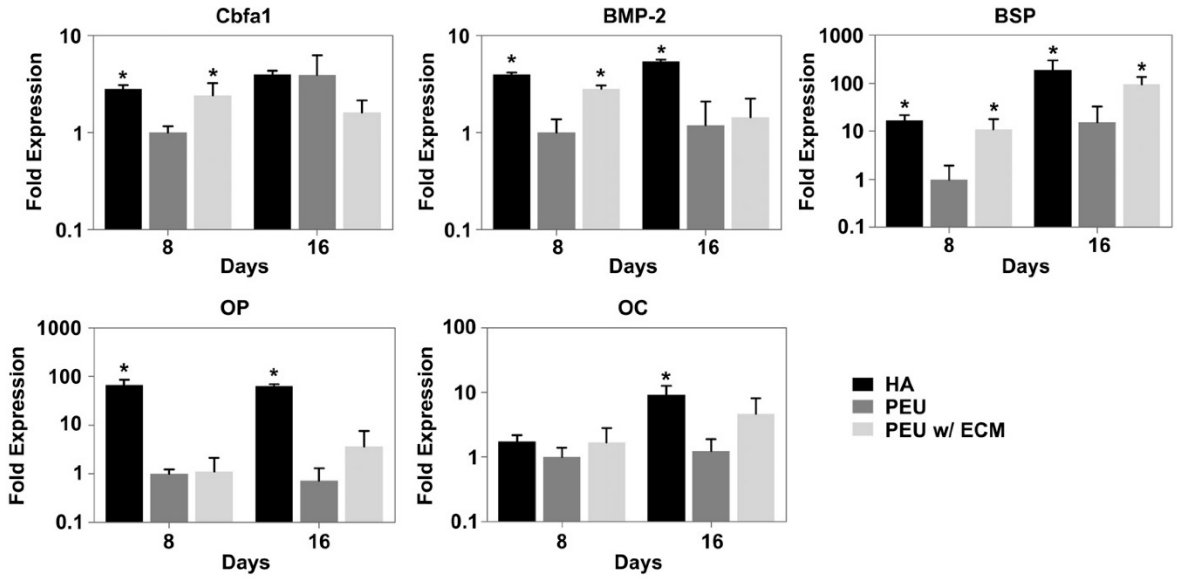


**Fig. 5.** Effect of the ECM on osteogenic marker gene expression. Real time RT-PCR analysis mRNA expression levels of hMSC reseeded on HA, PEU and PEU w/ECM for: Cbfa-1, BMP-2, BSP, OP and OC genes. Expression levels were calculated by normalizing the quantified mRNA amount to GAPDH and by further dividing the resulting value by that obtained on PEU at day 8. Gene expression analysis evidenced a coordinated up-regulation of the osteoblastic markers, in PEU w/ECM similarly to HA, with PEU controls expressing generally lower levels. (* — Statistically significant difference from PEU).

hMSC cultured on HA. At day 16, BSP expression increased for all conditions, being however higher on PEU w/ECM and HA with similar trends. Cbfa-1 expression level increased on PEU and was slightly down-regulated on PEU w/ECM. BMP-2 expression was similar on PEU and PEU w/ECM and lower than on HA. At the same time point, expression levels of mid-late osteoblastic genes (OP and OC) were up-regulated for hMSC cultured on PEU w/ECM (more than 4-fold for OC) as compared to PEU, with a trend similar to that of hMSC cultured on HA. Taken together, these results suggest that the presence of ECM enhanced the osteoblastic differentiation of freshly seeded immature hMSC in a similar fashion to ceramic substrates while preserving a higher percentage of STRO-1+ cells.

### *3.4. Evaluation of decellularized hybrid ECM-polymer scaffold's performance in vivo*

To further investigate the osteoinductive potential of the hybrid ECM-polymer scaffolds, following decellularization constructs were ectopically implanted in nude mice. After 8 weeks, samples were explanted and bone formation assessed by means of SR-μCT and histological analyses. SR-μCT performed on constructs before in vivo implantation show the polymeric porous structure and only few visible mineral deposits (bottom-left side of the construct) with most of the calcium phosphate spherulites evidenced in SEM being below the minimal resolved dimension (Fig. 6A, in vitro; arrow). After explantation the samples presented scattered regions that displayed a significant degree of mineralization (Fig. 6A, in vivo; circled region). Histological and immunohistochemical staining of the explants based on the hybrid ECM-polymer scaffolds demonstrated the uniform colonization by cells and indicated the formation of a connective tissue with rather loose structure but intensely positive for alizarin red and for BSP (Fig. 6B). Importantly, no evidences of either BSP or mineralization were found in the explants based on control plain PEU scaffolds (Fig. 6b) or in the ceramic ones (Supplementary Data 3). As expected, in situ hybridization for human alu sequences excluded the presence of cells of human origin in all PEU w/ECM explants (Supplementary Data 3).

## 4. Discussion

In this study, we have demonstrated the feasibility to generate hybrid ECM-polymer constructs relying on a multi-step, bioreactor-based approach. The mineralized ECM deposition was followed by a decellularization process under perfusion flow that minimally affected ECM bioactive components (collagen and calcium) while effectively removing cell debris. We further established that the resulting hybrid substrates enhanced the osteogenic differentiation of hMSC in vitro, similarly to ceramic scaffolds, by up-regulating the expression of typical osteoblastic gene markers and increasing calcium deposition as compared to plain PEU. Coherently, only the decellularized hybrid ECM-polymer constructs induced in vivo a BSP co-localized mineralization, indicative of an immature osteoid tissue.

The multiblock polyesterurethane chosen for this study has been widely used in tissue engineering applications [31] [32], and [33] and was combined here in a porous structure potentially compliant with BTE [22] and [23]. Nonetheless, plain polyesterurethane substrates lack bone-specific bioactive signals leading to impaired use in BTE applications [34] [35], and [36]. We took advantage of this limit, common to the majority of plain synthetic polymers, in order to study the bioactivity of mineralized ECM grown into inert polymer scaffolds. For the generation of adequate ECM-polymer hybrids, our protocol relied on three main steps: i) seeding and ii) culturing appropriately the hMSC within the pores of PEU to foster mineralized ECM deposition, and iii) decellularizing the resulting constructs. To tackle these three phases we adopted a bioreactor based approach that has been previously demonstrated to achieve reproducibly uniform ECM deposition into porous 3D scaffolds [21], crucial to the generation of consistent hybrid ECM-polymer constructs. The seeding step is especially critical to the homogeneity of the construct but also to the

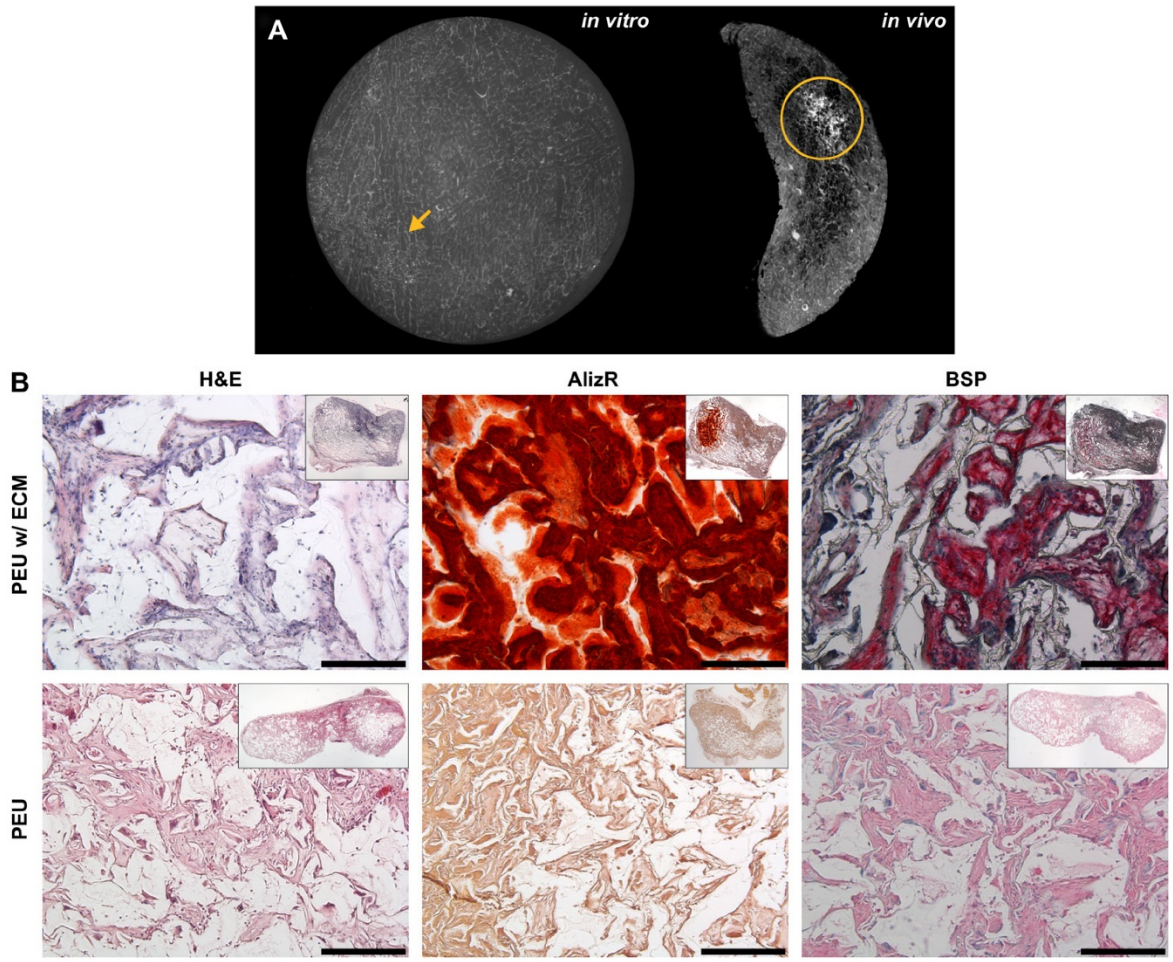


**Fig. 6.** Effect of the ECM following implantation in a nude mouse ectopic model. (A) Representative SR-μCT images acquired before and after implantation of PEU w/ECM displayed a significant mineralization in vivo. (B) Histological analyses of explanted PEU w/ECM and PEU constructs. Hematoxylin and eosin (H&E) staining revealed a loose ECM that displayed in PEU w/ECM a strong positive stain for Alizarin Red (AlizR) and bone sialoprotein (BSP). Both BSP and AlizR were negative in PEU constructs. (Scale bars = 200 μm).

efficiency of the production process [20]. Within the present experimental setup, the number of cells inoculated to the bioreactor system was defined by optimizing the seeding efficiency and yielding a final amount of adherent cells in a range that has been previously reported to prime cell proliferation and extracellular matrix synthesis [37]. The sequence of the external soluble factors we supplied to the culture medium here aimed to promote initially the proliferation of hMSC with their subsequent osteoblastic differentiation, thus providing for a progressive collagen and mineral spherulites deposition with consequent coating of the polymer surface with bone-like ECM.

To devitalize and remove the remaining cellular debris while preserving the mineralized ECM, we combined a chemo-physical cell lysis with a perfusion-based wash-off of. The cellular remnants represent indeed a major source of antigenic epitopes which may drive adverse immune responses and possibly interfere with the remodeling of biologic scaffolds [38] and [39]. With the bioreactor-based washing step, DNA residues, recently proposed as a general index of cell remnants [39] and directly correlated with adverse host reaction [40], were dramatically reduced, yielding a final DNA concentration (37.5 ng/mg) below the adverse reaction threshold (50 ng/mg) suggested by Crapo et al. [39]. At the same time, collagen and calcium deposits were substantially unaltered, suggesting that the ultra-structure disruption potentially associated with freeze/thaw process [41] was minimal and however compatible with the maintenance of the mineralized ECM. Although further analyses are required to evaluate the effect of decellularization also to non-collagenous proteins, the results indicate the feasibility to use bioreactor-based perfusion and salt buffer solutions as an alternative to more disruptive chemical and/or more costly DNase-based treatments [39].

To assess the bioactivity of the ECM, expanded hMSC were newly seeded on the decellularized hybrid constructs. Although it has been previously shown that cell adhesion is positively modulated in the presence of proteins and peptides on polymer surfaces [8] and [42], our findings showed that the presence of the ECM complex did not affect the cell seeding efficiency. Currently there is no consensus on how cell adhesion is affected by the presence of cell-laid ECM and controversial data have been reported describing either decreased or unaltered cell affinity to ECM coated surfaces,

possibly due to different adopted methods [19] and [43]. Beside cell-substrate affinity, the seeding process under perfusion has also been shown to be dependent on the fluid dynamics occurring within the pores of 3D scaffold structures [44]. Even if the fluid dynamics were not specifically evaluated in this work, the observed ECM confinement to a thin coating on the PEU surface suggests minimal pore size variation, consistent with the unaltered cell seeding efficiency.

Upon adhesion, the presence of ECM favored calcium deposition by hMSC, which were previously expanded in FGF-2 to maintain an immature phenotype [25]. We observed a considerably anticipated onset of mineralization as compared to other studies using hMSC (2 weeks versus 8 weeks) [19], indicating a possible stimulating role of perfusion flow together with osteogenic factors, similarly to what was previously observed to a lesser extent with osteoblastic differentiated rat MSC [16] [17], and [45]. Despite the differences among the various experimental setups and animal species of the cells, these results suggest that the mineralization observed here may raise from the combined effect of ECM, exogenous osteogenic factors and flow induced shear stress [17].

Gene expression analysis evidenced a coordinated up-regulation of commonly assessed osteoblastic markers in PEU w/ECM as compared to PEU controls, similarly to what was previously demonstrated with pre-differentiated rat MSCs [24] and approaching the trends observed using a ceramic substrate, which is known to support the MSC osteoblastic differentiation [46]. On the other hand, as compared to HA, the flow cytofluorometric results established the presence in PEU w/ECM of a higher percentage of STRO-1+ cells, known as early mesenchymal progenitors or pre-osteoblastic cells [47]. Taken together, these findings indicate that the ECM-polymer hybrids are capable to favor hMSC osteogenic differentiation and, at the same time, to preserve a pool of their precursors. It would be tempting to speculate that the PEU w/ECM scaffolds thus establish a specialized microenvironment (niche), somehow recapitulating the homeostatic balance between hMSC self-renewal and differentiation [43].

To further evaluate the in vivo osteoinductive potential of ECM-polymer hybrids, decellularized constructs were implanted subcutaneously in nude mice. MSC-generated ECM has previously been demonstrated to enhance vascularization [18] and improve engraftment in rat models [19] but with no evidences of bone formation or enhanced mineralization. Our findings indicated construct invasion by host cells and the accumulation of a mineral phase, as evidenced by the SR-μCT analysis. Notably, the mineral accumulations occurred in close proximity to BSP, a bone-related protein known to be involved in the nucleation of hydroxyapatite [48]. Due to experimentally proven cross-species reactivity of the primary human antibody, with the present data it is not possible to conclude whether BSP was of human origin and consequently already present on the constructs prior to implantation, or of mouse origin and thereby result of an induction process. Considering the BSP expression data during in vitro generation of hybrid constructs and the extent of this protein found histologically, the possible chimeric nature of BSP (i.e. produced both from human and mouse cells) cannot be excluded. This co-localized mineral-BSP presence was anyhow overlapping with loosely packed and organized ECM similar to woven osteoid matrix. Although at the assessed explantation time point no frank bone tissue formation can be claimed, these observations along with the in vitro results confirm that ECM noticeably improved the biological performances of the polymer scaffolds. These results warrant further in vivo investigation of optimized ECM compositions/structures (e.g., using alternative cell sources or different maturation stages), possibly based on protocols that been proven to enhance osteogenic differentiation in vitro [43] [45], [49] and [50]. Moreover, the ectopic nude mouse model used in our study does not mimic the complex biological environment of bone and is considered as one of the most challenging models for osteoinduction [51]. In this regard, a physiological orthotopic environment, known to be rich in osteogenic factors, will provide a more suitable and relevant milieu to investigate the bone forming capacity of our hybrid ECM-polymer constructs.

## 5. Conclusions

The developed hybrid ECM-polymer materials have been shown to regulate cell osteogenic commitment while maintaining a progenitor cell pool. The concept of decellularized engineered constructs could be extended to other cells and tissues, with the ultimate goal to generate "off the shelf" products alternative to xenogeneic or allogeneic acellular matrices. The use of bioreactors will potentially streamline the manufacturing process and provide standardized, clinically compliant and cost-effective products. Polymeric scaffolds decorated with decellularized matrices can also be used as models of engineered niches physiologically presenting customized signals to cells.

## Author contribution

NS, AP, and IM designed the study with the contribution of SM; NS, AP, and BEP performed the experiments; NS, AP, and BEP analyzed the data; NS and AP interpreted the results; NS, AP, IM and BEP wrote the paper. All the authors discussed the results, commented and revised the paper.

## Acknowledgments

The research leading to these results has received funding from the European Community's Seventh Framework Programme (MultiTERM, grant agreement nr 238551). We are grateful to Prof. Bert Müller and Dr. Marco Stampanoni for the help in interpreting microtomography results. The authors thank Ab Medica S.p.A. for kindly providing DegraPol® biomaterial (ETH Zurich and University of Zurich are owners and ab medica S.p.A is exclusive licensee of all IP Rights of DegraPol®) and Dr. Eliana Bonavoglia and Prof. Peter Neuenschwander for their expert assistance with DegraPol® scaffold. The authors acknowledge Fin-Ceramica Faenza S.p.a, Italy for the generous supply of Engipore scaffolds.

## Appendix A. Supplementary data

Supplementary data related to this article can be found online at doi:10.1016/j.biomaterials.2012.03.082.

## References

[1] Rosso F, Giordano A, Barbarisi M, Barbarisi A. From cell-ECM interactions to tissue engineering. J Cell Physiol 2004;199:174–80.
[2] Allori AC, Sailon AM, Warren SM. Biological basis of bone formation, remodeling, and repair-part II: extracellular matrix. Tissue Eng Part B Rev 2008;14:275–83.
[3] Owen SC, Shoichet MS. Design of three-dimensional biomimetic scaffolds. J Biomed Mater Res A 2010;94:1321–31.
[4] Bueno EM, Glowacki J. Cell-free and cell-based approaches for bone regeneration. Nat Rev Rheumatol 2009;5:685–97.
[5] Moroni L, de Wijn JR, van Blitterswijk CA. Integrating novel technologies to fabricate smart scaffolds. J Biomater Sci Polym Ed 2008;19:543–72.
[6] Hutmacher DW, Schantz JT, Lam CX, Tan KC, Lim TC. State of the art and future directions of scaffold-based bone engineering from a biomaterials perspective. J Tissue Eng Regen Med 2007;1:245–60.
[7] Chan G, Mooney DJ. New materials for tissue engineering: towards greater control over the biological response. Trends Biotechnol 2008;26:382–92.
[8] Shekaran A, Garcia AJ. Extracellular matrix-mimetic adhesive biomaterials for bone repair. J Biomed Mater Res A 2011;96:261–72.

Keselowsky BG, Collard DM, Garcia AJ. Integrin binding specificity regulates biomaterial surface chemistry effects on cell differentiation. Proc Natl Acad Sci 2005;102:5953–7.
Tsai SW, Chen CC, Chen PL, Hsu FY. Influence of topography of nanofibrils of three-dimensional collagen gel beads on the phenotype, proliferation, and maturation of osteoblasts. J Biomed Mater Res A 2009;91:985–93.
Carson AE, Barker TH. Emerging concepts in engineering extracellular matrix variants for directing cell phenotype. Regen Med 2009;4:593–600.
Kundu AK, Khatiwala CB, Putnam AJ. Extracellular matrix remodeling, integrin expression, and downstream signaling pathways influence the osteogenic differentiation of mesenchymal stem cells on Poly(Lactide-Co-Glycolide) substrates. Tissue Eng Part A 2008;15:273–83.
Reing JE, Zhang L, Myers-Irvin J, Cordero KE, Freytes DO, Heber-Katz E, et al. Degradation products of extracellular matrix affect cell migration and proliferation. Tissue Eng Part A 2009;15:605–14.
Chen XD, Dusevich V, Feng JQ, Manolagas SC, Jilka RL. Extracellular matrix made by bone marrow cells facilitates expansion of marrow-derived mesenchymal progenitor cells and prevents their differentiation into osteoblasts. J Bone Miner Res 2007;22:1943–56.
Pei M, He F, Kish V. Expansion on extracellular matrix deposited by human bone marrow stromal cells facilitates stem cell proliferation and tissue-specific lineage potential. Tissue Eng Part A 2011;17:3067–76.
Datta N, Holtorf HL, Sikavitsas VI, Jansen JA, Mikos AG. Effect of bone extracellular matrix synthesized in vitro on the osteoblastic differentiation of marrow stromal cells. Biomaterials 2005;26:971–7.
Datta N, Pham QP, Sharma U, Sikavitsas VI, Jansen JA, Mikos AG. In vitro generated extracellular matrix and fluid shear stress synergistically enhance 3D osteoblastic differentiation. Proc Natl Acad Sci 2006;103:2488–93.
Pham QP, Kasper FK, Mistry AS, Sharma U, Yasko AW, Jansen JA, et al. Analysis of the osteoinductive capacity and angiogenicity of an in vitro generated extracellular matrix. J Biomed Mater Res A 2009;88:295–303.
Deutsch ER, Guldberg RE. Stem cell-synthesized extracellular matrix for bone repair. J Mater Chem 2010;20:8942–51.
Wendt D, Marsano A, Jakob M, Heberer M, Martin I. Oscillating perfusion of cell suspensions through three-dimensional scaffolds enhances cell seeding efficiency and uniformity. Biotechnol Bioeng 2003;84:205–14.
Wendt D, Stroebel S, Jakob M, John GT, Martin I. Uniform tissues engineered by seeding and culturing cells in 3D scaffolds under perfusion at defined oxygen tensions. Biorheology 2006;43:481–8.
Karageorgiou V, Kaplan D. Porosity of 3D biomaterial scaffolds and osteogenesis. Biomaterials 2005;26:5474–91.
Shimko DA, Nauman EA. Development and characterization of a porous poly(methyl methacrylate) scaffold with controllable modulus and permeability. J Biomed Mater Res B Appl Biomater 2007;80:360–9.
Pham QP, Kasper FK, Scott Baggett L, Raphael RM, Jansen JA, Mikos AG. The influence of an in vitro generated bone-like extracellular matrix on osteoblastic gene expression of marrow stromal cells. Biomaterials 2008;29:2729–39.
Martin I, Muraglia A, Campanile G, Cancedda R, Quarto R. Fibroblast growth factor-2 supports ex vivo expansion and maintenance of osteogenic precursors from human bone marrow. Endocrinology 1997;138:4456–62.
Piccinini E, Sadr N, Martin I. Ceramic materials lead to underestimated DNA quantifications: a method for reliable measurements. Eur Cell Mater 2010;20:38–44.
Braccini A, Wendt D, Jaquiery C, Jakob M, Heberer M, Kenins L, et al. Three-dimensional perfusion culture of human bone marrow cells and generation of osteoinductive grafts. Stem Cells 2005;23:1066–72.
Barbero A, Ploegert S, Heberer M, Martin I. Plasticity of clonal populations of dedifferentiated adult human articular chondrocytes. Arthritis Rheum 2003;48:1315–25.
Livak KJ, Schmittgen TD. Analysis of relative gene expression data using real-time quantitative PCR and the 2(-Delta Delta C(T)) Method. Methods 2001;25:402–8.
[30] Gronthos S, Graves SE, Ohta S, Simmons PJ. The STRO-1+ fraction of ac human bone marrow contains the osteogenic precursors. Blood 1994;4164–73.
[31] Buschmann J, Welti M, Hemmi S, Neuenschwander P, Baltes C, Giovanol et al. 3D co-cultures of osteoblasts and endothelial cells in DegraPol foa histological and high field MRI analyses of pre-engineered capillary netwc in bone grafts. Tissue Eng Part A 2011;17:291–9.
[32] Danielsson C, Ruault S, Simonet M, Neuenschwander P, Frey P. Polyester ethane foam scaffold for smooth muscle cell tissue engineering. Biomater 2006;27:1410–5.
[33] Riboldi SA, Sampaolesi M, Neuenschwander P, Cossu G, Mantero S. Elect spun degradable polyesterurethane membranes: potential scaffolds for sl etal muscle tissue engineering. Biomaterials 2005;26:4606–15.
[34] Boissard CI, Bourban PE, Tami AE, Alini M, Eglin D. Nanohydroxyapat poly(ester urethane) scaffold for bone tissue engineering. Acta Biomater 20 5:3316–27.
[35] Guelcher SA. Biodegradable polyurethanes: synthesis and applications regenerative medicine. Tissue Eng Part B Rev 2008;14:3–17.
[36] Kavlock KD, Pechar TW, Hollinger JO, Guelcher SA, Goldstein AS. Synthesis a characterization of segmented poly(esterurethane urea) elastomers for b tissue engineering. Acta Biomater 2007;3:475–84.
[37] Zhou YF, Sae-Lim V, Chou AM, Hutmacher DW, Lim TM. Does seeding den affect in vitro mineral nodules formation in novel composite scaffol J Biomed Mater Res A 2006;78:183–93.
[38] Brown BN, Valentin JE, Stewart-Akers AM, McCabe GP, Badylak SF. Mac phage phenotype and remodeling outcomes in response to biologic scaffc with and without a cellular component. Biomaterials 2009;30:1482–91.
[39] Crapo PM, Gilbert TW, Badylak SF. An overview of tissue and whole or decellularization processes. Biomaterials 2011;32:3233–43.
[40] Keane TJ, Londono R, Turner NJ, Badylak SF. Consequences of ineffect decellularization of biologic scaffolds on the host response. Biomaterials 20 33:1771–81.
[41] Teo KY, DeHoyos TO, Dutton JC, Grinnell F, Han B. Effects of freezing-indu cell-fluid-matrix interactions on the cells and extracellular matrix of er neered tissues. Biomaterials 2011;32:5380–90.
[42] Hidalgo-Bastida LA, Cartmell SH. Mesenchymal stem cells, osteoblasts a extracellular matrix proteins: enhancing cell adhesion and differentiation bone tissue engineering. Tissue Eng Part B Rev 2010;16:405–12.
[43] Hoshiba T, Kawazoe N, Tateishi T, Chen G. Development of stepw osteogenesis-mimicking matrices for the regulation of mesenchymal stem functions. J Biol Chem 2009;284:31164–73.
[44] Melchels FP, Tonnarelli B, Olivares AL, Martin I, Lacroix D, Feijen J, et al. 7 influence of the scaffold design on the distribution of adhering cells a perfusion cell seeding. Biomaterials 2011;32:2878–84.
[45] Liao J, Guo X, Nelson D, Kasper FK, Mikos AG. Modulation of osteoge properties of biodegradable polymer/extracellular matrix scaffolds genera with a flow perfusion bioreactor. Acta Biomater 2010;6:2386–93.
[46] Habibovic P, de Groot K. Osteoinductive biomaterials–properties and re vance in bone repair. J Tissue Eng Regen Med 2007;1:25–32.
[47] Gronthos S, Zannettino AC, Graves SE, Ohta S, Hay SJ, Simmons PJ. Differen cell surface expression of the STRO-1 and alkaline phosphatase antigens discrete developmental stages in primary cultures of human bone cells. J Bc Miner Res 1999;14:47–56.
[48] Hunter GK, Goldberg HA. Nucleation of hydroxyapatite by bone sialoprot Proc Natl Acad Sci 1993;90:8562–5.
[49] Evans ND, Gentleman E, Chen X, Roberts CJ, Polak JM, Stevens MM. Ext cellular matrix-mediated osteogenic differentiation of murine embryc stem cells. Biomaterials 2010;31:3244–52.
[50] Sun Y, Li W, Lu Z, Chen R, Ling J, Ran Q, et al. Rescuing replication a osteogenesis of aged mesenchymal stem cells by exposure to a yo extracellular matrix. Faseb J 2011;25:1474–85.
[51] Scott MA, Levi B, Askarinam A, Nguyen A, Rackohn T, Ting K, et al. Brief Revi of models of ectopic bone formation. Stem Cells Dev 2012;21:655–67.

**Supplementary data**

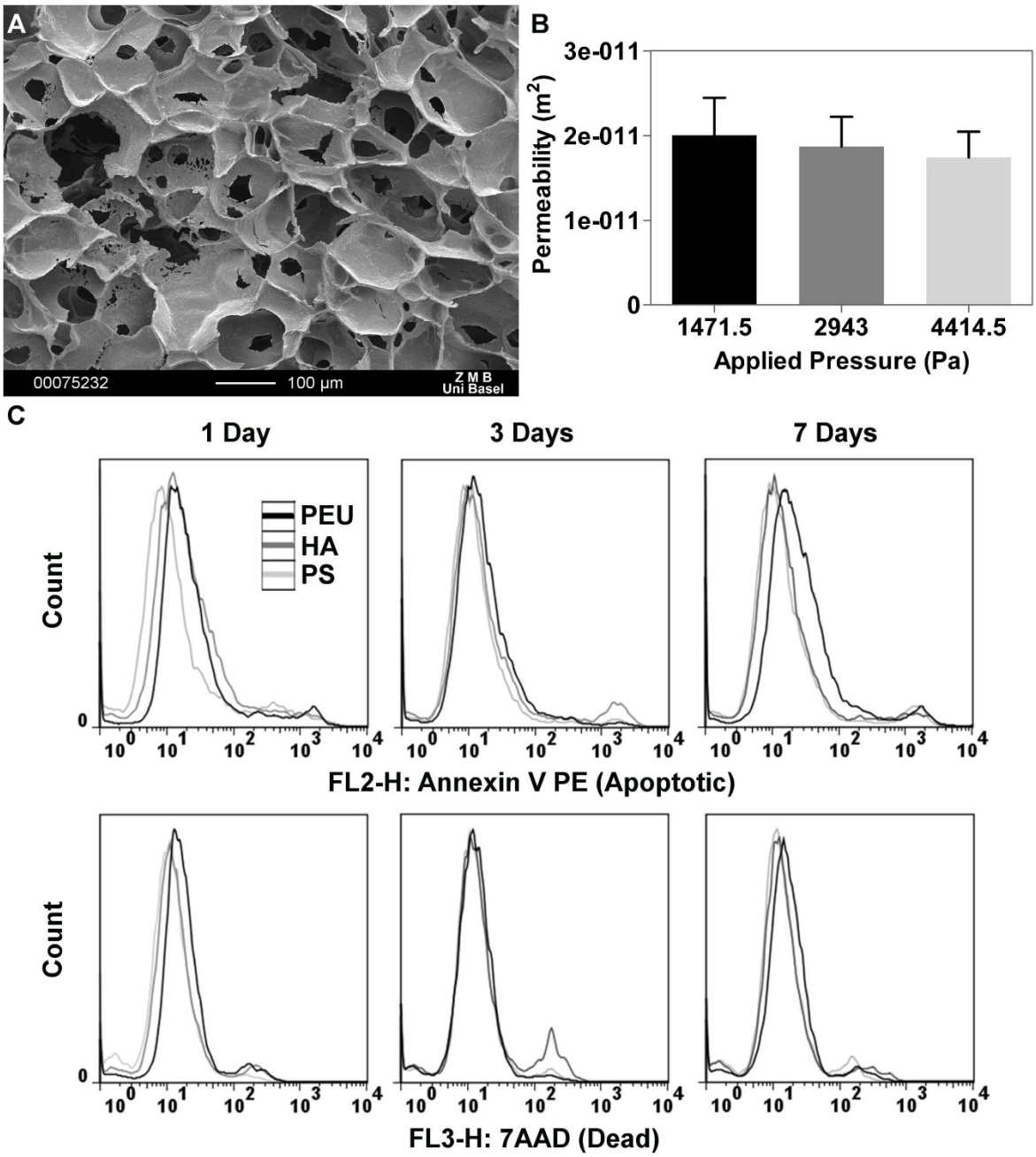


Supplementary Data 1.

PEU scaffold characterization. (A) SEM images of the scaffold showing an open interconnected pore structure with average pore dimensions of 153 ± 44 µm (B) permeability evaluation at different working pressures. (C) Cytotoxicity tests show a viability similar to those of ceramic (HA) and tissue culture polystyrene (PS) controls.

| | | |
|---|---|---|
| Collagen I | Primer R | CAG CCG CTT CAC CTA CAG C |
| | Primer F | TTT TGT ATT CAA TCA CTG TCT TGC C |
| | Probe | CCG GTG TGA CTC GTG CAG CCA TC |
| Cbfa1 | Primer R | GCC TTC AAG GTG GTA GCC C |
| | Primer F | CGT TAC CCG CCA TGA CAG TA |
| | Probe | CCA CAG TCC CAT CTG GTA CCT CTC CG |
| BMP-2 | Primer R | AAC ACT GTG CGC AGC TTC C |
| | Primer F | CTC CGG GTT GTT TTC CCA C |
| | Probe | CCA TGA AGA ATC TTT GGA AGA ACT ACC AGA AAC TG |
| BSP | Primer R | TGC CTT GAG CCT GCT TCC |
| | Primer F | GCA AAA TTA AAG CAG TCT TCA TTT TG |
| | Probe | CTC CAG GAC TGC CAG AGG AAG CAA TCA |
| OP | Primer R | CTC AGG CCA GTT GCA GCC |
| | Primer F | CAA AAG CAA ATC ACT GCA ATT CTC |
| | Probe | AAA CGC CGA CCA AGG AAA ACT CAC TAC C |
| OC | Primer R | GAA GCC CAG CGG TGC A |
| | Primer F | CAC TAC CTC GCT GCC CTC C |
| | Probe | TGG ACA CAA AGG CTG CAC CTT TGC T |
| GAPDH | Primer R | ATG GGG AAG GTG AAG GTC G |
| | Primer F | TAA AAG CAG CCC TGG TGA CC |
| | Probe | CGC CCA ATA CGA CCA AAT CCG TTG AC |

Supplementary Data 2.

List of the adopted primers and probes.

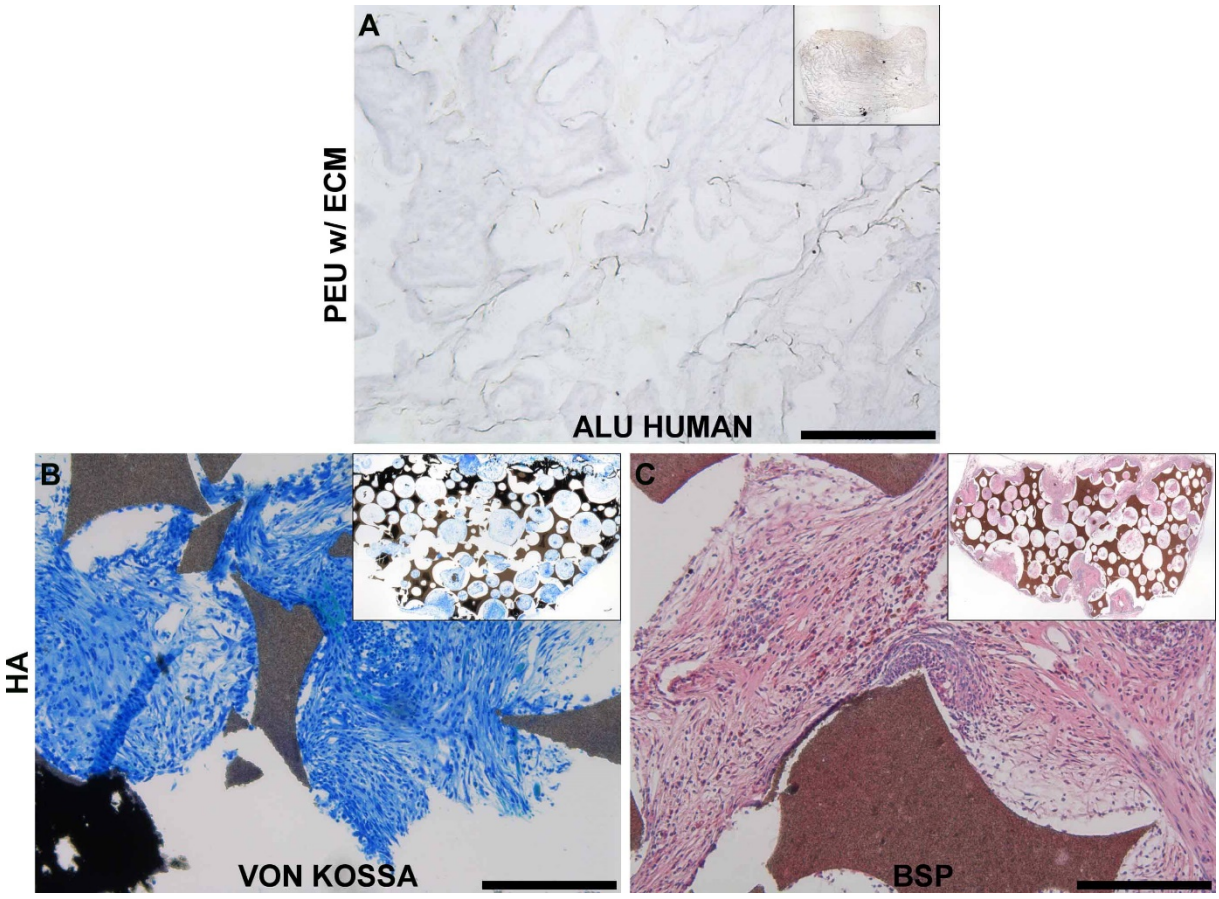


Supplementary Data 3.

Histological analyses of explanted PEU w/ECM. Constructs were negative for human alu hybridization confirming the absence of cells of human origin (A). The pores of cell-free implants of control HA samples were negative for Von Kossa staining (B) and BSP (C). The HA samples embedded in MMA (without undergoing decalcification treatment), the scaffold itself was positive to Von Kossa due to the phosphate present in the substrate material. (Scale bars = 200 μm).

| Days | STRO-1 Positive Population (%) | | |
|---|---|---|---|
| | HA | PEU | PEU w/ ECM |
| 8 | 4.9 | 11.8 | 8.0 |
| 16 | 3.6 | 7.9 | 7.4 |

Table 1.

hMSC expression levels for STRO-1 osteogenic precursor marker after 8 and 16 days culture on HA, PEU and PEU w/ECM. Positive expression was defined as the level of fluorescence greater than 99% of corresponding control.

Biomaterials. 2013 Jul;34(26):6099-6108
doi: 10.1016/j.biomaterials.2013.04.058

# Tissue decellularization by activation of programmed cell death

Paul Bourgine[a], Benjamin E. Pippenger[a], Atanas Todorov Jr. [a], Laurent Tchang[a], Ivan Martin[a]

[a] Department of Surgery, University Hospital Basel, Hebelstrasse 20, CH-4031 Basel, Switzerland

*Correspondence to: Prof. Ivan Martin
ICFS, University Hospital Basel
Hebelstrasse 20, ZLF, Room 405
4031 Basel, Switzerland
Phone: + 41 61 265 2384; fax: + 41 61 265 3990
E-mail: Ivan.Martin@usb.ch

## ABSTRACT

Decellularized tissues, native or engineered, are receiving increasing interest in the field of regenerative medicine as scaffolds or implants for tissue and organ repair. The approach, which offers the opportunity to deliver off-the-shelf bioactive materials without immuno-matching requirements, is based on the rationale that extracellular matrix (ECM)-presented cues can be potently instructive towards regeneration. However, existing decellularization protocols typically result in damage to the source ECM and do not allow the controlled preservation of its structural, biochemical and/or biomechanical features. Here we propose the deliberate activation of programmed cell death as a method to selectively target the cellular component of a tissue and thereby to preserve the integrity of the decellularized ECM. In the case of engineered tissues, the approach could be complemented by the use of (i) an immortalized cell line, engineered to undergo apoptosis upon exposure to a chemical inducer, and (ii) a perfusion bioreactor system, supporting efficient removal of cellular material. The combination of these tools may lead to the streamlined development of more appropriate materials, based on engineered and decellularized ECM and including a customized set of signals specifically designed to activate endogenous regenerative processes.

Biomaterials 34 (2013) 6099–6108

Contents lists available at SciVerse ScienceDirect

Biomaterials

journal homepage: www.elsevier.com/locate/biomaterials

Leading opinion

# Tissue decellularization by activation of programmed cell death

Paul E. Bourgine, Benjamin E. Pippenger, Atanas Todorov Jr., Laurent Tchang, Ivan Martin*

*Departments of Surgery and of Biomedicine, University Hospital Basel, University of Basel, Hebelstrasse 20, CH-4031 Basel, Switzerland*

ARTICLE INFO

*Article history:*
Received 19 April 2013
Accepted 27 April 2013
Available online 27 May 2013

*Keywords:*
Decellularization
Apoptosis
Bioreactor
Regenerative medicine
Extra-cellular matrix

ABSTRACT

Decellularized tissues, native or engineered, are receiving increasing interest in the field of regenerative medicine as scaffolds or implants for tissue and organ repair. The approach, which offers the opportunity to deliver *off-the-shelf* bioactive materials without immuno-matching requirements, is based on the rationale that extracellular matrix (ECM)-presented cues can be potently instructive towards regeneration. However, existing decellularization protocols typically result in damage to the source ECM and do not allow the controlled preservation of its structural, biochemical and/or biomechanical features. Here we propose the deliberate activation of programmed cell death as a method to selectively target the cellular component of a tissue and thereby to preserve the integrity of the decellularized ECM. In the case of engineered tissues, the approach could be complemented by the use of (i) an immortalized cell line, engineered to undergo apoptosis upon exposure to a chemical inducer, and (ii) a perfusion bioreactor system, supporting efficient removal of cellular material. The combination of these tools may lead to the streamlined development of more appropriate materials, based on engineered and decellularized ECM and including a customized set of signals specifically designed to activate endogenous regenerative processes.



## 1. Introduction

The extracellular matrix (ECM) is a combination of structural and functional proteins, proteoglycans, lipids and crystals that has a unique composition and physical properties for every tissue and organ in the body. Acting as a reservoir for morphogens while providing mechanical support for resident cells, ECM participates in cell communication as well as in defining the shape and stability of tissues [5]. ECM cues have been demonstrated to specifically promote cell recruitment, adhesion, migration, proliferation and differentiation in a way that reflects the functional needs and biological identity of tissues [6]. Such instructive elements may retain at least in part their functionality even in the absence of the living cellular component.

Based on this rationale, decellularized ECM has received increased attention in the field of regenerative medicine as an *off-the-shelf* and immune-compatible alternative to living grafts for tissue and organ repair (Fig. 1). Decellularized ECM is expected to induce regenerative processes not only through specific "organomorphic" structures [8], but also by the physiological presentation of different cocktails of regulatory molecules in a mechanically suitable environment. The instructive scaffold materials derived from decellularized ECM could be activated by living cells prior to implantation, with the assumption that ECM is capable of directing the differentiation fate of the seeded cells [9–12]. In an even more attractive paradigm, the decellularized ECM could be directly used to instruct resident cells towards endogenous tissue repair by leveraging principles of morphogenesis. Starting from decellularized bone as a prototype ECM graft [13], the field has received convincing proof-of-principle evidences of the latter approach for epithelial [14], musculoskeletal [15] and vascular [16] tissue regeneration, as well as for the engineering of myocardial [17], pulmonary [4], renal [18,19] and pancreatic implants [20]. More recently, thanks to the progress in guiding cell differentiation towards specific lineages, *in vitro*-engineered tissues are also being considered as a substrate for decellularization. This approach opens the perspective to the generation of large quantities of standardized, customized grafts.

A variety of chemical, enzymatic and physical procedures have been developed to eliminate the cellular component of both native and engineered tissues while minimally disrupting the ECM (Box 1). Protocols described in literature tend to combine several of these principal methods in order to increase the efficiency of decellularization and at the same time reduce damage to the ECM by using less destructive conditions.

* Corresponding author. Institute for Surgical Research and Hospital Management, Basel University Hospital, Hebelstrasse 20, 4031 Basel, Switzerland. Tel.: +41 61 265 2384; fax: +41 61 265 3990.
*E-mail addresses:* ivan.martin@usb.ch, imartin@uhbs.ch (I. Martin).

0142-9612/$ – see front matter © 2013 Elsevier Ltd. All rights reserved.
http://dx.doi.org/10.1016/j.biomaterials.2013.04.058

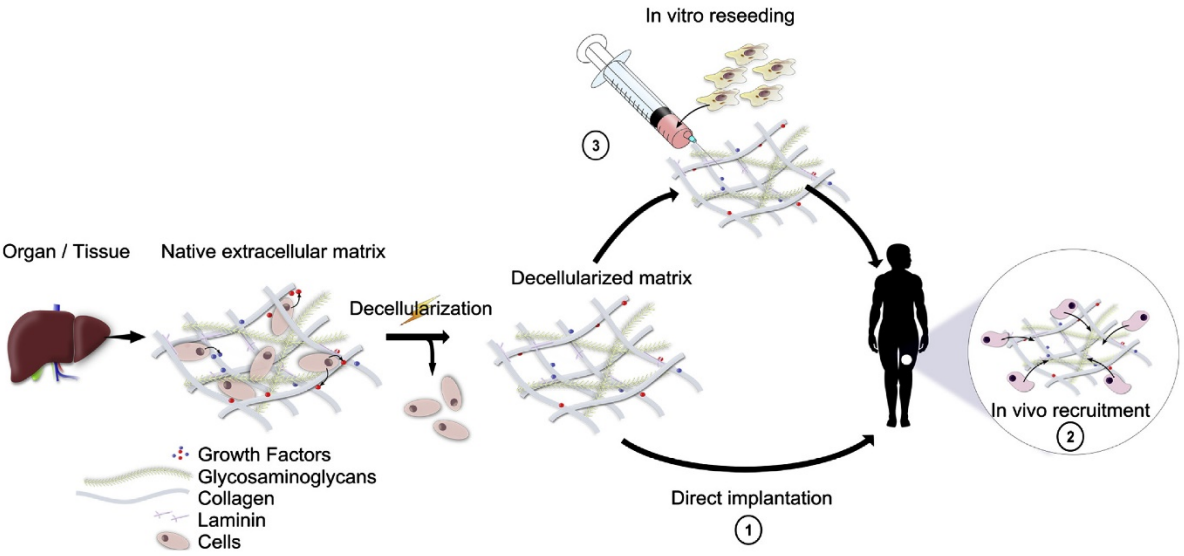


**Fig. 1.** Concept of tissue decellularization. Cell-free tissue can be generated by decellularization of native or engineered tissue. The resulting ECM can be directly transplanted into a patient (1), entirely relying on the capacity to instruct resident cells towards endogenous tissue repair (2). Alternatively, prior to implantation the ECM can be seeded with cells that "prime" the material (e.g., to enhance its remodeling or vascularization) and/or "get primed" toward a specific function (e.g., to proliferate or differentiate) (3). The latter implants could induce regeneration by the combined action of the seeded and recruited cells.

**Box 1**
Overview of existing decellularization procedures. A more comprehensive analysis can be found in recent reviews [6,22,23].

*Acids and bases* [1] react with and denature proteins, solubilize cell components and alter nucleic acids, thus bursting cells. They are not selective and hence alter also ECM components, especially collagens, glycosaminoglycans (GAG) and growth factors.

*Hypertonic and hypotonic solutions* [2] disrupt cells through osmotic shock and also interfere with DNA-protein interactions. They have a relative efficiency and do not allow for an effective removal of cellular residues.

*Detergents* [3] may be ionic, non-ionic or a combination of both. They disrupt DNA-protein, lipid and lipid–protein interactions and may denature proteins. Additionally to their action on cells, they also damage the ECM ultrastructure, leading to a loss of collagens, growth factors and GAG.

*Enzymes* [4] can be used to target the remnant nucleic acids after cell rupture or the peptide bonds which anchor the cells to the ECM. They tend to remain in significant quantities in the tissue and may provoke an additional immune response. Prolonged exposition can also result in removal of collagens, laminin, fibronectin, elastin and GAG, as well as destruction of the ECM ultrastructure.

*Physical methods* [7] are widely used for the decellularization of tissues. The most common ones consist of repeated freeze and thaw cycles. Cells burst due to the formation of intra- and extra-cellular ice crystals, which lead to drastic changes in ion concentrations and mechanical destruction of the cell membrane. The ice crystals also damage the ultrastructure and proteins contained in the ECM and can inactivate some growth factors (e.g., Vascular Endothelial Growth Factor (VEGF)).

All of the above mentioned methods, which have been subject of several review assays [6,21–23], can reach variable degrees of decellularization efficiency, but some problems remain common to all. First, all existing techniques rely on cell lysis. The resulting cell debris can then freely adsorb to the remaining matrix, leading to a paradoxical increase in immunogenicity [24]. Second, existing techniques have been demonstrated to alter the ECM, leading to the degradation of some of its components [6].

In principle, maintaining the integrity of the ECM following decellularization could support a more predictable, reproducible and effective clinical use of the resulting material. Moreover, from a scientific standpoint, preservation of the ECM would be instrumental to possibly identify the role of specific molecules and their organization in eliciting tissue repair processes. However, the typical procedures used necessarily imply an impairment of the ECM integrity. Aiming at avoiding the side effects inherent to current strategies, we propose here an alternative approach to tissue decellularization based on the controlled activation of programmed cell death.

## 2. Processes of cell death

Cell death can occur by either necrosis or apoptosis. During necrosis, the cell membrane rapidly becomes permeable, leading to the leakage of the intra-cellular content. Necrosis is a non-lysosomal, uncontrolled process typically caused by external events and signals [25], associated with distinct morphological patterns (Fig. 2). Since necrosis involves the early loss of the membrane integrity, it induces a massive inflammation linked to the leakage of cellular content [26].

Instead, apoptosis is a genetically determined process, consequently referred to as the "programmed cell death", leading to the suicide of the cells [27,28]. Apoptosis typically occurs during tissue and organ development but may also act as a homeostatic mechanism or as a means to eliminate infected or tumorigenic cells [29]. Towards the induction of apoptosis for tissue decellularization, it is necessary to distinguish two different pathways, namely the

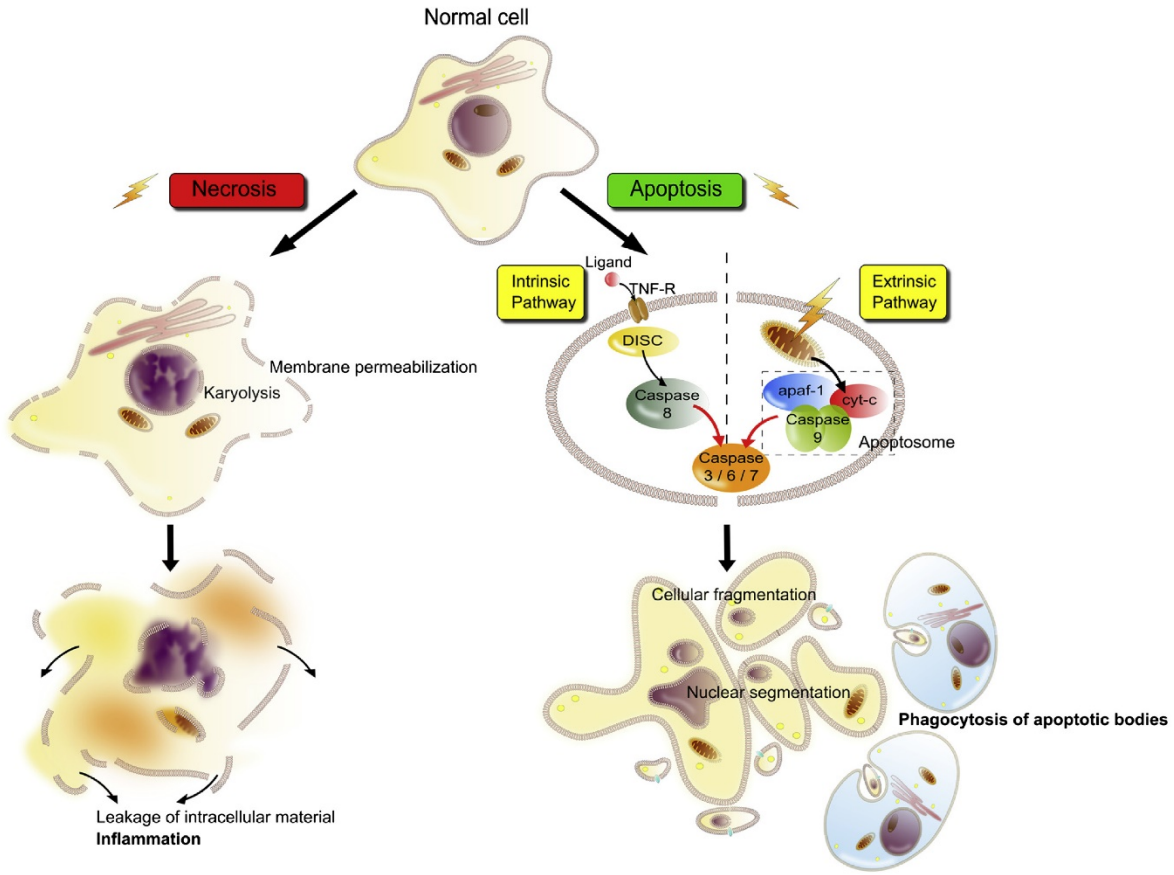


**Fig. 2.** Processes of cell death. Cell death occurs through either necrosis or apoptosis. Necrosis implies permeabilization of the cell membrane and consequently the leakage of the intra-cellular content, potentially inducing massive inflammation. Instead, the activation of the apoptotic program, through either the intrinsic or extrinsic pathway, involves a cascade of molecular events that results in cellular condensation and disruption into small apoptotic bodies. During the process, the cellular content is degraded and strictly kept within the cell membrane, avoiding an inflammatory reaction. Abbreviations: TNFR = tumor necrosis factor receptor; apaf-1 = apoptotic protease activating factor 1; cyt-c = cytochrome-c.

intrinsic or extrinsic ones. While the two pathways differ in their initial activation, they converge in the final cell suicide execution (Fig. 2). The molecular mechanisms driving both apoptotic pathways are highly complex and not fully understood, but can be shortly described as follows.

The intrinsic pathway, triggered upon stress stimuli (e.g. change of environmental conditions), is initiated by the permeabilization of the mitochondrial outer membrane, resulting in the release of the cytochrome-c (cyt-c) into the cytosol [30]. This protein forms a complex called apoptosome, together with the Apoptotic protease activating factor 1 (Apaf-1) and caspase-9. The formation of this complex turns on the initiator caspase-9, which in turn activates the effectors caspase-3, 6, and 7 [31–33]. Due to the essential role of the mitochondria in this process, the intrinsic pathway is also referred to as the "mitochondrial pathway".

The extrinsic pathway is triggered by external signals binding to specific cell surface death receptors (DR) of the tumor necrosis factor family (TNF, Table 1) [34,35]. Such binding results in the formation of a death inducing signaling complex (DISC), leading to the transduction of the signal within the cytosol [36]. Following caspase-8 dimerization, the same effector caspases involved in the intrinsic route are activated.

After initiation of the suicide program by either the intrinsic or extrinsic pathway and following the activation of the effector caspases, different endonucleases and proteases respectively lead to DNA fragmentation and the degradation of cytoskeletal and nuclear proteins [28]. As a consequence, cytomorphological changes are

**Table 1**
Death receptors of the TNF superfamily and their cognate ligands. Abbreviations: TNFR1 = tumor necrosis factor receptor 1; TNFα = Tumor necrosis factor α; Apo-3 = Apoptosis antigen 3; TRAIL = TNF-related apoptosis inducible ligand; TRAILR = TNF-related apoptosis inducible ligand receptor; NGF = nerve growth factor; NGFR = nerve growth factor receptor; EDA = ectodysplasin A; EDAR = ectodysplasin A receptor [38,39,81,82] .

| Receptor | Cognate ligand |
|---|---|
| TNFR1 (DR-1) | TNFα |
| Fas/CD95 (DR-2) | FasL |
| Apo-3 (DR-3) | TL1A |
| TRAILR (DR-4 and DR-5) | TRAIL |
| DR-6 | Unknown |
| NGFR | NGF |
| EDAR | EDA |

observed like the chromatin and cytosol condensation, associated with a global cell shrinkage [28]. As a final step, cells are disrupted into small apoptotic bodies that are then phagocytosed by immune cells [37]. This common end stage cellular morphology of intact apoptotic bodies is particularly interesting when considering the decellularization of tissues and matrices, as described below.

## 3. Apoptosis, the holy grail for tissue decellularization?

Existing decellularization methods require a tradeoff between efficient cellular removal and ECM preservation, as increasing the treatment severity for a more complete decellularization fatally results in an enhanced ECM disruption. As a result, current decellularization protocols rather aim at minimizing effects on the ECM rather than avoiding them [6]. Here we propose an alternative approach based on the exploitation of programmed cell death. The apoptotic pathways can be deliberately activated through a clean and controlled process by the delivery of appropriate signals. Importantly, this strategy of decellularization would selectively target the cell component of a tissue, in a way which remains decoupled from compromising the ECM integrity.

A closer analysis of the mechanism of apoptosis identifies key features that make it attractive in view of a decellularization procedure. During apoptosis, the cell membrane undergoes structural changes that lead to the loss of cell contact with the ECM [38]. This combined with the reduced size of apoptotic bodies (0.5–2 μm), cell removal with virtually no structural or functional changes to the tissue matrix may be achievable. Moreover, during the whole apoptotic process, the cellular content is kept strictly within the cell membrane and the apoptotic bodies [39]. The immunogenic cellular constituents do not leak into the surrounding matrix [40–42], thus preventing an unnecessary inflammatory reaction. This is in contrast to existing decellularization techniques, inducing a necrotic cell-death, cell bursting and the release of immunogenic cellular material within the neighboring environment [24]. Without appropriate rinses, such material may generate a high immune-reaction following implantation and subsequently lead to the rejection of the graft.

A possible additional advantage of ECM decellularization by induction of apoptosis is related to the association between the activation of effector caspases [3,6,7] and the release of Prostaglandin $E_2$ ($PGE_2$). This process has been recently reported to be involved in tissue regeneration by stimulating proliferation of neighboring progenitor cells [43]. Thus, decellularizing a tissue through the apoptotic pathway may contribute to prime the matrix towards regeneration programs through the release of key paracrine signals.

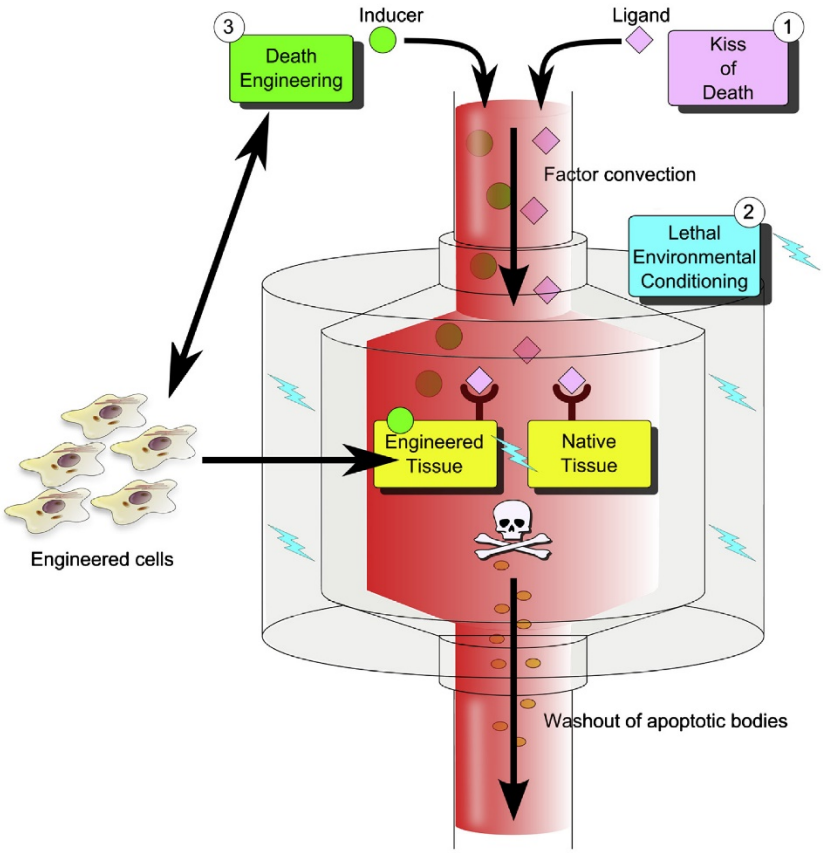


**Fig. 3.** Tissue decellularization by apoptosis induction within 3D perfusion bioreactor. Three different approaches are proposed in order to decellularize a tissue by apoptosis-induction; *Kiss-of-death* (1), *Lethal Environmental Conditioning* (2), *Death-engineering* (3). The decellularization procedure within a 3D perfusion bioreactor system increases the convection of the apoptotic inducer, establishes controlled environmental conditions and facilitates the washout of apoptotic bodies. In particular, when considering the decellularization of engineered tissues, this system could be the basis for a streamlined process to generate an ECM and subsequently induce apoptosis within a single, closed device.

Apoptosis is also a physiological process during embryogenesis, normal tissue development and immunological events. Induction of apoptosis, as the predominant pathway to cell death, thus has the potential to mimic natural developmental steps in tissue formation and remodeling [44,45]. Hence, the proposed strategy appears to be in compliance with the recently described concept of "developmental engineering" [46], namely the recapitulation of developmental processes for the engineering of regeneration.

## 4. Apoptosis induction strategies

The method used to implement the apoptotic concept for ECM decellularization will critically determine the killing efficiency and overall success of the strategy. Here we propose different approaches, which notably differ according to the type of pathway (i.e., intrinsic vs. extrinsic) to be activated.

### 4.1. Kiss-of-death

This strategy entirely relies on the extrinsic pathway activation through the delivery of specific ligands that bind their corresponding death receptors (DRs) of the TNF superfamily (Table 1). As the DRs are ubiquitously expressed [47], the activation of the extrinsic apoptotic pathway can be considered for the decellularization of virtually any tissue/organ. Nevertheless, the choice of the ligand, and consequently the type of DR to target has to be carefully considered. While some ligands are known to specifically activate the programmed cell death, others (DR-1, DR-3, DR-6 and EDAR) may have also anti-apoptotic effects, leading to the activation of survival signals [35]. Furthermore, each cell type might have a different sensitivity to each ligand, since a differential expression of the DRs is observed from tissue to tissue. Some cells may also be more prone than others to escape apoptosis through the survival pathway. For instance, TRAIL was shown to induce apoptosis in cancer cells, but not in normal cells [48,49]. Therefore, when elaborating a decellularization strategy, the type of DR to target should be selected according to the specific cellular system.

A certain number of pro-apoptotic ligands were already reported to successfully induce apoptosis in a variety of cell types. Human bone marrow-derived mesenchymal stromal cells (hMSC) were shown to be sensitive to FasL, in both an undifferentiated and differentiated status [50]. FasL was also shown to induce apoptosis of cardiomyocytes [51] and epidermal cells [52]. Moreover, it is abundantly expressed in a variety of organs, such as the heart, kidney, pancreas and the liver [53]. The delivery of TNFα was described as an efficient inducer in lung [54] and intestinal epithelial cells [55]. This factor also promotes chondrocyte [56] and renal endothelial cell apoptosis [57].

This non-exhaustive list of references demonstrates the diversity of the studies reporting the successful use of DR ligands as apoptotic inducers. However, none of them aimed at optimizing the observed killing, which may require screening not only for the appropriate ligand, but also for a suitable concentration and time of induction. One possible optimization strategy could rely on the combination of ligands, to generate a "customized death cocktail". This can be used to obtain synergistic effects, as for example one ligand would prime cells to increase their sensitivity to a second one. It was thus shown that treating lung fibroblast and hepatocytes with TNFα sensitizes them to FasL induced apoptosis [58,59].

A potential limit of the *Kiss-of-death* strategy possibly involves the inflammatory effect of some ligands. A certain quantity of those factors may remain entrapped in the ECM, requiring additional rinsing for their removal from the graft. Furthermore, depending on the required concentrations of the selected ligands, the process may become costly.

### 4.2. Lethal-environmental-conditioning

Upon environmental stress, cells can naturally undergo apoptosis by activation of the intrinsic "mitochondrial" pathway. An apoptotic response could thus be induced by modulating

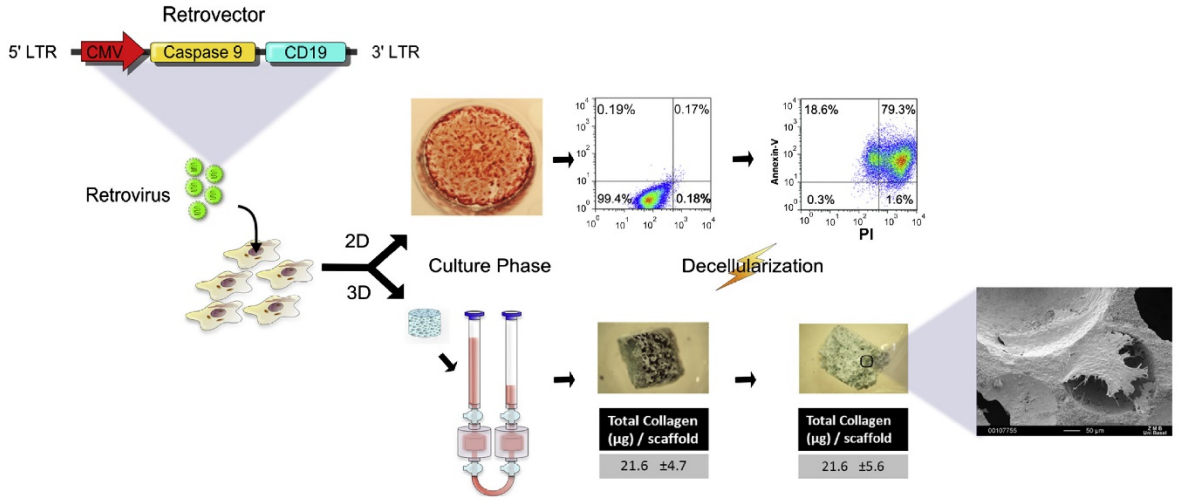


**Fig. 4.** Generation of ECM-decorated materials by apoptosis-driven decellularization. A hMSC cell line was generated and transduced with an inducible caspase 9 gene (iCaspase 9) [71]. Cells were shown to deposit a mineralized ECM (Alizarin-red staining) in Petri dishes (2D) while being efficiently inducible toward apoptosis (>95% positivity for Annexin-V and/or PI). After perfusion-mediated seeding on porous ceramic scaffolds (3D), the cell line was capable to adhere, colonize the scaffold (MTT staining) and deposit a collagen-rich ECM. The apoptotic decellularization performed within the bioreactor system led to the generation of an ECM-decorated material without a measurable reduction of the total collagen content. As a comparison, the freeze&thaw method applied to the same constructs resulted in a collagen loss of 74% (final content: 5.61 ± 1.06 µg/scaffold). These findings provide a proof-of-principle for the decellularization of ECM produced by osteogenic cells following the described apoptotic *Death-engineering* strategy, in a perfusion bioreactor setup.

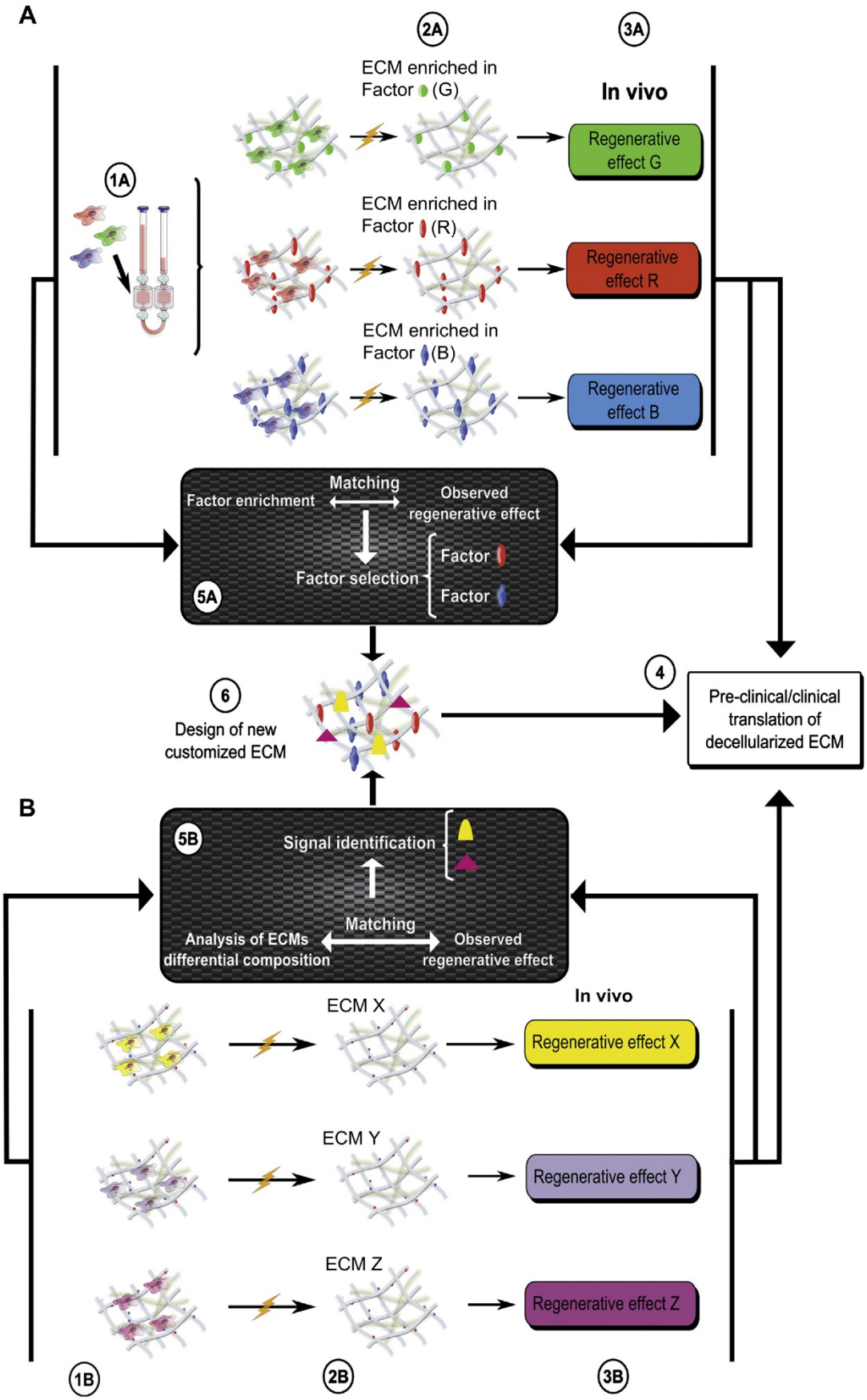
A
2A
3A
ECM enriched in Factor (G)
In vivo
Regenerative effect G
1A
ECM enriched in Factor (R)
Regenerative effect R
ECM enriched in Factor (B)
Regenerative effect B
Factor enrichment
Matching
Observed regenerative effect
Factor selection
Factor
Factor
5A
6
Design of new customized ECM
4
Pre-clinical/clinical translation of decellularized ECM
B
5B
Signal identification
Matching
Analysis of ECMs differential composition
Observed regenerative effect
In vivo
ECM X
Regenerative effect X
ECM Y
Regenerative effect Y
ECM Z
Regenerative effect Z
1B
2B
3B

environmental factors, including temperature, pH, as well as $CO_2/O_2$, nitric oxide (NO), and $H_2O_2$ content. As opposed to the physical freeze & thaw method, leading to a necrotic response, induction of apoptosis by temperature changes requires low variations, in either hyperthermic [60] or hypothermic [61] ranges. Ideally, temperature fluctuations from 10 °C to 45 °C are advised, whereby the effect on the matrix will also depend on the incubation time. NO has been described as a potent inducer of mitochondrial apoptosis [62], especially for cardiomyocytes [63], pancreatic cells [64] and chondrocytes [65]. The use of hypoxic conditions was also reported to activate the apoptotic program in pancreatic cells [66] or cardiomyocytes [67].

The advantages of the *lethal-environmental-conditioning* strategy rely on the minimal cost and simplicity of the setup required to modulate and control the operating conditions. However, an efficient killing might only be obtained after an extensive and possibly multi-parametric screening for optimal conditions.

### 4.3. Death-engineering

This strategy relies on the activation of any of the two apoptotic pathways by the use of a genetic approach. Since it requires the genetic engineering of cells prior to the generation of a tissue, this strategy relates mainly to the decellularization of engineered grafts. Apoptosis activation could in principle be achieved by modulating the expression level of key genes involved in the pathway. Nevertheless, since apoptosis implies phosphorylation and dimerization of specific molecular players, it cannot be triggered by simply overexpressing or silencing key genes of the transduction pathway.

One possibility to engineer cells to death consists in overexpressing death-receptors at the cell surface. This was shown to enhance cell sensitivity to the death-inducing ligand [68] and could thus be used in conjunction with the *Kiss-of-death* strategy.

An alternative option relies on the implementation of a toxic transgene (e.g. apoptin, lectin), whose expression is under strict control. In this regard, the use of a tight and inducible expression system is a requirement in order to activate cell-suicide post-tissue generation and to avoid an excessive "leakiness" that may also result in premature cell-death. The stable integration of such a genetic construct is also critical as existing transient expression systems were shown to persist only from days to a few weeks within the cells [69]. Considering modified cells would be induced towards death after the synthesis of a tissue, which implicates an extensive culture time, transient systems may result in a poor killing due to the non-persistence of the genetic construct.

As a suitable genetic device addressing the above mentioned requirements, an elegant inducible system was described [70] and shown to lead to a high killing efficiency in transduced cells. This device is based on the constitutive expression of a modified caspase 9, whose dimerization can be activated through the delivery of a clinically approved inducer. This genetic approach was originally developed to improve the safety of cell-based therapy, but could also be used to induce the decellularization of a tissue. The efficiency of killing was already demonstrated in primary and differentiated hMSC [71]. The advantage of this system relies in the absence of leakiness and the downstream activation of the apoptotic pathway, thus avoiding activation of the survival pathway.

The three aforementioned strategies (*Kiss-of-death, lethal environmental conditioning and death-engineering*) differ in protocol but are fully compatible and their combination may in fact synergize the final cell killing efficiency.

## 5. Tissue/organ decellularization within perfusion systems

Devitalization can be considered as the first step of a decellularization procedure, ultimately aiming not only at killing, but also at removing the cellular fraction. Typical methods to eliminate the cell debris are based on extensive rinsing but risk to either lead to mechanical disruption of the tissue or to a non-efficient removal of the immunogenic material. Following the concepts of whole organ perfusion elegantly developed in the recent years [5,17], here we propose the use of perfusion bioreactor systems combined with induction of apoptosis in order to achieve an efficient and controlled tissue decellularization (Fig. 3).

The use of a bioreactor system would allow for a superior control of the process parameters, such as temperature or gas content, which would be directly relevant for the *lethal-environmental-conditioning* strategy. Moreover, the perfusion may enhance the killing efficiency by increasing the convection of the pro-apoptotic factors throughout the graft, especially while considering the *Kiss-of-death* or *Death engineering* strategies (Fig. 3). The use of perfusion systems would also play a critical role in the efficient and controlled removal of the previously killed cellular component. Controlling the flow patterns and associated induced shear may be of interest during the washing step in order to eliminate the apoptotic bodies from the ECM as they form, thus allowing for a non-invasive, yet efficient and standardized wash-out of any cellular material.

The use of perfusion-based bioreactor systems, forcing a cell suspension or culture medium directly through the pores of a scaffold material, was previously shown to support the engineering of tissues with superior properties than typical static cultures [72–74]. Thus, one could envision a streamlined manufacturing process for *off-the-shelf* decellularized grafts, whereby the same perfusion system would be used first to develop the tissue and subsequently to decellularize the deposited ECM. Additional features and benefits of such paradigm, derived from other biotechnology settings, would include automation, standardization, control and possibly cost-effectiveness of the process implementation.

## 6. Tissues engineered to death: a proof of principle

In the context of bone regeneration, one attractive strategy is to generate decellularized grafts with osteo-inductive properties by decoration of materials with a cell-laid ECM. In contrast to the delivery of over-doses of single morphogens (e.g., defined bone

**Fig. 5.** Alternative pathways towards the design of customized, decellularized ECM (A) Cells can be engineered (1A) to secrete specific factors/morphogens. Following 3D culture, possibly in a bioreactor system and subsequent apoptosis-driven decellularization, the produced tissues are enriched in specific morphogens (2A). The differences in composition are expected to trigger specific regenerative effects *in vivo* (3A) that could result in their direct pre-clinical/clinical translation [4]. The matching between the elicited *in vivo* response (e.g. angiogenic, osteo-inductive or proliferative effect) and the ECM composition could lead to the selection of a set of factors (5A) capable to induce a desired regenerative process. Ultimately, the design of the resulting customized ECM would represent a new generation of instructive materials with enhanced performance for a predictable regeneration (6). (B) The decellularization by apoptosis also offers the exciting but challenging possibility to investigate the properties of ECM from engineered/native tissues (1b), through the removal of the cellular fraction without compromising the integrity of the ECM (2b). This may allow to better understand the role and function of the different ECMs in the absence of the cellular component. The instructive capacity of such acellular constructs can be evaluated upon *in vivo* implantation in suitable models (3b) and the observed regenerative effect can either lead to a direct pre-clinical/clinical translation of the generated ECM (4), or can be matched with the respective ECM composition (5b). A combinatorial analysis of this matching may allow the identification of new signals (5b) that critically drove the regenerative process. Ultimately, these factors could be implemented within the design of customized ECM (6), converging with the approach described above (Fig. 5A) towards the generation of instructive materials that contain the necessary set of signals required for the repair of specific tissues/organs.

morphogenetic proteins), associated with cost and safety concerns [75,76], this approach relies on the embedding and presentation by the ECM of a cocktail of different factors in more physiological concentrations to activate a regenerative process (e.g., by acting on resident osteoblastic and endothelial lineage cells). In this context, human bone marrow-derived Mesenchymal Stromal Cells (hMSC) have already been used in the attempt to generate ECM with osteo-inductive properties [77,78], as a niche for reseeded MSC or for priming of endogenous progenitor cells. So far, however, the ECM deposited during *in vitro* culture could not be shown to be capable of inducing ectopic *in vivo* bone formation if deprived of the living cellular component [9]. Combining the approaches of decellularization by apoptosis with a 3D perfusion culture system [79], together with the utilization of a suitable cell source, could offer the opportunity to enhance the osteo-inductive properties of decellularized ECM. We recently reported the successful generation of an immortalized hMSC line with properties similar to the original primary cells and controlled survival. The cell line maintains the capacity to differentiate towards the osteogenic lineage, is not tumorigenic and – thanks to the implementation of a genetic device – can be pushed to programmed cell death by the delivery of a clinically approved chemical inducer [80].

Here we report that the cell line could deposit a mineralized ECM in 2D culture and still be efficiently induced towards apoptosis (>95%, Fig. 4). Moreover, when seeded on a porous ceramic scaffold within a 3D perfusion-based bioreactor system, the engineered cell line was capable to adhere, proliferate and deposit an ECM. The generated constructs could be directly and efficiently decellularized by the direct perfusion of the apoptotic-inducer through the ECM, leading to the successful generation of ECM-decorated, cell-free materials. As compared to the living counterparts, the "apoptized" tissues maintained the amount of total collagen, as representative ECM protein, in contrast to those decellularized by a conventional freeze/thaw protocol, where a marked loss of total collagen content (74%) was measured (Fig. 4). This setting thus provides a proof-of-principle for the decellularization of ECM produced by osteogenic cells following the described apoptotic *Death-engineering* strategy, in a perfusion bioreactor setup.

Further studies are required to assess (i) to which extent the apoptotic treatment may better preserve the deposited ECM, beyond total collagen, as compared to traditional protocols of decellularization and (ii) whether the resulting "apoptized" grafts have osteo-inductive properties. The paradigm could obviously be extended to other cell lines, for the deposition of a customized ECM specifically competent to induce regeneration of different tissues.

## 7. Conclusion & perspective

The deliberate activation of programmed cell death is here proposed as an elegant alternative to conventional approaches for decellularization of native or engineered ECM. Thanks to the possibility to specifically target the cellular component, decellularization by apoptosis-induction is expected to better preserve the integrity of the structural and instructive components of an ECM and ultimately to lead to the generation of *off-the-shelf* grafts with enhanced regenerative properties. The different apoptosis induction strategies described above offer a wide range of possibilities which could also be combined with a 3D perfusion culture system for a streamlined process implementation and/or with the use of immortalized cell lines, genetically implemented with an inducible death device.

The use of a cell line for the engineering of ECM to be decellularized would support not only repeatable production of batches with standardized properties, but also optimization and customization of the ECM regenerative potency. In fact, a cell line could be further engineered to overexpress defined factors, for example specific BMPs for enhanced osteoinduction or VEGF for more efficient vascularization. The design of customized ECM (Fig. 5A) to elicit specific repair would allow establishing a new generation of instructive materials matching the structural and molecular cues required for a predictable regeneration.

The use of apoptosis as decellularization technique goes beyond the generation of grafts with enhanced performance. The concept would also offer the unprecedented possibility to investigate the properties of decellularized but theoretically intact ECM and – by correlating an observed regenerative capacity with a specific composition – to identify a set of cues critical to elicit certain functions (Fig. 5B). The investigation and validation of the relevance of such features could then ultimately support a transition from the paradigm of decellularization of engineered biological ECM to the vision of entirely synthetic matrices, designed to contain the necessary and sufficient set of signals required for the repair of specific tissues/organs.

## Author contributions

Paul Bourgine: conception and design, collection and assembly of data, data analysis and interpretation, and manuscript writing; Benjamin Pippenger: experimental design, collection and assembly of data, data analysis and interpretation, manuscript writing; Atanas Todorov Jr.: manuscript writing; Laurent Tchang: figures conception; Ivan Martin: conception and design, financial support, manuscript writing, and final approval of manuscript.

## Acknowledgments

The research leading to these results has received funding from the European Community's Seventh Framework Programme (MultiTERM, grant agreement nr 238551). The authors acknowledge Fin-Ceramica Faenza S.p.a, Italy for the generous supply of Engipore scaffolds.

## References

[1] Reing JE, Brown BN, Daly KA, Freund JM, Gilbert TW, Hsiong SX, et al. The effects of processing methods upon mechanical and biologic properties of porcine dermal extracellular matrix scaffolds. Biomaterials 2010 Nov;31(33):8626–33.
[2] Yang B, Zhang Y, Zhou L, Sun Z, Zheng J, Chen Y, et al. Development of a porcine bladder acellular matrix with well-preserved extracellular bioactive factors for tissue engineering. Tissue Eng Part C Methods 2010 Oct;16(5):1201–11.
[3] Shupe T, Williams M, Brown A, Willenberg B, Petersen BE. Method for the decellularization of intact rat liver. Organogenesis 2010 Apr;6(2):134–6.
[4] Petersen TH, Calle EA, Zhao L, Lee EJ, Gui L, Raredon MB, et al. Tissue-engineered lungs for in vivo implantation. Science 2010 Jul 30;329(5991):538–41.
[5] Song JJ, Ott HC. Organ engineering based on decellularized matrix scaffolds. Trends Mol Med 2011 Aug;17(8):424–32.
[6] Crapo PM, Gilbert TW, Badylak SF. An overview of tissue and whole organ decellularization processes. Biomaterials 2011 Apr;32(12):3233–43.
[7] Wainwright JM, Czajka CA, Patel UB, Freytes DO, Tobita K, Gilbert TW, et al. Preparation of cardiac extracellular matrix from an intact porcine heart. Tissue Eng Part C Methods 2010 Jun;16(3):525–32.
[8] Toni R, Tampieri A, Zini N, Strusi V, Sandri M, Dallatana D, et al. Ex situ bioengineering of bioartificial endocrine glands: a new frontier in regenerative medicine of soft tissue organs. Ann Anat 2011 Oct 20;193(5):381–94.
[9] Sadr N, Pippenger BE, Scherberich A, Wendt D, Mantero S, Martin I, et al. Enhancing the biological performance of synthetic polymeric materials by decoration with engineered, decellularized extracellular matrix. Biomaterials 2012 Jul;33(20):5085–93.
[10] Decaris ML, Binder BY, Soicher MA, Bhat A, Leach JK. Cell-derived matrix coatings for polymeric scaffolds. Tissue Eng Part A 2012 Oct;18(19–20):2148–57.
[11] Evan G. Getting one's Fak straight. Dev Cell 2010 Aug 17;19(2):185–6.
[12] Kang Y, Kim S, Bishop J, Khademhosseini A, Yang Y. The osteogenic differentiation of human bone marrow MSCs on HUVEC-derived ECM and beta-TCP scaffold. Biomaterials 2012 Oct;33(29):6998–7007.
[13] Freiberg RA, Ray RD. Studies of devitalized bone implants. Arch Surg 1964 Sep;89:417–27.

Carragee EJ, Hurwitz EL, Weiner BK. A critical review of recombinant human bone morphogenetic protein-2 trials in spinal surgery: emerging safety concerns and lessons learned. Spine J 2011 Jun;11(6):471–91.
Gautschi OP, Frey SP, Zellweger R. Bone morphogenetic proteins in clinical applications. ANZ J Surg 2007 Aug;77(8):626–31.
Datta N, Holtorf HL, Sikavitsas VI, Jansen JA, Mikos AG. Effect of bone extracellular matrix synthesized in vitro on the osteoblastic differentiation of marrow stromal cells. Biomaterials 2005 Mar;26(9):971–7.
Datta N, Pham QP, Sharma U, Sikavitsas VI, Jansen JA, Mikos AG. In vitro generated extracellular matrix and fluid shear stress synergistically enhance 3D osteoblastic differentiation. Proc Natl Acad Sci U S A 2006 Feb 21;103(8):2488–93.
[79] Wendt D, Marsano A, Jakob M, Heberer M, Martin I. Oscillating perfusio cell suspensions through three-dimensional scaffolds enhances cell see efficiency and uniformity. Biotechnol Bioeng 2003 Oct 20;84(2):205–14.
[80] Bourgine P, Pippenger B, Güven S, Scherberich A, Martin I. Enginee of customizable devitalized extracellular matrices using clonal, de inducible, immortalized human mesenchymal stromal cells. Vienna: TER 2012.
[81] Wilson NS, Dixit V, Ashkenazi A. Death receptor signal transducers: node coordination in immune signaling networks. Nat Immunol 2009 Apr;1( 348–55.
[82] Ashkenazi A, Dixit VM. Death receptors: signaling and modulation. Scie 1998 Aug 28;281(5381):1305–8.

## III. Conclusions and Perspectives

Biology remains a finicky system, prone to auto-regulation/transformation independent of the engineered input and remarkably resistant to current protocol-based control methods. Based on this lack of control, the implementation of biologicals in humans is a difficult process that requires years of development and regulatory procedures, after which, results often demonstrate a lack of reproducibility and/or clinically-relevant outcomes. This is evident in the fact that 90% of clinical trials for tissue engineering products stop after phase I, never reaching the market [109]. Despite the technical and regulatory challenges associated with tissue engineered products, their perspective as a reliable treatment option is quite good [110]. Replacement/repair solutions to less complex tissues have met with overwhelming success and recent developments in material science and 3D culture systems have offered a slow evolution to more and more complex tissue replacements [111–114]. So far, the uniting element for all aforementioned implant technologies is based on the autologous use of cells to render a scaffolding material more receptive and prone to a regenerative response in vivo. This type of personalized medicine relies on many parameters for a successful clinical outcome, but this thesis treats the subject of optimizing two of these parameters in particular: the cell source and standardization of implant production.

The first two chapters dealt with cartilage and bone tissue engineering, respectively, investigating a novel cell source specifically chosen for its hypothetical capacity to integrate and communicate with the chosen implant sites. Adult human nasal chondrocytes, being derived from an embryological layer known for its remarkable capacity to differentiate into a variety of tissue types, were shown to not only maintain their capacity to differentiate into different cell types, but also to be capable of integrating into heterotopic sites, eventually participating in tissue repair. In Chapter 1, the adaptive capacity of nasal chondrocytes was investigated via their cartilage repair capabilities in an articular cartilage defect site. We demonstrated their latent self-renewal and progenitor capacity and correlated their tissue repair abilities to their specific Hox genetic signature. In Chapter 2, the multi-differentiation potential of nasal chondrocytes was explored by testing their capacity to differentiate into a bone forming osteoblast capable of orchestrating frank bone formation upon orthotopic

implantation. Interestingly, while nasal chondrocytes have now been shown to be capable of forming and repairing both cartilage and bone tissue types, it appears their capacity to do so is governed by the implant site itself. For regenerative medicine purposes, this is not only extremely clinically relevant, but highlights an important factor to be considered when choosing an appropriate cell source for graft production. Indeed, currently successful autologous cell-based approaches to graft production rely on using either multipotent stromal or fully-differentiated cells from the defective tissue itself for the engineering of a replacement graft. Interestingly and demonstrated in this thesis, nasal chondrocytes alone seem to fill both criteria for cartilage and bone applications: the demonstration of multipotent capacities and being derived from either a cartilage layer or from a craniofacial tissue. The clinical impact of these findings are therefore beyond our initial hopes. An adult chondrocyte cell source capable of articular cartilage repair already represents a significant step forward for regenerative medicine in cartilage applications. Nasal chondrocytes' ability to form a stable cartilage, even in long term implant experiments (up to 1 year) combined with their apparent resistance to endochondral ossification stimulation suggests this cell type helps to fills the gap present in articular cartilage tissue engineering. Indeed, the phase 1 clinical trials currently underway in Basel using autologous nasal chondrocytes to treat both homo- and heterotopic cartilage defects demonstrates their promise of versatility and safety in cartilage applications. While at an earlier stage of development, nasal chondrocytes' demonstrated ability to contribute to cranial bone repair broadens their clinical application to potentially include homotopic bone defects, possibly representing a unique cell source to repair craniofacial defects involving both cartilage and bone tissues. Autologous cell-based graft production represents a promising field in regenerative medicine and nasal chondrocytes seem to have their place in this emerging technology. Awaiting the final results from the clinical studies currently underway, nasal chondrocytes already present convincing preliminary results in humans that they do indeed have the capacity to reproducibly form a stable repair cartilage in defects. Further optimization of nasal chondrocyte-based bone grafts could also lead to similar positive findings in craniofacial bone applications.

The second parameter treated by this thesis for the optimization of clinically relevant graft production is standardization. As previously mentioned, cell-based systems demonstrate inherent adaptability to user input which tends to reduce the reproducibility of the constructed graft. One approach to minimize this effect but which continues to profit from the positive biological response presented by cells is based on the activation of a graft material using a cell-laid extracellular matrix (ECM). While the presence of cells on a graft material represents several problems for implant production standardization (reproducibility, donor variability, expensive and time consuming graft production costs and limited to one-off personalized grafts), ECM-based grafts produced in a perfusion bioreactor system promises to address these drawbacks.

Steps are currently underway to optimize both graft production strategies detailed in this thesis. While both technologies (living- and ECM-based graft production) are still hindered by the large amount of parameters to control throughout the production process, emerging technologies are helping to minimize and control the variable effects present in any biological system. 3D perfusion bioreactor systems are helping to reduce user manipulation of the graft material and standardize the biomechanical signals given to the cells during graft production. This technology theoretically allows for the use of any cell, as long as it is combined with an appropriate material for seeding and culture. For nasal chondrocytes, future work should first test if the biological signals present in the ECM produced during culture is enough to elicit a cartilage and bone repair response in vivo similar to the cell containing grafts demonstrated in this thesis. Production of ECM-based grafts could then be transferred to a 3D perfusion-based bioreactor system. Concurrently, current work is underway to test the feasibility to enrich the cell-laid ECM in chosen growth factors to augment to regenerative response upon implantation [115,116]. The power of this work resides in its potential to be transferred to other cell systems for targeted implant site graft production. ECM-based grafts with controlled repair signals combined with bioreactor production represent exciting new tools for tissue engineering, offering the possibility to tailor grafts to a specified regenerative and clinical need.